AD_____

Award Number: W81XWH-04-1-0580

TITLE: Regulation of hTERT Expression and Function in Newly Immortalized p53(+) Human Mammary Epithelial Cell Lines

PRINCIPAL INVESTIGATOR: Martha R. Stampfer, Ph.D.

CONTRACTING ORGANIZATION: University of California, Berkeley
Berkeley, CA 94720

REPORT DATE: June 2008

TYPE OF REPORT: Final

PREPARED FOR: U.S. Army Medical Research and Materiel Command
Fort Detrick, Maryland 21702-5012

REPORT DOCUMENTATION PAGE

Form Approved
OMB No. 0704-0188

1. REPORT DATE *(DD-MM-YYYY)*	**2. REPORT TYPE**	**3. DATES COVERED** *(From - To)*
01-06-2008	Final	1 Jun 2004 – 31 May 2008

4. TITLE AND SUBTITLE

Regulation of hTERT Expression and Function in Newly Immortalized p53(+) Human Mammary Epithelial Cell Lines

5a. CONTRACT NUMBER

5b. GRANT NUMBER
W81XWH-04-1-0580

5c. PROGRAM ELEMENT NUMBER

6. AUTHOR(S)

Martha R. Stampfer, Ph.D.

E-Mail: MRStampfer@lbl.gov

5d. PROJECT NUMBER

5e. TASK NUMBER

5f. WORK UNIT NUMBER

7. PERFORMING ORGANIZATION NAME(S) AND ADDRESS(ES)

University of California, Berkeley
Berkeley, CA 94720

8. PERFORMING ORGANIZATION REPORT NUMBER

9. SPONSORING / MONITORING AGENCY NAME(S) AND ADDRESS(ES)
U.S. Army Medical Research and Materiel Command
Fort Detrick, Maryland 21702-5012

10. SPONSOR/MONITOR'S ACRONYM(S)

11. SPONSOR/MONITOR'S REPORT NUMBER(S)

12. DISTRIBUTION / AVAILABILITY STATEMENT
Approved for Public Release; Distribution Unlimited

13. SUPPLEMENTARY NOTES – Original contains colored plates: ALL DTIC reproductions will be in black and white.

14. ABSTRACT

Telomerase is reactivated in almost all human breast cancers; loss of telomeric protection can lead to genomic instability. This proposal is to study telomerase reactivation and telomere protection in newly immortal, p53+ human mammary epithelial cells (HMEC), and to determine if these cells may be especially sensitive to therapies that target telomerase activity and telomere protection. Prior work showed that p53 can suppress most, but not all, telomerase expression in newly immortal p53+ HMEC lines until telomeres become extremely short, when an unknown mechanism (termed conversion) relieves this repression. We hypothesized that the observed upregulation of cyclin-dependent kinase inhibitor p57 might protect cells with critically short telomeres by inhibiting growth until there is sufficient telomerase to protect the telomeric ends. Our research in the past year supports a role of p57 in arresting growth prior to a p53-mediated DNA damage response being evoked, as well as a novel role in telomere homeostasis. Inhibition of p57 produced a result similar to inhibition of telomerase – accelerated, complete growth arrest without telomerase reactivation. Unlike telomerase inhibition, p57 inhibition led to a p53-mediated DNA damage arrest. Our data support a potential role for inhibition of p57 and/or telomerase in preferentially killing newly immortal p53+ HMEC.

15. SUBJECT TERMS
No subject terms provided.

16. SECURITY CLASSIFICATION OF:			**17. LIMITATION OF ABSTRACT**	**18. NUMBER OF PAGES**	**19a. NAME OF RESPONSIBLE PERSON**
a. REPORT	**b. ABSTRACT**	**c. THIS PAGE**			USAMRMC
U	U	U	UU	76	**19b. TELEPHONE NUMBER** *(include area code)*

Standard Form 298 (Rev. 8-98)
Prescribed by ANSI Std. Z39.18

Table of Contents

INTRODUCTION:

Acquisition of an immortal potential is considered crucial for human carcinogenesis, in order for a single cell to accumulate the multiple errors necessary for malignancy. In human carcinomas, attaining immortality is associated with reactivation of telomerase activity, which maintains the telomeric ends. Loss of telomeric protection usually leads to telomeric associations and genomic instability. In the continuing absence of telomerase activity, cell death or irreversible growth arrest will ensue. This proposal was designed to study the mechanisms involved in telomerase reactivation and telomere protection in newly immortalized human mammary epithelial cells (HMEC) that retain wild type p53 function, and to determine if these cells may be especially sensitive to killing by agents that target telomerase activity and telomere protection. Prior work showed that p53 can suppress most, but not all, telomerase expression in newly immortal p53+ HMEC lines, leading to a gradual erosion in telomere length until telomeres become extremely short (mean TRF $\leq$3 kb) (Stampfer et al., 2003, Stampfer et al., 1997). At that point, most growth stops, and levels of the cyclin-dependent kinase inhibitor p57 ^{KIP2} are elevated (Nijjar et al., 1999). An unknown mechanism (termed conversion) then gradually relieves this p53-mediated repression, although all other tested p53 functions are retained (Stampfer et al., 2003, Stampfer et al., 1997), leading to telomerase reactivation, stabilization of telomere length, and resumption of good growth; levels of p57 are gradually reduced concordant with these conversion-associated changes. Based on preliminary data we hypothesized that p57, a known cell cycle inhibitor, might be acting to protect these critically shortened telomeres by inhibiting growth until there was sufficient telomerase reactivation to protect the telomeric ends. This could explain our puzzling observation that although telomere lengths were exceedingly short, there was no evidence of widespread genomic instability before or during the conversion process. Therefore, our aims were to (1) Test whether the very low levels of telomerase present in newly immortal p53+ HMEC lines preferentially maintain the shortest telomere ends, until the conversion associated relief of p53-mediated suppression of telomerase activity occurs. (2) Test whether the low telomerase activity, along with the elevated p57 expression, suppress the genomic instability that is seen in senescent cells with critically short telomeres without telomerase expression (Romanov et al, 2001, Chin et al., 2004), and whether inhibition of telomerase activity and p57 function might efficiently kill the newly immortal cells. (3) Determine how p53 regulates telomerase activity in newly immortal HMEC lines. We have been able to address Aims 1 and 2, and to a lesser extent, Aim 3. Altogether, our data confirmed part of our original hypothesis, and led to an unanticipated result. As expected from the hypothesis in Aim 1, inhibition of telomerase activity led to early growth arrest and elevation of p57, without evidence of induction of a p53 damage response. As expected from the hypothesis in Aim 2, inhibition of p57 function also led to an early growth arrest, however in this case associated with p53 activation. These results support the hypothesis that p57 elevation serves to arrest cells prior to the presence of critically short telomeres that can form telomere associations leading to genomic instability. In the absence of p57, proliferation continues until the critically short telomeres elicit ap53-dependent response. What was unexpected was the total absence of telomerase reactivation/conversion process occurring when p57 was inhibited, implicating a role for p57 in initiating the conversion process. We now hypothesize that growth inhibition resulting from the elevated p57 may indeed be protecting the p53+ pre-conversion HMEC lines from genomic instability; however, expression of p57 is also required for the alleviation of the p53-mediated telomerase suppression. Our data support a potential role for inhibition of p57 and/or telomerase in preferentially killing newly immortal p53+ HMEC.

BODY:

Our prior work indicated that p53-dependent p57 expression is elevated in pre-conversion populations of newly immortal p53+ HMEC lines (Nijjar et al., 1999). In the p53+ immortally transformed line 184A1, we have shown that p57 elevation in the cycling population is coincident with the time when the mean TRF declines to <3 kb and most cells enter a growth arrest. p57 levels then very gradually decrease as telomerase activity gradually increases, and the population gradually resumes active proliferation. In a preliminary experiment, telomerase activity was inhibited in pre-conversion 184A1 using a dominant negative (DN) construct against hTERT, GRN385, transduced into 184A1 at passage 12. Treated cultures showed earlier growth arrest and p57

elevation than controls (passage 14 vs. passage 17-18). The morphology of the growth-arrested cells was similar in both cases. However, the control cultures contained cells with slow growth that gradually reactivated telomerase and underwent conversion, whereas all the GRN385-transduced cells showed a very gradual loss of viability over 1-2 months. We had postulated that the elevated levels of p57, a known cell cycle inhibitor, might be involved in restraining proliferation at this arrest until the p53 repression of telomerase was relieved and sufficient telomerase was reactivated to protect the telomeric ends and the cells' viability. In the absence of reactivated telomerase, ongoing proliferation with such critically short telomeres (< 3 kb) would lead to telomeric associations and mitotic failure. Our data have shown that while p57 does prevent critically short telomeres that can lead to genomic instability, it was also required for the conversion process, and full telomerase reactivation, to occur. Our data further suggest that, in the absence ofp57 expression (and conversion-associated telomerase reactivation), critically short telomeres may elicit a p53-dependent growth arrest and damage response.

Inhibition of hTERT in early 184A1 results in rapid growth arrest, elevation of p57, and prevents transformation to full immortality. We repeated our previous preliminary study with GRN385 and documented similar results (Fig. 1). 184A1 was transduced at passage (p) 13. As expected, control 184A1-LXSN cells overcame conversion associated with up-regulated p57 levels (not shown, see also Fig. 2), and gave rise to fully immortal cells. Telomerase activity was reduced in 184A1-GRN385 (DNhTERT) cells within one passage after retroviral transduction, and this population showed complete growth arrest with significantly up-regulated p57 prior to p57 elevation in the control population. No evidence of p53 activation was seen in either 184A1 population at 16p. These results suggest that p57 can slow down cell proliferation prior to or at the onset of conversion, before the telomeres become functionally critically short, or p53 is activated.

Abrogation of p57 expression in early 184A1 results in rapid growth arrest, and prevents transformation to full immortality. p57 expression was abrogated in pre-conversion 184A1 at 12p using retroviruses containing p57shRNA, or the scrambled shRNA vector (LNH1X). The levels of p57 in these cells were monitored by Western blotting (Fig. 2A) in growth-arrested cell extracts. Growth arrest by EGF withdrawal (Stampfer et al., 1993) was necessary for p57 detection, because pre-conversion cells express p57 only in the G0 phase of the cells cycle, until they approach the onset of conversion (Nijjar et al., 1999). The expression of p57shRNA reduced the levels of p57 in pre-conversion Go cells by 90%. Protein levels of $p27^{KIP1}$, a homolog of $p57^{KIP2}$, were unchanged (Fig. 2A), demonstrating the specificity of the shRNA.

Contrary to our initial expectations, cells with reduced p57 expression growth-arrested shortly after the introduction of the p57shRNA and never progressed to full immortality (Figs. 2B and 3A), while 184A1-LNH1X cells produced fully immortal populations (Fig. 3A). The 184A1-p57shRNA cells tested negative for apoptosis by TUNEL assay (data not shown).

To test the specificity of this shRNA effect, we introduced p57 shRNA into 184A1 at 50p, which had already overcome conversion and become fully immortal (increased levels of hTERT and stabilized telomeres). As in pre-conversion cells, protein levels of p57 were measured in growth-arrested G0 extracts. Western analysis demonstrated that introduction of p57shRNA resulted in a 75% reduction of p57 levels (Fig. 2C). Contrary to growth inhibition achieved in pre-conversion 184A1-p57shRNA cells, fully immortal cells with p57shRNA continued to proliferate robustly (Figs. 2D and 3B). These results demonstrate that p57shRNA-induced growth arrest is specific to pre-conversion 184A1.

To confirm our findings by an independent method, we introduced a dominant-negative p57 mutant (DNp57) into pre-conversion and fully immortal 184A1. DNp57 contains mutations in the 3_{10} helix, which is the key structural component of p57, responsible for Cdk inhibition (Hashimoto et al. 1998). As shown in Figures 3C and 3D, like p57shRNA, Dnp57 caused rapid growth arrest in pre-conversion, but not in fully immortal 184A1.

p57 may protect HMEC from DNA damage that could be induced by critically short telomeres, while

abrogation of p57 can lead to activation of p53-mediated DNA damage signaling. The p53 pathway is activated in response to DNA damage evoked by critically short telomeres in many cell types, including HMEC at senescence due to telomere dysfunction (Garbe et al., 2007). We found that, despite their short telomeres, 184A1 undergoing conversion with p57 elevation did not exhibit a markedly activated p53 damage response pathway at the passages examined (Fig. 4); note p53 appears constitutively phosphorylated at low levels in pre-conversion cells. Similarly, a DNA damage response (activated γH2AX; increased Chk2 phosphorylation; up-regulation of $p21^{CIP1}$) was not seen in the early growth arrest produced by GRN385 that is associated with elevated p57 levels (Fig. 1C). These results are consistent with our observation that conversion is not associated with genomic instability.

In contrast, evidence of an activated DNA damage response was apparent in cells transduced with the p57shRNA. As shown in Figure 4B, upstream (Chk2) and downstream ($p21^{CIP1}$) members of the p53 signaling cascade were activated in 184A1-p57shRNA cells and the levels of p53 Ser15 phosphorylation were increased. The phosphorylation status of p53 at Ser15 was also evaluated on a single-cell basis, using immunofluorescence, to account for cell-to-cell variability within the population (Fig. 5); increased phosphorylation was observed in 184A1-p57shRNA as early as 14p (two passages after p57shRNA transduction). These data indicate that pre-conversion 184A1 with abrogated p57 expression can arrest via a p53 damage response pathway. Our results suggest that the p57 elevation induced by short telomeres, and the associated growth arrest, may as we originally postulated, play a role in preventing the genomic instability associated with critically short telomeres producing DNA damage and telomeric associations. In the absence of elevated p57 levels, telomere erosion may be accelerated until DNA damage evokes a p53-mediated growth arrest. We still need to assay mean TRF lengths in these populations to determine the telomere lengths associated with these different conditions. These data should let us know if inhibition of p57 is correlated with more rapid shortening of the mean TRF, and if the induction of a p53 response correlates with attainment of critically shortened telomeres.

Our current model of regulatory interactions in newly immortal p53+ HMEC lines is as follows (Figure 6): p57 is up-regulated in p53+ newly immortal 184A1 in response to short, but still protected telomeres. Elevated p57 stops growth prior to the telomeres becoming critically shortened to the point of causing DNA damage. Additionally, by a mechanism we have not yet uncovered, p57 expression appears essential for pre-conversion HMEC to overcome the p53-mediated repression of hTERT and proceed through conversion to full immortality. If p53 function is abrogated in pre-conversion 184A1 by transducing GSE22 into these cells, p57 expression is prevented, hTERT expression is up-regulated, and cells immortalize efficiently. If p57 is abrogated, then ongoing telomere erosion produces DNA damage and a p53-mediated arrest, which we predict will be associated with some genomic instability. The latter possibility is consistent with our recent report that p53 is responsible for a similar growth arrest in senescent HMEC when the mean TRF of the population declines below 5 kb (Garbe et al., 2007). In the senescent population, telomere length would be assumed to be heterogeneous, so that critically shortened telomeres could induce a p53-mediated DNA damage response with a mean TRF of ~4-5 kb. In the situation with the pre-conversion 184A1, we hypothesize that the telomere lengths are more homogeneous because the low level of telomerase normally present, while not sufficient to preclude ongoing telomere erosion, may preferentially maintain the shortest telomeres lengths; therefore telomere dysfunction is not seen until a shorter mean TRF length of < 3 kb.

A novel aspect of this work is the potential association of p57 up-regulation in response to short telomeres in p53+ newly immortal HMEC with reactivated telomerase expression. It has been well established that p57 is up-regulated during differentiation processes in various cell types, however this gene has not, to date, been associated with telomere homeostasis. Our data suggest that the p53-dependent p57 expression may be necessary to relieve the p53-mediated repression of telomerase activity. In any case, these results support a potential clinical use for inhibition of p57 and/or telomerase in early stage p53+ breast carcinogenesis, since inhibition of p57 led to premature cell growth arrest and death.

Another goal of this proposal was to examine the effects of joint inhibition of p57 and telomerase activity. For this purpose, we wanted to use the oligonucleotide telomerase inhibitor GRN163L (whose effect can be reversed) from our collaborators at Geron. However, there was an extensive delay in obtaining this proprietary material from Geron Corporation, such that we received the material only a short time before the funding for ongoing research on this project ended. We were able to perform one initial study with this compound (and mismatch control). Pre-conversion and fully immortal 184A1 were exposed to varying doses of GRN163L and the control oligonucleotide GRN140833 for one passage at concentrations recommended by Geron (Fig. 7). Our results indicated that these HMEC are much more sensitive to GRN163L than most previous cells examined by Geron. We would like to repeat this study using lower doses for a longer period of time. The pre-conversion 184A1 cells were wiped out at the lowest concentration of GRN163L tested. Although cells exposed to GRN140833 were also inhibited, visual inspection showed that these cells still retained a normal appearance (Fig. 7B). In fully immortal 184A1, exposure to GRN163L was also more toxic than GRN140833, but not to the extent seen with the pre-conversion 184A1. These results are consistent with our hypothesis that the newly immortal p53+ lines with low telomerase activity and very short telomeres might be preferentially vulnerable to telomerase inhibition.

We were not able to perform all our proposed studies to determine how p53 regulates telomerase activity in the newly immortal p53+ HMEC lines. For the studies performed, we utilized the genetic suppressor element (GSE22) that acts as a dominant negative inhibitor of p53 tetramer formation (Stampfer et al. 2003). When GSE22 was transduced into a newly immortalized p53+ line, 184A1, levels of hTERT mRNA and telomerase activity quickly increased, and telomere length was stabilized (Stampfer et al, 2003). As a first step in determining the mechanism of p53 repression of hTERT, the timing of telomerase reactivation in GSE22-transduced 184A1 was measured. Telomerase activity was up-regulated within 96 hours of p53 inactivation (Figure 8), suggesting that the repression of telomerase by endogenous p53 is indirect. It is conceivable, though unlikely, that p53 could be acting directly to induce a long-lived repressor of telomerase transcription, so that the effect of p53 inactivation could take time to manifest. We do believe that p53 is acting on hTERT transcription because of our previously demonstrated effect of GSE22 on hTERT expression (Stampfer et al., 2003) and because the hTERT promoter showed increased activity in GSE22-transduced cells (Figure 9). Preliminary studies (Figure 10) suggested that the histone deacetylase inhibitor trichostatin A can increase telomerase activity in pre-conversion 184A1, implying a possible role of chromatin conformation in the suppression of telomerase in this population.

In related studies, we collaborated with Steven Haney at Wyeth, Cambridge MA, to perform expression array profiles of p53(+) vs. p53(-) immortalized HMEC lines, and finite vs. immortal HMEC (Li et al., 2007). We saw that greatest changes in expression occur in the transition from finite strains to non-malignant immortal lines (such as the 184A1 line), and that immortalized non-malignant lines like 184A1 resemble cells found in DCIS in vivo. These studies support the use of this cell line as a model of early stage human breast carcinogenesis, and the testing of effects of potential therapeutics on these cells. The data also reinforce our concern that immortally transformed non-malignant lines should not be referred to (as is commonly done) as normal, since they have already acquired the rate-limiting steps in carcinogenesis.

Another paper referred to above (Garbe et al., 2007) examined the role of p53 in the senescence barriers encountered by finite lifespan HMEC. We showed that p53 can be activated by critically shortened telomeres evoking a DNA damage response. In this situation telomere dysfunction activates p53, which produces a mostly viable arrest, without evidence of apoptosis, but with genomic instability. These results bear directly upon the studies on the newly immortal 184A1 line, as we believe our data reported above indicate that a similar situation is occurring when p57 is abrogated in the pre-conversion 184A1 line.

Preliminary studies also examined a possible role of telomere structure in the conversion process. We looked at expression of telomere-associated proteins, to see if there were any changes in their expression or localization that might correlate with immortalization or conversion. No significant changes were seen in expression of

TRF1, Tin2, Rap1, Ku70, Ku80, or WRN when comparing finite, newly immortal and fully immortal HMEC lines. However, increased expression of TRF2 was observed by Western blotting in the fully immortal lines (as well as many breast tumor cell lines) compared to both pre-conversion and finite HMEC (Nijjar et al, 2005). To determine if this change in TRF2 expression correlated with conversion and telomerase reactivation, the same population of 184A1 transduced with GSE22 that had been studied for telomerase expression was assayed for TRF2 protein expression by Western blotting and protein localization by IF. Increased TRF2 expression correlated with increased telomerase expression during conversion. Since overexpression of hTERT in pre-conversion 184A1 by itself did not result in increased TRF2 expression (Nijjar et al, 2005), this change must be due not simply to the expression of telomerase, but as a consequence of other changes occurring during conversion and endogenous reactivation of telomerase activity. We postulate that conversion in newly immortal p53+ HMEC is triggered by a change in telomere structure when the mean TRF has declined to $\leq$3 kb. The observed alteration in TRF2 expression and localization may provide a clue to the nature of the changes incurred when these cells enter conversion/reactivate telomerase.

In this final year of the grant (no cost extension for10% of PI time), the collected results have been evaluated and prepared for publication. However, we will still need to perform TRF analyses of the cultures described above before we are ready to submit a manuscript.

KEY RESEARCH ACCOMPLISHMENTS:

• Shown that inhibition of p57 in pre-conversion p53+ immortalized HMEC produces some effects similar to inhibition of telomerase activity, i.e., earlier growth arrest, suppression of conversion, and eventual cell death. However, inhibition of p57 leads to activation of a p53-mediated DNA damage response, whereas no evidence of p53 activation is seen during normal conversion or when telomerase is inhibited.

• Provided data that support our hypothesis that elevated levels of p57 may be responsible for the lack of genomic instability observed before and during conversion, while also suggesting a novel role for p57 in regulating telomerase expression during conversion.

• Shown that pre-conversion immortal HMEC are exceptionally sensitive to a telomerase-inhibiting compound in preliminary clinical trials.

• Shown that critically shortened telomeres can elicit a p53-mediated DNA damage response in finite lifespan HMEC that produces a growth arrest similar to what is seen in newly immortal HMEC when p57 is abrogated.

REPORTABLE OUTCOMES:

Mechanisms of hTERT up-regulation during immortalization of human mammary epithelial cells, Ekaterina Bassett, James C. Garbe, Tarlochan Nijjar, Martha R. Stampfer, and Paul Yaswen, abstract, AACR Annual Meeting, Washington DC, April 2006

Functional interactions of $p57^{KIP2}$ and p53 during immortalization of human mammary epithelial cells, Ekaterina Bassett, James C. Garbe, Tarlochan Nijjar, Alain Beliveau, Martha R. Stampfer, and Paul Yaswen, abstract, AACR Annual Meeting, Los Angeles CA, April 2007

Li Y, Pan J, Li J-L, Lee J-H, Tunkey C, Saraf K, Garbe J, Jelinsky S, Stampfer MR, Haney, SA, Transcriptional Changes Associated with Breast Cancer Occur as Normal Human Mammary Epithelial Cells Overcome Senescence Barriers and Become Immortalized. Mol Can 6:7, 2007.

Garbe, J, Holst, CR, Bassett, E, Tlsty, T, Stampfer, MR, Inactivation of p53 Function in Cultured Human Mammary Epithelial Cells Turns the Telomere-Length Dependent Senescence Barrier from Agonescence into Crisis. Cell Cycle 6:1927-1936, 2007.

CONCLUSIONS:

Telomerase is reactivated in almost all human breast cancers; the immortal potential conferred by telomerase is thought to be crucial for malignant progression. Expression of hTERT, the catalytic subunit of human telomerase, is the rate-limiting component of telomerase activity.

Our research has uncovered novel steps involving telomerase repression and reactivation during the immortalization of p53+ HMEC. These studies have shown that newly immortal p53+ HMEC possess exceedingly short telomeres, yet are protected from the widespread genomic instability that could lead to cell death - such as we have observed in finite lifespan HMEC with critically short telomeres. We hypothesize that the short telomeres result from the observed p53-mediated repression of most telomerase activity, while the protection results from low levels of telomerase present preferentially maintaining the shortest telomeres until the conversion process relieves the p53-mediated repression of telomerase. This proposal has sought to expand upon this data, both in terms of understanding the basic mechanisms regulating telomerase expression in these cells, and to determine if such cells, with exceedingly short telomeres, could be especially vulnerable to therapies that target telomerase activity and/or propel cells into catastrophic genomic instability.

Our results support the possibility that newly immortal p53+ HMEC may be especially vulnerable to specific molecular manipulation. Inhibiting the function of the cyclin-dependent kinase inhibitor p57, as well as inhibition of telomerase activity, led to premature growth arrest and death of the entire newly immortal p53+ population, with no cells showing telomerase reactivation and conversion to full immortality. Our data support the hypothesis that elevated levels of p57, in response to short but not yet dysfunctional telomeres, elicits a growth arrest that prevents further proliferation that could lead to critically shorted telomeres, genomic instability, and a p53-mediated DNA damage response. Our data also posit a novel role for p57 in alleviating the p53-mediated repression of telomerase that is present in newly immortal p53+ HMEC lines, i.e., p53-dependent expression of p57 may be part of a feedback mechanism necessary for relief of the p53-mediated repression of telomerase activity.

REFERENCES:

Chin, K, Ortiz de Solorzano, C, Knowles, D, Jones, A, Chou,W, Rodriguez, E, Kuo, W-L, Ljung, B-M, Chew, K, Krig, S, Garbe, J, Stampfer, M, Yaswen, P, Gray, JW, Lockett, SJ. *In Situ* Analysis of Genome Instability in Breast Cancer. Nature Genetics:36, 984-988 2004.

Garbe, J, Holst, CR, Bassett, E, Tlsty, T, Stampfer, MR, Inactivation of p53 Function in Cultured Human Mammary Epithelial Cells Turns the Telomere-Length Dependent Senescence Barrier from Agonescence into Crisis. Cell Cycle, in press.

Hashimoto Y, Kohri K, Kaneko Y, *et al.* Critical role for the 310 helix region of p57(Kip2) in cyclin-dependent kinase 2 inhibition and growth suppression. JBC:273, 16544-50, 1998.

Li Y, Pan J, Li J-L, Lee J-H, Tunkey C, Saraf K, Garbe J, Jelinsky S, Stampfer MR, Haney, SA, Transcriptional Changes Associated with Breast Cancer Occur as Normal Human Mammary Epithelial Cells Overcome Senescence Barriers and Become Immortalized. Mol Can 6:7, 2007.

Nijjar, T, Wigington, D, Garbe, JC, Waha, A, Stampfer, MR, Yaswen, P, $p57^{KIP2}$ expression and loss of heterozygosity during immortal conversion of cultured human mammary epithelial cells, Cancer Res 59:5112-5118, 1999.

Nijjar, T, Bassett, E, Garbe, J, Takenaka, Y, Stampfer, MR, Gilley, D, Yaswen, P, Accumulation and altered localization of telomere-associated protein TRF2 in immortally transformed and tumor-derived human breast cells, Oncogene:24, 3369–3376, 2005.

Romanov, SR, Kozakiewicz, K, Holst, CR, Stampfer, MR, Haupt, LM, Tlsty, TD, Normal human mammary epithelial cells spontaneously escape senescence and acquire genomic changes, Nature 409:633-637, 2001.

Stampfer, M.R., Pan, C.-H., Hosoda, J., Bartholomew, J., Mendelsohn, J., and Yaswen, P. Blockage of EGF receptor signal transduction causes reversible arrest of normal and immortal human mammary epithelial cells with synchronous reentry into the cell cycle. Exp. Cell Res. 208, 175-188, 1993.

Stampfer, M, Garbe, J, Nijjar, T, Wigington, D, Swisshelm, K, Yaswen, P, Loss of p53 function accelerates acquisition of telomerase activity in indefinite lifespan human mammary epithelial cell lines, Oncogene 22:5238-5251, 2003.

Stampfer, MR, Bodnar, A, Garbe, J, Wong, M, Pan, A, Villeponteau, B, Yaswen, P, Gradual phenotypic conversion associated with immortalization of cultured human mammary epithelial cells, Mol Biol Cell 8:2391-2405, 1997.

FIGURES 1-10

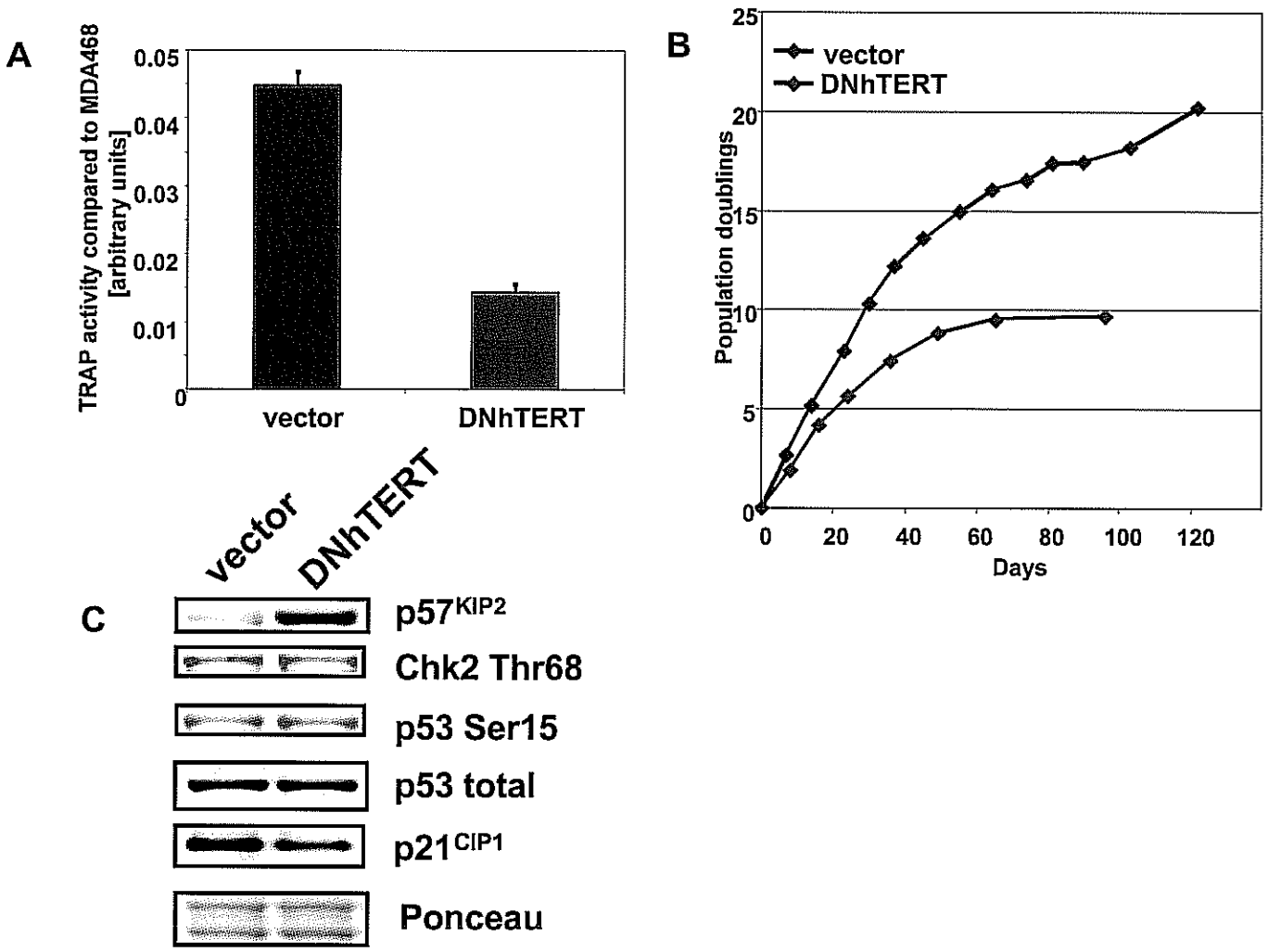

Figure 1. Inhibition of hTERT in pre-conversion 184A1 leads to a premature growth arrest associated with p57 expression. 184A1 pre-conversion HMEC were retrovirally transduced with DNhTERT at 13p. A. Telomerase (TRAP) activity in 184A1-DNhTERT 14p cells (DNhTERT), compared to the control 184A1-LXSN 14p cells (vector). B. 184A1-DNhTERT cells (DNhTERT) enter permanent growth arrest, while 184A1-LXSN cells (vector) proceed through conversion and become fully immortal. C. Western blot showing accelerated up-regulation of p57 in 184A1-DNhTERT cells 16p (DNhTERT), compared to 184A1-LXSN cells 16p (vector), three passages after retroviral transduction. Note the absence of any indication of p53 activation under either condition.

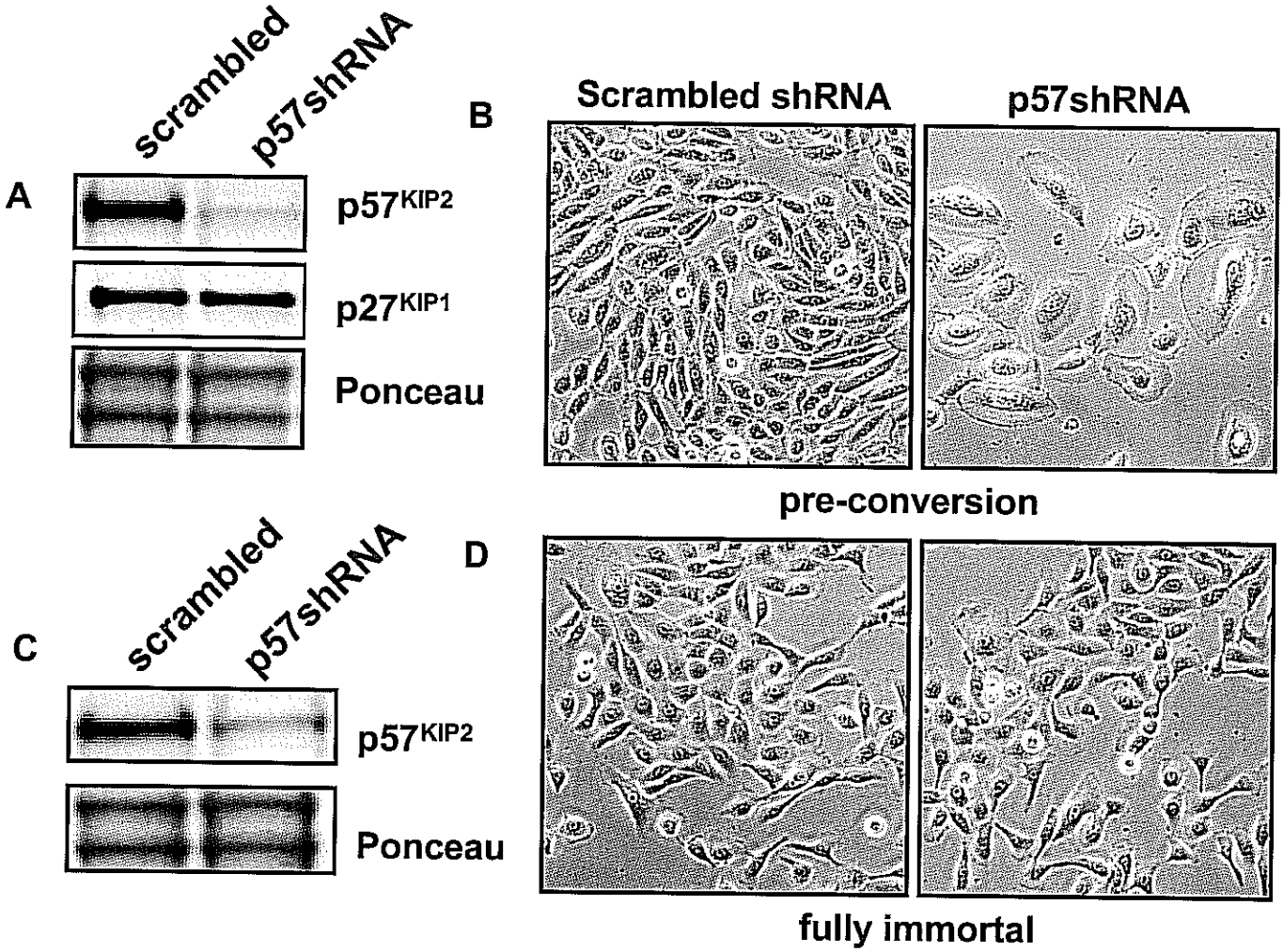

Figure 2. Abrogation of p57 expression causes early growth arrest, and prevents immortalization of pre-conversion 184A1, but has no effect on proliferation of fully immortal 184A1. A. Western blot showing a decrease of p57 expression in pre-conversion 184A1-p57shRNA 16p (p57shRNA), compared to the 184A1-LNH1X 16p (scrambled). The expression of $p27^{KIP1}$, a $p57^{KIP2}$ homolog, is unaffected by shRNA targeted against $p57^{KIP2}$. B, 184A1-p57shRNA cells display growth arrest, while the scrambled shRNA-expressing cells (184A1-LNH1X) proliferate robustly. C. Western blot showing a reduction of p57 expression in fully immortal 184A1-p57shRNA cells 51p (p57shRNA), as compared to the 184A1-LNH1X 51p (scrambled). D. No difference in phenotype is observed when expression of p57 is reduced in fully immortal 184A1.

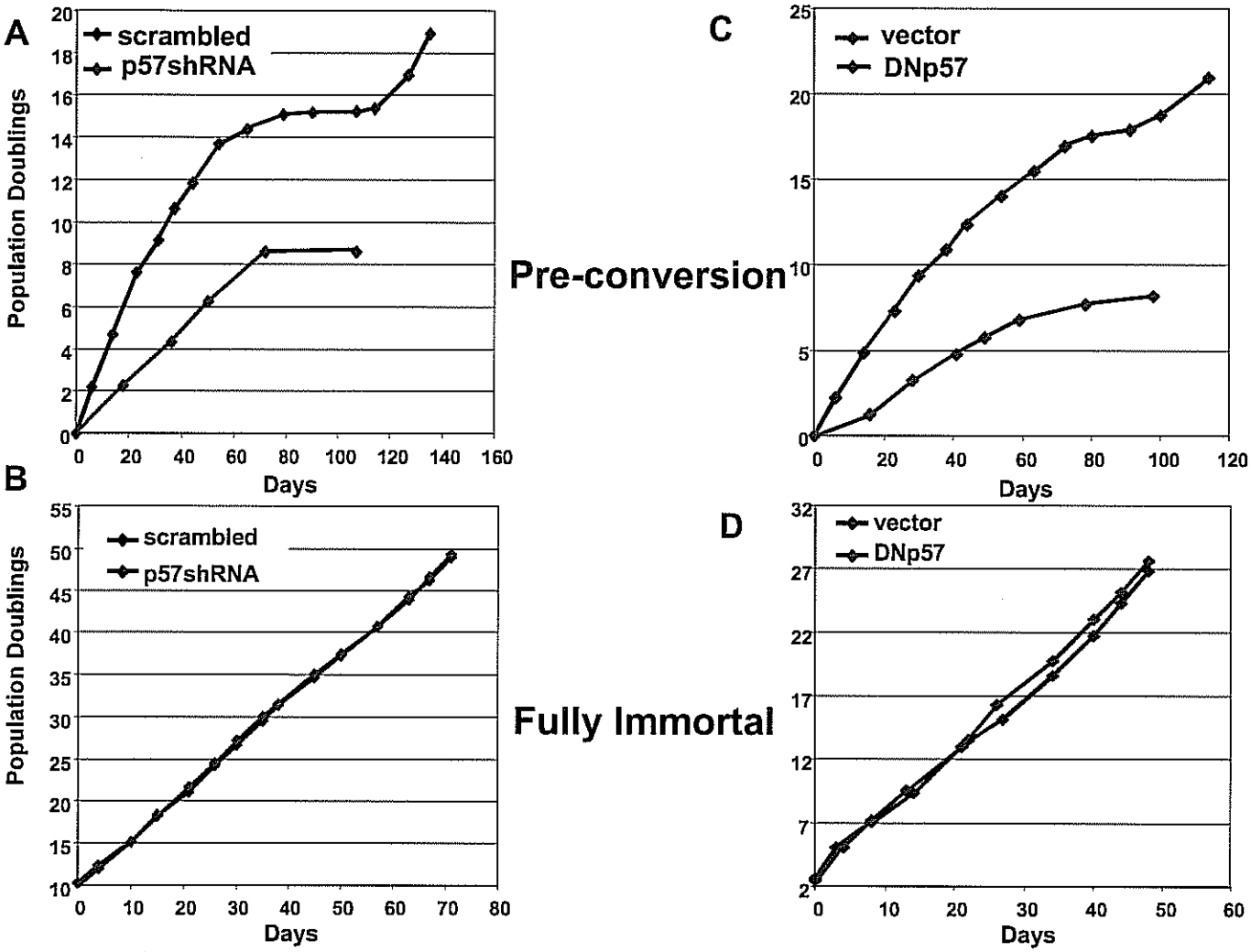

Figure 3. Inhibition of p57 expression or function induces growth arrest in pre-conversion, but not fully immortal HMEC. A and B, Growth curves for 184A1-LNH1X (scrambled) and 184A1-p57shRNA (p57shRNA), infected at 12p (pre-conversion) or 49p (Fully Immortal). C and D, Growth curves for 184A1-LXSN (vector) and 184A1-DNp57 (DNp57), infected at 12p (pre-conversion) or 49p (Fully Immortal).

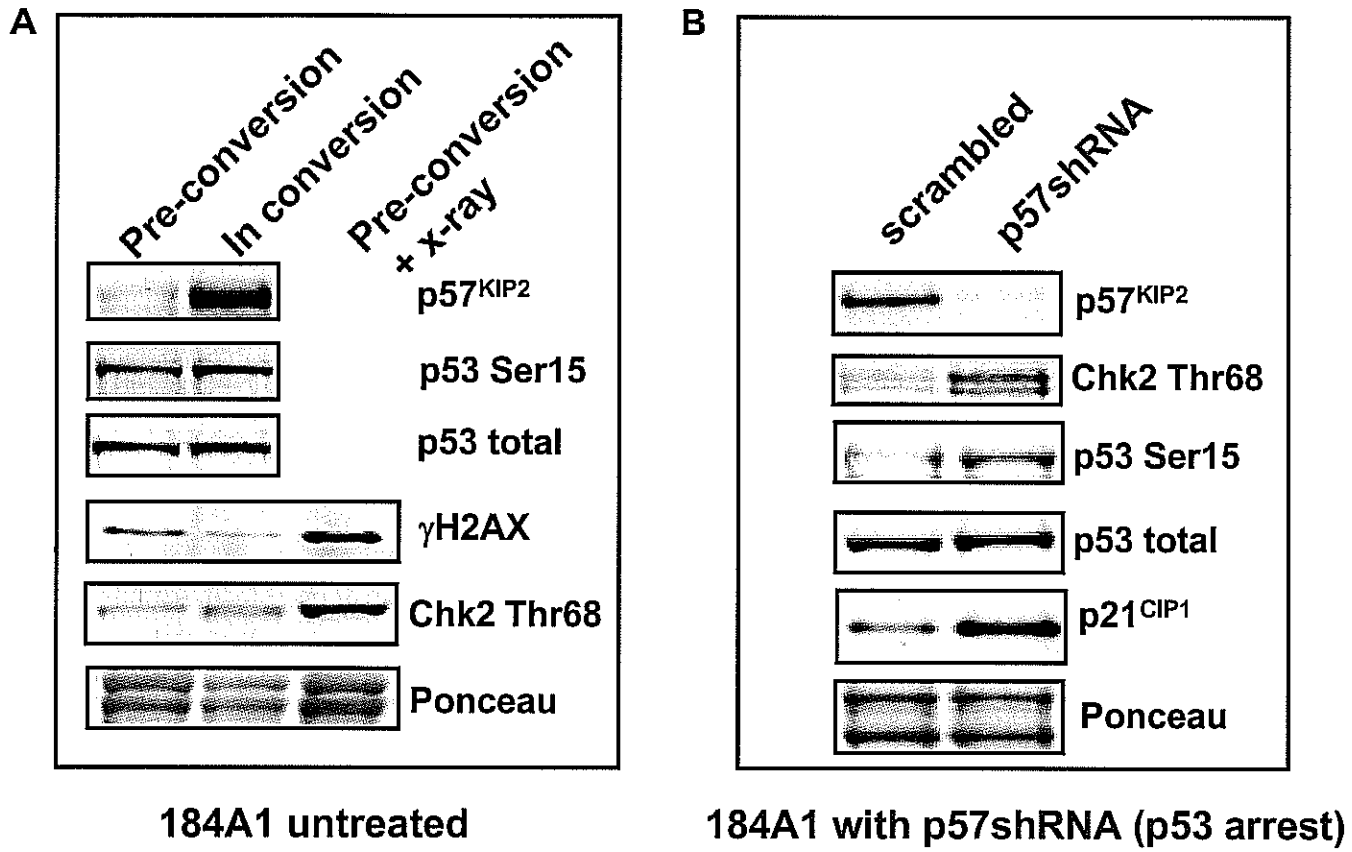

Figure 4. Growth arrest in pre-conversion HMEC with inhibited p57 expression correlates with activation of the p53 pathway. A. Western blots for DNA damage signaling pathway proteins in 184A1, 14p (pre-conversion), and 20p (in conversion). B. Western blots for DNA damage signaling pathway proteins in 184A1-LNH1X 16p (scrambled) and 184A1-p57shRNA 16p (p57shRNA).

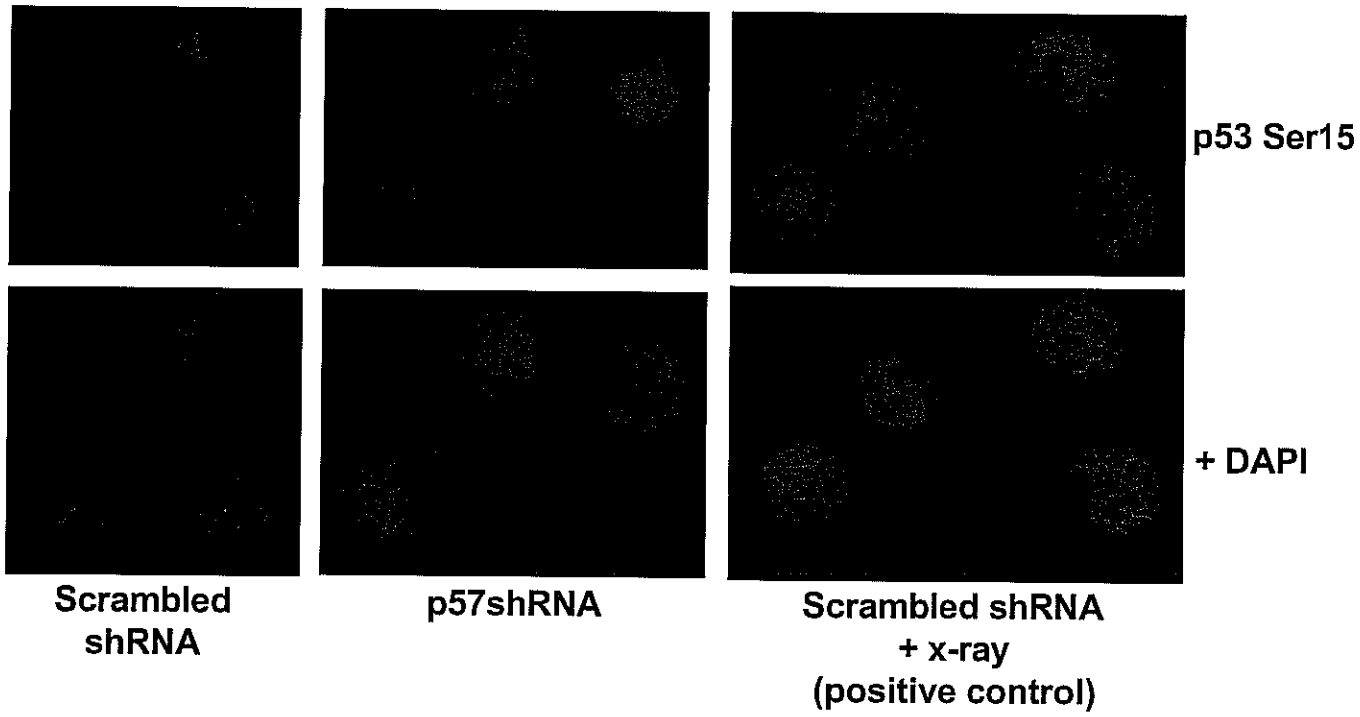

Figure 5. Growth arrest in pre-conversion HMEC with inhibited p57 expression correlates with an increase in p53Ser15 phosphorylation as detected by immunofluorescence. Scrambled shRNA, 184A1-LNH1X 14p. p57shRNA, 184A1-p57shRNA 14p. Scrambled shRNA + x-ray, 184A1-LNH1X 14p treated with 10Gy of x-ray.

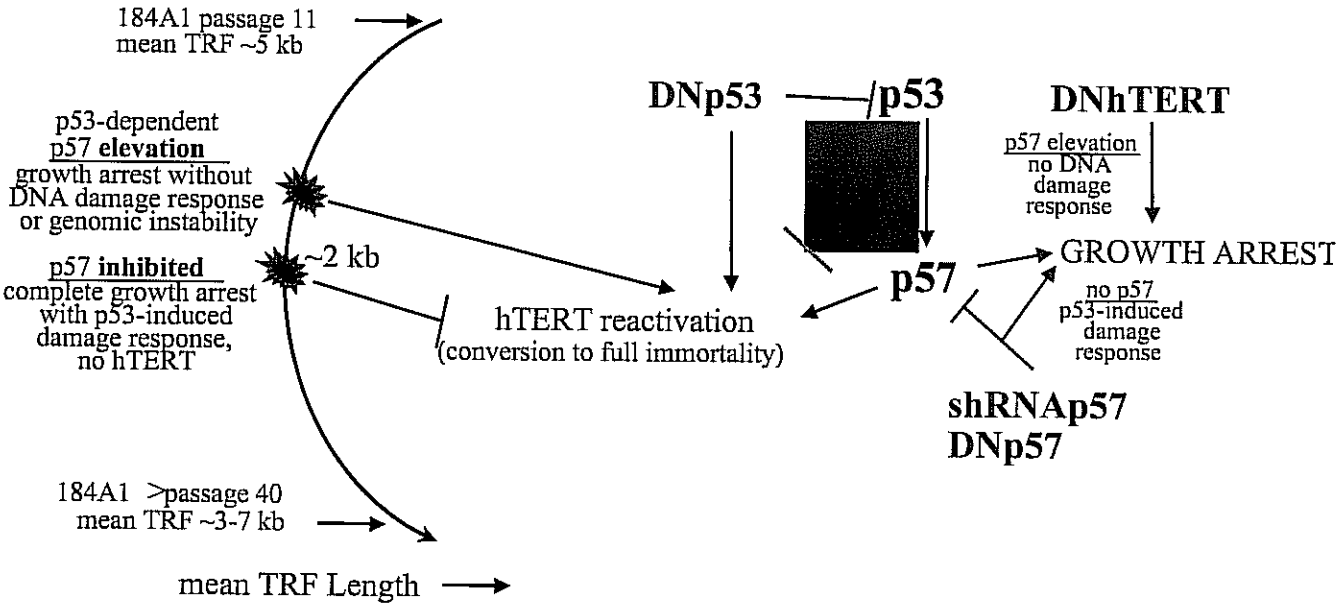

Figure 6. Model of Regulatory Interactions in Newly Immortal p53(+) 184A1

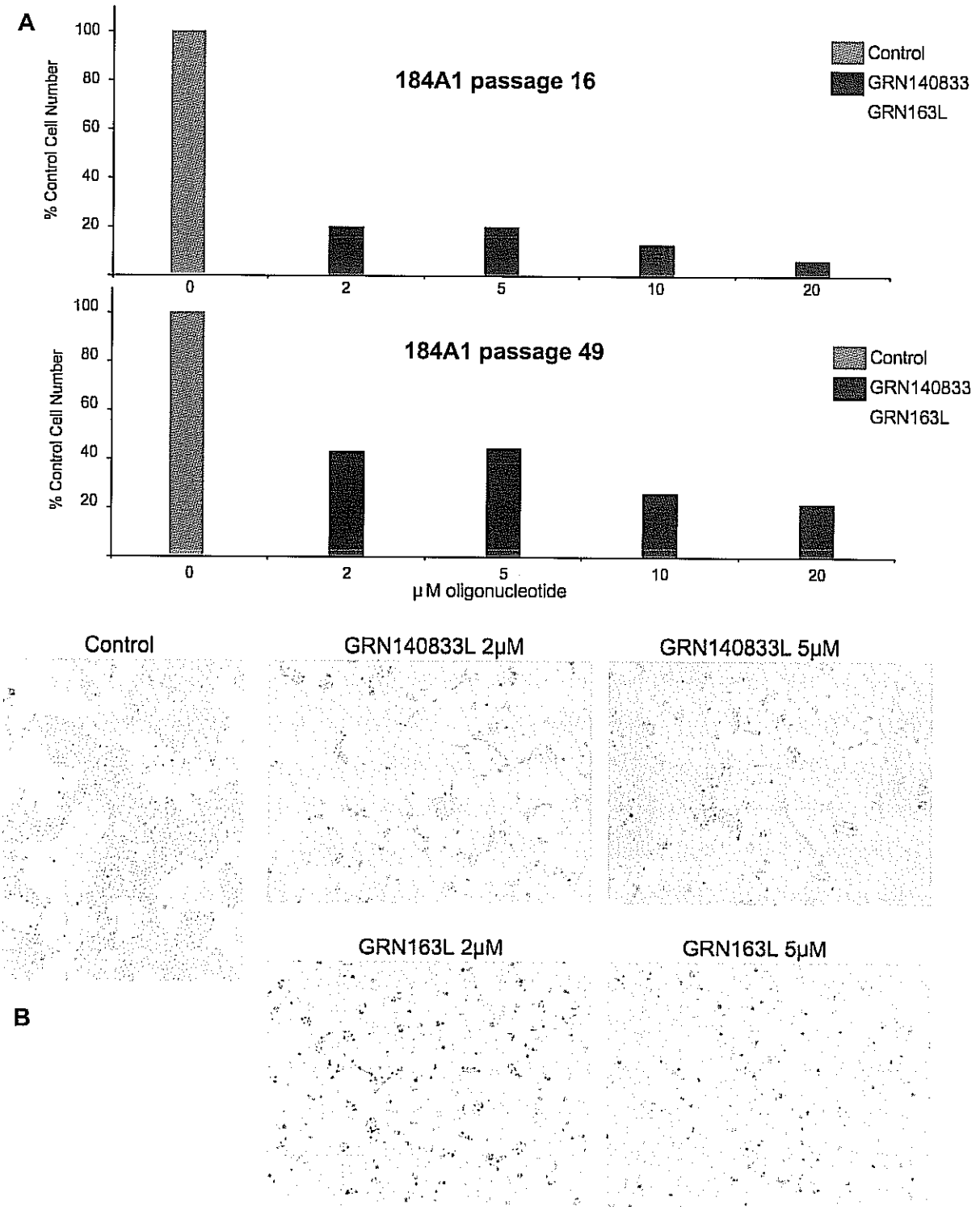

Figure 7. Effect of telomerase oligonucleotide inhibitor GRN163L on growth of pre-conversion and fully immortal 184A1. Cells were seeded into duplicate 35 mm dishes ($5x10^4$ cells/dish) and all dishes were counted when the controls became subconfluent to confluent. Control cell numbers for passage 16 were $4.1x10^5$ and for passage 49 were$8.8x10^5$. Although the mismatch oligo was also inhibitory to cell growth, visual inspection showed cells still growing with the expected morphology, while the cells exposed to GRN163L looked quite sick.

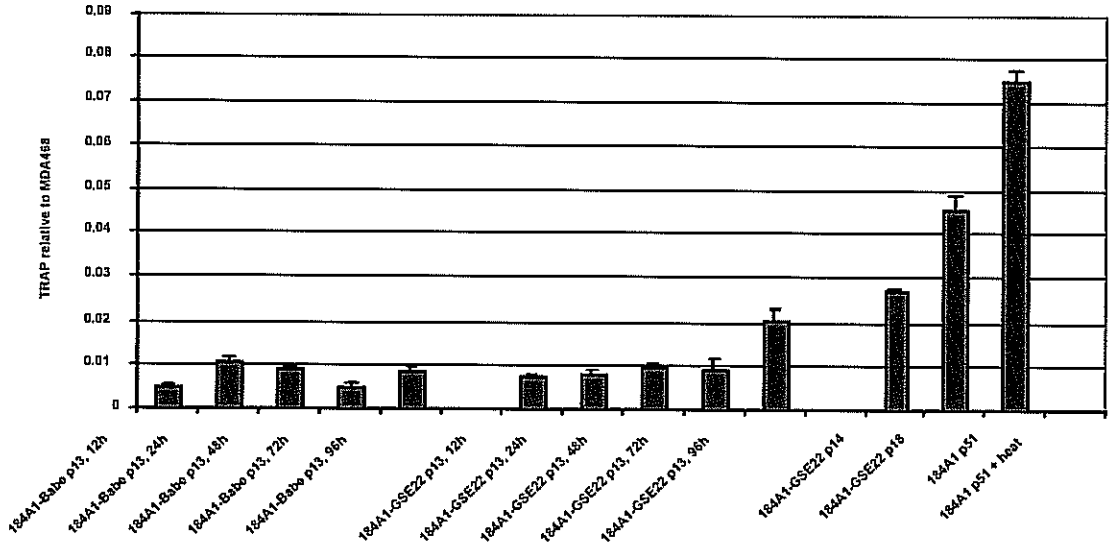

Figure 8. Telomerase activity in pre-conversion 184A1 is up-regulated within 96 hours of GSE22 transduction. 184A1 were infected with high-titer retroviruses carrying either the empty pBabe vector, or the pBabe-GSE22 construct at passage 13. At the indicated time points, ranging from 12h to 96h, subclonfluent cultures were collected by trypsinization, and the cell pellets were processed for real-time TRAP assay using the Quantitative Telomerase Detection Kit (Allied Biotech), following the manufacturer's protocols. 184A1-GSE22 at the later passages, and fully immortal 184A1 cells at passage 51, were used as positive controls for increased telomerase activity.

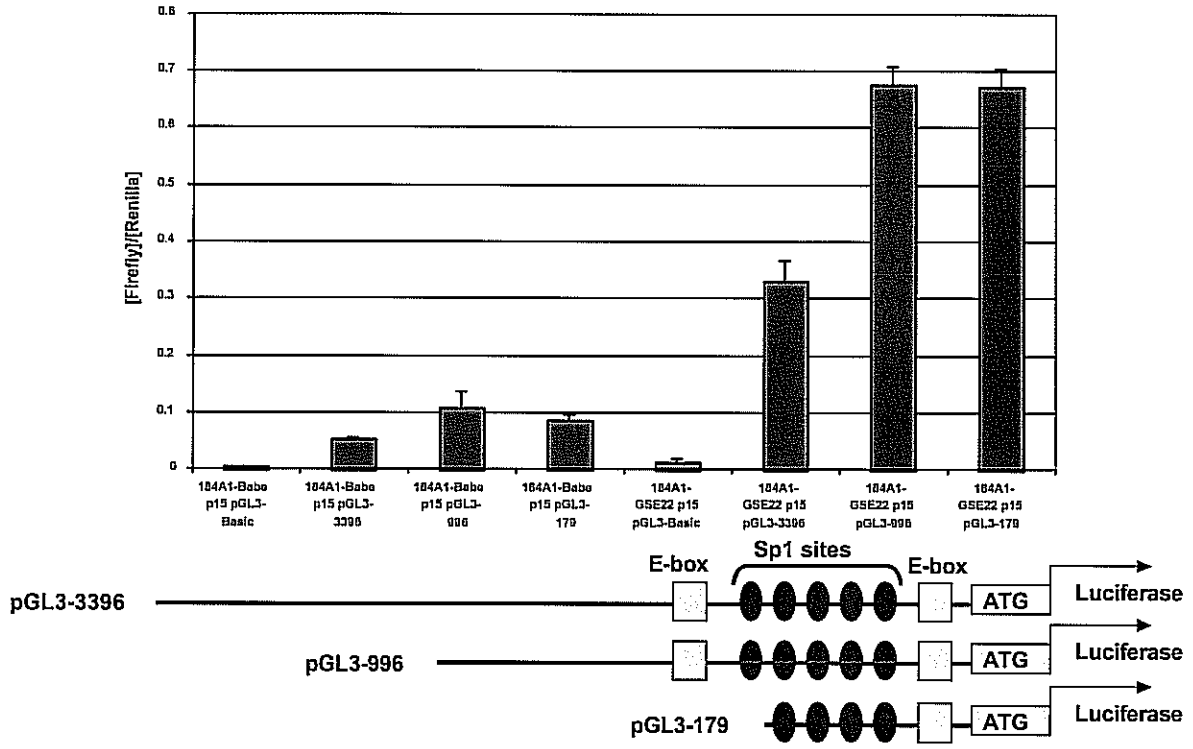

Figure 9. hTERT promoter activity of the firefly luciferase reporter in pre-conversion 184A1 with and without GSE22 inactivation of p53 function. Schematics were adapted from Won *et al.*, *JBC* 277:38230, 2002, and the firefly luciferase hTERT reporter plasmids were obtained from Dr. Tae Kook Kim, Advanced Institute of Science and Technology, Daejeon, South Korea. The firefly luciferase reporter plasmids were co-transfected into 184A1-Babe and 184A1-GSE22 cells at a 1:1 ratio with the promoterless Renilla reporter plasmid (pRL-Null). Following a 48h incubation, subclonfluent cultures were lysed and assayed using the Dual-Luciferase Reporter Assay (Promega). The results are reported as ratios of the firefly reporter luminescence to the Renilla reporter luminescence.

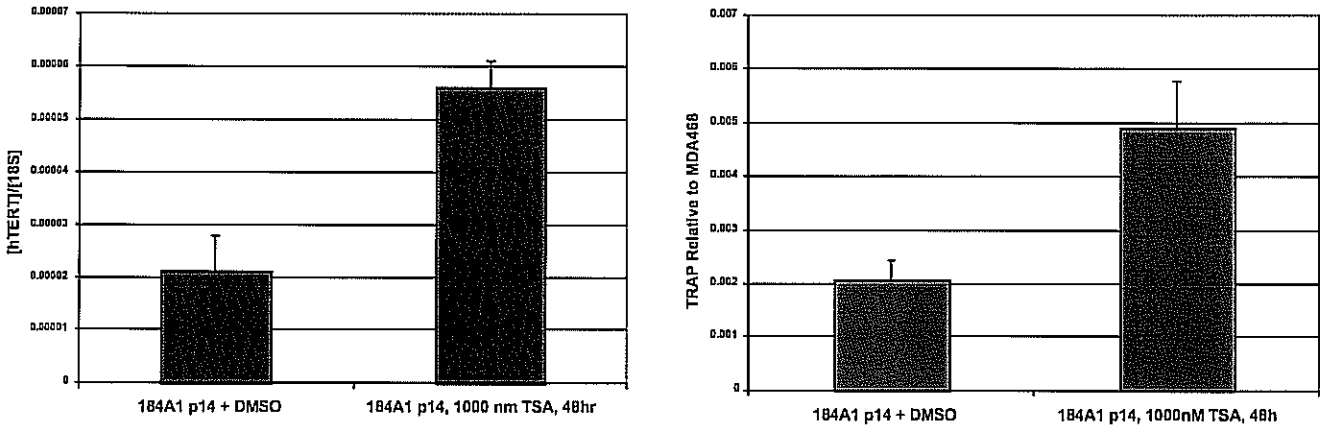

Figure 10. hTERT expression and telomerase activity in pre-conversion 184A1 are induced by the histone deacetylase inhibitor, trichostatin A. 184A1 at passage 14 were treated with either 1000 nM trichostatin A, or DMSO solvent. Following a 48h incubation, parallel subconfluent cultures were harvested for either real-time TRAP assay (Allied Biotech), or for RNA. RNA was isolated using RNeasy Mini Kit (Qiagen), and converted to cDNA using iScript cDNA Synthesis Kit (BioRad). The levels of hTERT expression were determined by real-time PCR, using iQ SYBR Green probe (BioRad). Specific primers were used to amplify hTERT mRNA as a full-length product. Quantification of the product was performed by comparing the levels of hTERT expression to the levels of expression of a housekeeping gene, 18S ribosomal RNA.

[Cell Cycle 6:15, 1927-1936, 1 August 2007]; ©2007 Landes Bioscience

Report

Inactivation of p53 Function in Cultured Human Mammary Epithelial Cells Turns the Telomere-Length Dependent Senescence Barrier From Agonescence into Crisis

James C. Garbe[1]
Charles R. Holst[2,†]
Ekaterina Bassett[1,‡]
Thea Tlsty[2]
Martha R. Stampfer[1,*]

[1]Life Sciences Division; Lawrence Berkeley National Laboratory; Berkeley, California USA

[2]Department of Pathology; UCSF Comprehensive Cancer Center; University of California at San Francisco; San Francisco, California USA

†Current address: Department of Molecular and Cellular Pharmacology; Exelixis, Inc.; South San Francisco, California USA

‡Current address: Geron Corporation; Menlo Park, California USA

*Correspondence to: Martha R. Stampfer; Lawrence Berkeley National Laboratory; Life Sciences Division, Bldg.73; Berkeley, California 94720 USA; Tel.: 510.486.7273; Fax: 510.486.4545; Email: mrstampfer@lbl.gov

Original manuscript submitted: 05/25/07
Manuscript accepted: 05/30/07

Previously published online as a *Cell Cycle* E-publication:
http://www.landesbioscience.com/journals/cc/abstract.php?id=4519

KEY WORDS

p53, agonescence, crisis, senescence, genomic instability, stasis

ABBREVIATIONS

CKI	cyclin dependent kinase inhibitor
GSE	genetic suppressor element
HMEC	human mammary epithelial cells
LI	labeling index
OIS	oncogene-induced senescence
PD	population doublings
Rb	retinoblastoma protein
SA-β-Gal	senescence associated β-galactosidase
TRF	terminal restriction fragment

ACKNOWLEDGEMENTS

See page 1934.

ABSTRACT

Cultured human mammary epithelial cells (HMEC) encounter two distinct barriers to indefinite growth. The first barrier, originally termed selection, can be overcome through loss of expression of the cyclin-dependent kinase inhibitor $p16^{INK4A}$. The resultant $p16^{-}$, $p53^{+}$ post-selection HMEC encounter a second barrier, termed agonescence, associated with critically shortened telomeres and widespread chromosomal aberrations. Although some cell death is present at agonescence, the majority of the population retains long-term viability. We now show that abrogation of p53 function in post-selection HMEC inactivates cell cycle checkpoints and changes the mostly viable agonescence barrier into a crisis-like barrier with massive cell death. In contrast, inactivation of p53 does not affect the ability of HMEC to overcome the first barrier. These data indicate that agonescence and crisis represent two different forms of a telomere-length dependent proliferation barrier. Altogether, our data suggest a modified model of HMEC senescence barriers. We propose that the first barrier is Rb-mediated and largely or completely independent of telomere length. This barrier is now being termed stasis, for stress-associated senescence. The second barrier (agonescence or crisis) results from ongoing telomere erosion leading to critically short telomeres and telomere dysfunction.

INTRODUCTION

Human cells cultured from normal somatic tissues express senescence, i.e., a limited proliferative potential; spontaneous immortal transformation is virtually unknown. The mechanisms responsible for enforcing this finite lifespan have not been clearly defined. Critically shortened telomeres resulting from telomerase repression, and responses to various stresses and/or DNA damage have been proposed as major limiting factors.[1-5] Additionally, oncogene-induced senescence (OIS) can be induced by exposure to certain oncogenes.[6-9]

A commonly used model of immortal transformation of cultured human cells posits overcoming at least two barriers, which have been called senescence or M1, and crisis or M2.[10,11] As originally proposed, the first barrier, senescence, is postulated to be due to shortened telomeres signaling activation of p53 and retinoblastoma (Rb) controlled cell cycle checkpoints, causing a viable arrest. Extended life cultures, usually obtained through exposure to viral oncogenes that functionally inactivate both Rb and p53, eventually reach the M2 barrier and undergo crisis, i.e., critically shortened telomeres producing genomic instability and cell death. Overcoming crisis has been thought to require acquiring a rare mutation during crisis that reactivates telomerase activity.[12] This model has been complicated by the demonstration of nontelomere length dependent senescence resulting from oncogenic and other stresses in many cultured human cell types.[13-17]

Our data using cultured human mammary epithelial cells (HMEC), along with data from other human cell systems, suggests a modified model of the senescence barriers encountered by finite human cells in vitro. HMEC derived from reduction mammoplasty tissue have undergone ~15–60 population doublings (PD) in vitro prior to encountering a first proliferation barrier, with the variation in the number of PD attained dependent upon culture conditions (Garbe J, Stampfer M, unpublished).[2,18,19] HMEC arrested at this barrier show a low labeling index (LI) of ~2%, viable arrest in G_1, normal karyotypes, a variable mean telomere restriction fragment (TRF) length of ~6–8 kb, expression of senescence-associated β-galactosidase activity (SA-β-Gal), and a large, flat, vacuolated morphology.[20,21] Under some culture conditions, proliferating cells have spontaneously emerged from arrested cell populations.[19,22] We originally called this proliferative barrier

selection, and the emergent proliferative population post-selection.[19] Post-selection cells lack expression of the cyclin-dependent kinase inhibitor (CKI) $p16^{INK4A}$, associated with methylation of the p16 promoter.[23] Post-selection HMEC encounter a second proliferation barrier after ~30–70 additional PD. This barrier, recently termed agonescence, is associated with critically shortened telomeres and widespread chromosomal abnormalities, including telomere associations.[21,24] Agonescent HMEC show a moderate LI of ~15%, a mostly viable arrest at all phases of the cell cycle along with some cell death, expression of SA-β-Gal, and a large, flat, vacuolated morphology. A situation characteristic of crisis, i.e., a high LI and massive cell death, was not observed in our finite lifespan HMEC populations. In this study we tested the hypothesis that the functional p53 present in post-selection HMEC induces a senescence response in the presence of critically short telomeres, thereby preventing the massive cell death and ongoing genomic instability associated with crisis.

We now demonstrate that the presence of functional p53 represents the distinction between agonescence and crisis. Abrogation of p53 function in post-selection HMEC inactivates cell cycle checkpoints and changes the mostly viable agonescence barrier into a crisis-like barrier with massive cell death. Abrogation of p53 function prior to the first barrier did not affect growth of the HMEC population. Altogether, our data suggest a modified model of HMEC senescence barriers using molecular defined nomenclature (see Fig. 6). In this model, the first barrier (originally termed selection) represents a Rb-mediated, nontelomere-length dependent, stress associated arrest, which we are calling stasis.[1] Phenotypic markers suggest that stasis is most similar to what has been called senescence or M1 in other cell systems. The second barrier is due to critically shortened telomeres producing telomere dysfunction. This barrier manifests as the recently described agonescence when p53 is functional, and as crisis in the absence of p53-dependent checkpoint arrest.

MATERIALS AND METHODS

Cell culture. Finite lifespan prestasis HMEC strain 184 (batch F) and post-selection HMEC strains 184 (batch B, agonescence at ~passage 15) and 48R (batch S, agonescence at ~passage 23) were obtained from reduction mammoplasty tissue that showed no epithelial cell pathology. Cells derived from primary tissues were grown in serum-containing MM medium, or serum-free MCDB 170 medium (MEGM, Clonetics Division of Cambrex, Walkersville, MD), as described.[18] Post-selection HMEC were cultured in MCDB 170 as described.[19,25,26] Labeling index was determined by addition of 3H-thymidine (0.5 μCi/ml) for 4 or 24 hr following refeeding, and visualization by autoradiography was as described.[27] Immunohistochemical analysis for p16 expression was performed as described using the JC8 antibody.[28] SA-β-Gal activity was determined as described.[29] In growing populations, each passage represents ~3–4 PD. Complete details on the derivation and culture of these HMEC can be found on our web site, www.lbl.gov/~mrgs/mindex.html.

Retroviral transduction. The pBABE-GSE22-puro plasmid, encoding a p53 genetic suppressor element (GSE) in a retroviral vector[30] was provided by Drs. Andrei Gudkov and Peter Chumakov, U. Ill., Chicago. GSE22 encodes the p53 nucleotides 937–1199, and the resultant peptide acts as a dominant negative suppressor by inhibiting the p53 tetramerization domain. Retroviral stocks were generated by transient cotransfection of the vector plasmid along with a plasmid encoding packaging functions into the 293 cell line.[31] Retroviral supernatants were collected in serum free MCDB 170 media containing 0.1% bovine serum albumin, filter sterilized and stored at -80°C. For lentivirus infections, the GSE22 insert was cloned into the pRRL.SIN-18 vector[32] and virus stocks produced as described.[33] Viral infection of 184 and 48R HMEC cultures was in MCDB 170 media containing 0.1% bovine serum albumin and 2.0 μg/ml polybrene (Sigma).

p53 function. For G_1 checkpoint assays, HMEC in log phase growth were exposed to 10 Gy of ionizing radiation from a Pantak II x-ray generator at 150 kV and 20 mA with beam filtration of 1.02 mm aluminum and 0.5 mm copper. Dosimetry was performed using a NIST-calibrated Victoreen condenser R-meter. Mock irradiated and irradiated cells were collected at 24 and 48 hrs post treatment and prepared for FACS analysis. For a spindle assembly checkpoint assays, HMEC in log phase growth were cultured in media containing 50 ng/ml colcemid (Karyomax, Life Technologies, Bethesda, MD). Treated cultures were refed every 24 hrs and samples were collected and prepared for FACS analysis at 0, 24, 48, 72, and 96 hrs. All cells were labeled with 10 μM BrdU (Sigma, St. Louis, MO) for 4 hours immediately prior to harvest. Analyses of BrdU incorporation and total DNA content were performed using a Becton-Dickinson flow cytometer. All analyzed events were gated to remove debris and aggregates. The fractions of BrdU(+) cells with specific DNA contents were determined by dividing the number of BrdU(+) events by the total number of gated events.

DNA damage assays. Subconfluent HMEC grown on 4-well chamber slides were either irradiated with 10 Gy of ionizing radiation, or mock-irradiated, and allowed to recover at 37°C for 6 h. The cells were then fixed with 4% paraformaldehyde, and permeabilized with 0.1% Triton X-100 (Sigma). The slides were blocked with 10% goat serum (Sigma) in CAS-Block (Zymed), and incubated with primary antibodies, against the serine 15 phosphorylated form of p53 (#9284, Cell Signaling Technology, Danvers, MA), the serine 139 phosphorylated form of H2AX (Clone JBW301, Chemicon, Temecula, CA), and 53BP1 (#A300-273A, Bethyl Laboratories, Montgomery, TX), or normal mouse or rabbit IgG (Invitrogen) as negative controls. After extensive washing with 0.1% Tween 20 (Sigma) in PBS, the slides were incubated with Alexa 488-conjugated anti-mouse IgG, or Alexa 594-conjugated anti-rabbit IgG (Invitrogen). Stained cells were visualized using a Zeiss Axiovert 200M inverted fluorescence microscope and imaged by a Retiga EX camera (Q-Imaging) and Image-Pro® Plus software (MediaCybernetics).

Telomerase and mean TRF length assays. Telomerase assays were performed as described[20] using the TRAP-EZE telomerase detection kit (Chemicon) and 2 μg of protein per assay. The telomerase products were visualized by Syber Green staining (Molecular Probes, Eugene, OR) and detected using a STORM imaging system (Molecular Dynamics, Sunnyvale, CA). DNA isolation and mean TRF analysis were performed as previously described using 3 μg of digested genomic DNA.[34,35]

RESULTS

p53 function is inactivated following transduction of GSE22. To test the hypothesis that functional p53 prevented crisis-associated massive cell death, we inactivated p53 function in post-selection HMEC using the p53 dominant negative genetic suppressor element GSE22.[30] Post-selection 184B HMEC were transduced with retroviral vectors containing GSE22 or empty control vector at passage

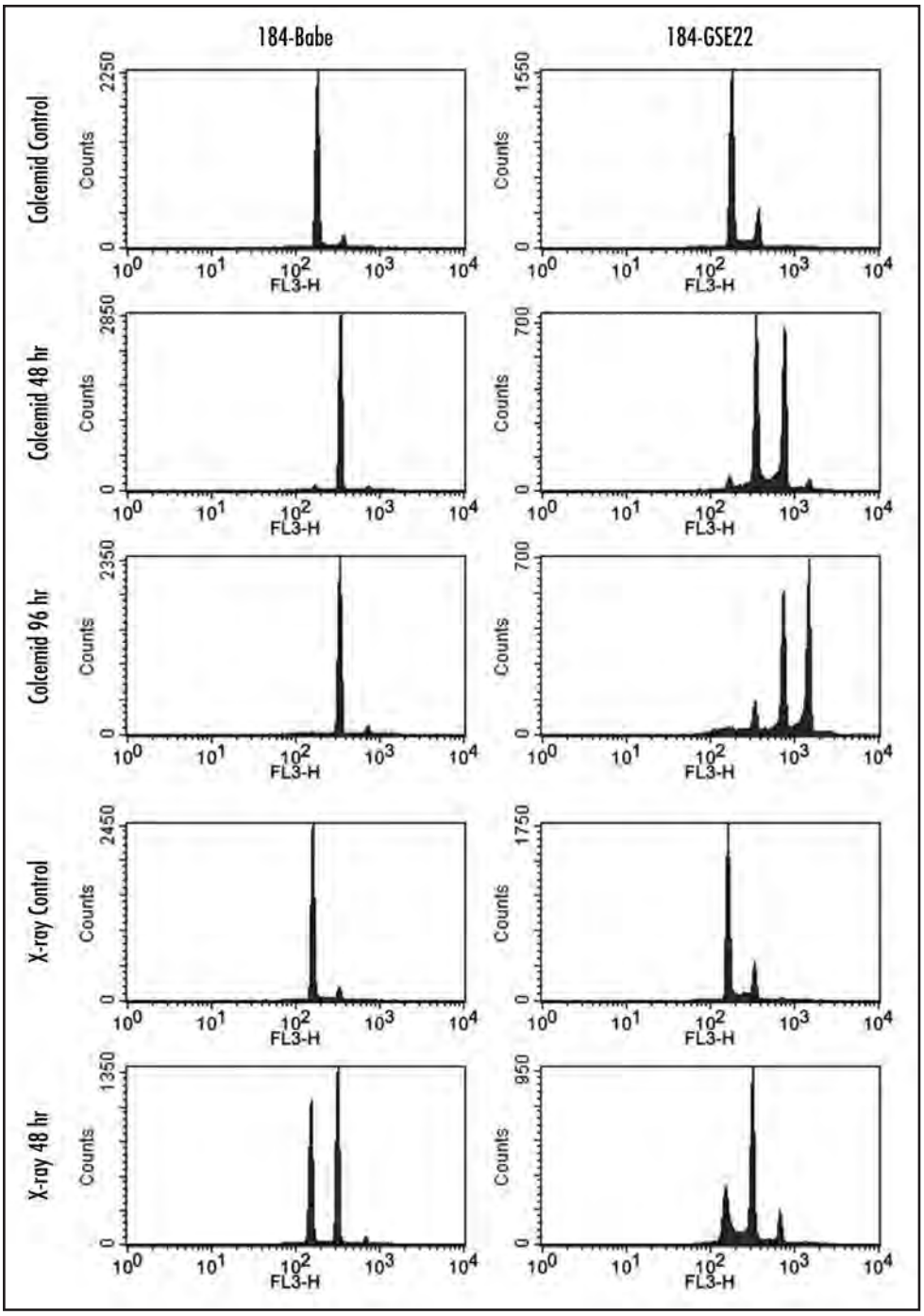

Figure 1. Transduction with GSE22 abrogates p53 function in post-selection 184 HMEC. 184B HMEC infected with GSE22-containing or control (Babe) vectors at passage 5 were analyzed by FACS analysis at passage 9 for DNA content in response to (A) 50 ng/ml colcemid and (B) 10 Gy of ionizing radiation.

5; ost-selection 48RS HMEC were transduced at passage 11. After selection with puromycin, the GSE transduced and control cells were assayed for p53 function following exposure to ionizing radiation or colcemid. Cells exposed to 10 Gy of x-irradiation were examined by FACS analysis after 24 and 48 hours, and cells exposed to 50 ng/ml colcemid were examined after 24, 48, 72 and 96 hrs. As shown in Figure 1 and Table 1, in unexposed cycling populations at passage 9, 184B-GSE22 compared to control 184B-Babe showed a modest increase in cells in S phase (~30% vs. 19%) and an increased fraction with a ≥4N DNA content (~3.5% vs. 0.6%). Following irradiation, 184B-Babe showed growth arrest in both G_1 and G_2, with few cells in S phase or with >4N DNA. In contrast, 184B-GSE22 failed to exhibit arrest; populations displayed ongoing DNA synthesis, with a major DNA peak at 4N as well as some cells with 8N DNA content. Following exposure to colcemid, the control population showed nearly complete growth arrest with 4N DNA content by 96 hr, with a small peak at 8N DNA content and almost no BrdU incorporation. In contrast, the 184B-GSE22 population continued to initiate DNA synthesis in the absence of mitosis and accumulated cells with ≥8N DNA content. Similar results were seen with specimen 48RS (data not shown).

These data indicate that p53 checkpoint-arresting functions have been abrogated in the GSE22-transduced populations. Additionally, the abundant p53 protein previously shown to be present in these post-selection HMEC,[35,36] does not show significant checkpoint-arresting activity in the absence of activating stimuli such as irradiation or colcemid.

p53 inactivation affects growth and morphology of post-selection HMEC. To determine the effect of abrogation of p53 function on growth capacity before and at agonescence, GSE22-transduced and control 184B HMEC populations were assayed for percentage of cells synthesizing DNA during 4 hr and 24 hr time periods starting from passage 8. Cells were also observed for morphology and viability.

There were no initial obvious differences between the GSE22-transduced and control cells at early passages after transduction. Both cell populations retained the typical cobblestone morphology of epithelial cells (Fig. 2A and C) and showed the same 24 hr LI of 93% (Table 2). The 184B-GSE22 population displayed a slight initial increased growth rate compared to 184B-Babe, which became more pronounced with ongoing subculture (Fig. 2G). By passage 12, there was a significant difference in the 24 hr LI between 184B-Babe (40%) vs. 184B-GSE22 (76%) (Table 2). As the control 184B-Babe population approached agonescence, its LI continued to decrease and its morphology changed, with an increasing percentage of the population exhibiting a senescent morphology of large, flat, vacuolated cells (Table 2 and Fig. 2B). By passage 15 there was no net increase in cell number and the 24 hr LI was ~15%. In contrast, 184B-GSE22 populations retained their small cobblestone morphology and a higher LI for an additional 2–3

Table 1 **BrdU incorporation of 184B-Babe and 184B-GSE22 after exposure to irradiation or colcemid at passage 9**

Cell	Control		Colcemid 96 hr		Control		X-ray 48 hr	
	% total	% BrdU+	% total	% BrdU+	% total	% BrdU+	% total	% BrdU+
184B-Babe								
<2n	0.48	0.03	0.32	0.02	0.51	0.05	0.32	0.00
2n	81.66	6.33	1.82	0.07	82.70	5.05	47.70	1.52
2n>4n	9.41	9.28	2.85	0.06	8.06	7.87	3.09	2.33
4n	7.84	4.38	88.59	0.19	8.17	4.67	44.33	4.02
>4n	0.61	0.34	6.41	0.95	0.56	0.35	4.55	2.58
Total	100	20.36	100	1.29	100	17.98	100	10.45
184B-GSE22								
<2n	0.38	0.08	2.88	0.32	0.44	0.03	1.27	0.20
2n	63.99	7.27	3.41	0.32	64.22	6.54	27.13	7.65
2n>4n	13.46	12.80	4.35	0.44	14.03	13.27	15.03	12.92
4n	19.02	8.91	7.95	0.49	17.45	7.26	41.13	9.01
>4n	3.16	2.04	81.40	26.19	3.86	2.22	15.44	8.63
Total	100	31.11	100	27.76	100	29.31	100	38.42

passages. By passage 15, the cell population contained a mixture of small proliferating cells along with large, vacuolated cells (Fig. 2D). The LI, 44%, was similar to that reported for cells in crisis.[37] With continuing time, either following subculture (data not shown), or observing the cell population remaining at passage 15, large vacuolated cells became predominant, with cultures eventually showing abundant cell debris (Fig. 2E and F) and a slowly declining LI (Table 2). These morphological changes are similar to those reported for cells in crisis. Both 184B-Babe and 184B-GSE22 showed an increasing percentage of SA-β-Gal(+) cells with passage. By passage 15, virtually all control cells were SA-β-Gal(+) (data not shown) as were the 184B-GSE22 cells with a senescent morphology (Fig. 2H).

To further demonstrate that loss of p53 function was responsible for the high LI seen in the late passage 184B-GSE22 cultures, GSE22 was transduced into an already agonescent culture of 184B HMEC at passage 15 using a lentiviral vector,[38] which allows infection of both dividing and nondividing cells. Seventy-two hours after infection the GSE22 transduced cultures had a 24 hr LI of 67%. In contrast, the cells transduced with the control lentivirus alone had a 24 hr LI of only 8%. Thus inactivation of p53 even at agonescence will allow growth-arrested cells exhibiting telomere dysfunction to resume DNA synthesis.

These data indicate that the abrogation of p53 function in post-selection HMEC initially does not have a significant effect on growth rate, but with continued proliferation leading to telomere erosion, eliminates the growth-restraining consequences of p53 activation, turning the largely viable agonescence arrest into a situation of crisis; i.e., high LI leading to massive cell death. We have not observed any instances of immortal clones arising from the 184B-GSE22 populations at crisis, based on observing the fate of more than 2×10^8 cells brought to crisis and maintained in culture for six months.

Post-selection HMEC at agonescence show evidence of a DNA damage response. To support the hypothesis that telomere dysfunction at agonescence is eliciting a DNA damage response that activates p53, we examined young and agonescent post-selection HMEC for γH2AX and 53BP1, markers associated with DNA damage,[39] and for activated p53 (phosphorylated on serine 15). Figure 3 shows the results for 184B and 48RS. In both cases, the agonescent culture was one passage away from no net increase in cell number, whereas the young cultures were 8 and 14 passages away respectively. As expected, numerous colocalized foci of 53BP1 and γH2AX were seen in the cells at agonescence and after x-irradiation, and expression of activated p53 was detected. In the young cultures, ~90% of the 48RS cells had 0–1 focus/nucleus, and faint expression of activated p53, while the 184B cultures had ~40% with 0–1 focus/nucleus, with no detectable expression of activated p53. Possibly, the greater expression of DNA damage foci in the young 184B cultures may reflect their closer proximity to agonescence. These data indicate that HMEC at agonescence show evidence of a DNA damage response and activation of p53.

Telomerase activity and mean TRF length. 184B-GSE22 and 184B-Babe populations were assayed for telomerase activity following retroviral infection at different passages. No activity was detected in control populations at any passage level. In two separate experiments, faint or no telomerase activity was seen in 184B-GSE22 (Fig. 4A). While faint activity could be detected at passage 7, this was largely absent at the passages closer to crisis (passages 13–14). Thus, inactivation of p53 function was insufficient to produce sustained reactivation of telomerase activity in $p16^-$ post-selection HMEC, consistent with the observed lack of immortal transformation. However, it is possible that inactivation of p53 function may elicit a transient increase in telomerase activity. Analysis of mean TRF length showed a reduced telomere length in 184B-GSE22 compared to 184B-Babe (3.1 vs. 3.8 kb), as well as a fainter signal, consistent with the extended proliferation of the p53-inactivated population (Fig. 4B).

p53 inactivation does not affect growth of prestasis HMEC. In other human cell types, e.g., keratinocytes and astrocytes, inactivation of p53, as well as p16 function, was necessary to overcome a telomere length independent proliferative barrier and permit efficient immortalization by hTERT transduction.[13,40] We have previously shown that $p16^-$ post-selection HMEC, which retain p53 function, could

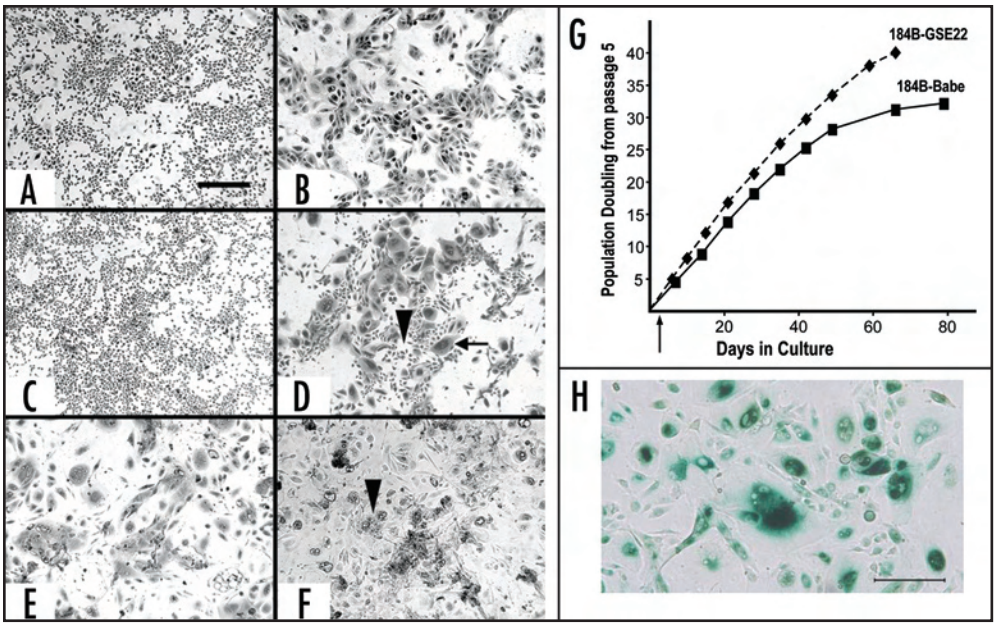

Figure 2. (A–F) Transduction of GSE22 leads to a crisis-like morphology rather than a mostly viable arrest in post-selection 184 HMEC. 184B HMEC infected with GSE22-containing or control (Babe) vectors at passage 5 were visually observed and photographed at subsequent passages. 184B-Babe (A) and 184B-GSE22 (C) at passage 7 show active growth of small cells with a cobblestone morphology. (B) 184B-Babe at agonescence, 2 months after plating at passage 15, contains mostly larger, flat cells with some vacuolization; the cell population can retain this morphology and viability for over a year. (D) 184-GSE22, two weeks after plating at passage 15, shows areas of small proliferating cells and many very large flat cells. (E) 184B-GSE22, two months after plating at passage 15, shows many large multi-nucleated vacuolated cells, cell debris, and some smaller cells. (F) 184B-GSE22, four months after plating at passage 15, shows mostly large multi-nucleated, vacuolated cells and abundant cell debris. The bar represents 200 microns. All photographs are at the same magnification. (G) Growth of 184B-Babe and 184B-GSE22 following transduction at passage 5 (arrow). (H) Post-selection 184B-GSE22 in crisis at passage 15 is SA-β-Gal(+).

Table 2 **Labeling Index (LI) of 184B-Babe and 184B-GSE22 at different passage levels**

	24 hr LI		4 hr LI	
Passage Number	**184B-Babe**	**184B-GSE22**	**184B-Babe**	**184B-GSE22**
8	93	93	39	42
12	40	76	6.9	30
13	17	70	3.2	20
14	16	44	3.7	19
15 (2 weeks)	15	43	2.3	16
15 (2 months)	5.6	25	1.9	15

be efficiently immortalized by hTERT,[28] indicating that HMEC do not need p53 inactivation to become immortal. To directly assess the role of p53 in enforcing stasis, primary 184F HMEC were grown in MM and transduced with the GSE22 or empty control vector at passage 2 or 3. Both cell populations showed similar growth rates and nearly complete growth arrest by passage 4, with expression of p16 and SA-β-Gal seen by immunohistochemistry in the large, senescent-appearing cells at passage 5 (Fig. 5B and C). As expected for HMEC grown in MM, no control cells showed escape from stasis; however, in two independent experiments a small number of clonal outgrowths appeared in the passage 5 GSE22-transduced cultures. Clonal outgrowths from one experiment ceased growth after an additional ~25 PD, with a morphology that resembled the post-selection 184B-GSE22 at crisis. Unlike post-selection HMEC, low levels of p16 expression were detectable in these populations (Fig. 5D). A clonal outgrowth from the second experiment maintained indefinite proliferative potential; this line has been called 184FGS1. These data indicate that in HMEC, p53 inactivation does not provide a proliferative advantage to prestasis populations as a whole. The very rare emergence of cells that overcame this first barrier suggests that these GSE22-transduced clones arose as a secondary, rather than a direct consequence of the loss of p53 function.

DISCUSSION

A variety of models and nomenclature have been employed in cultured human cell systems to describe senescence barriers; i.e., mechanisms that limit proliferative potential thereby precluding immortality. A commonly used model postulates two barriers, M1 or senescence, and M2 or crisis, that are both proposed to be consequences of shortened telomeres.[11,12] An M0 was later added to this model as a new name for the barrier we originally called selection.[41] More recently, telomere-length independent senescence barriers have been proposed.[1,2,13,15,17,40,42] These have been called senescence, extrinsic senescence, M1, M1.5, M^{INT}, and stasis. Other barriers to ongoing proliferation of finite lifespan cells have also been described, such as "stress-associated senescence" or "culture shock", due to sub-optimal culture conditions.[43,44] In most cases, these nomenclatures have not been defined and distinguished by specific molecular properties of the arrested cell populations. Cells are frequently called senescent based solely on their expression of SA-β-Gal, and a "senescent" (large, flat, vacuolated) morphology.

The data presented in this report, along with our long-term studies on HMEC, have led us to propose a simplified model and nomenclature for the senescence barriers encounter by cultured HMEC, based on expression of specific molecular properties (Fig. 6). Our model proposes that cultured HMEC encounter two mechanistically distinct senescence barriers: a stress-associated, telomere-length independent barrier, which we are calling stasis,[1] and a barrier due to ongoing telomere erosion leading to telomere dysfunction. Additionally, prestasis and post-selection finite lifespan HMEC in vitro are vulnerable to OIS, which induces a phenotype distinct from stasis and telomere dysfunction.[7]

We demonstrate here that the phenotype of the telomere dysfunction senescence barrier in HMEC depends upon whether or not p53 is functional. When p53 is functional, critically shortened telomeres produce a largely viable arrest, termed agonescence, due to the ability of p53 to respond to DNA damage by inducing cell cycle checkpoints. Thus, similar to what has been shown in in vivo mouse models, genomic instability based on telomere dysfunction

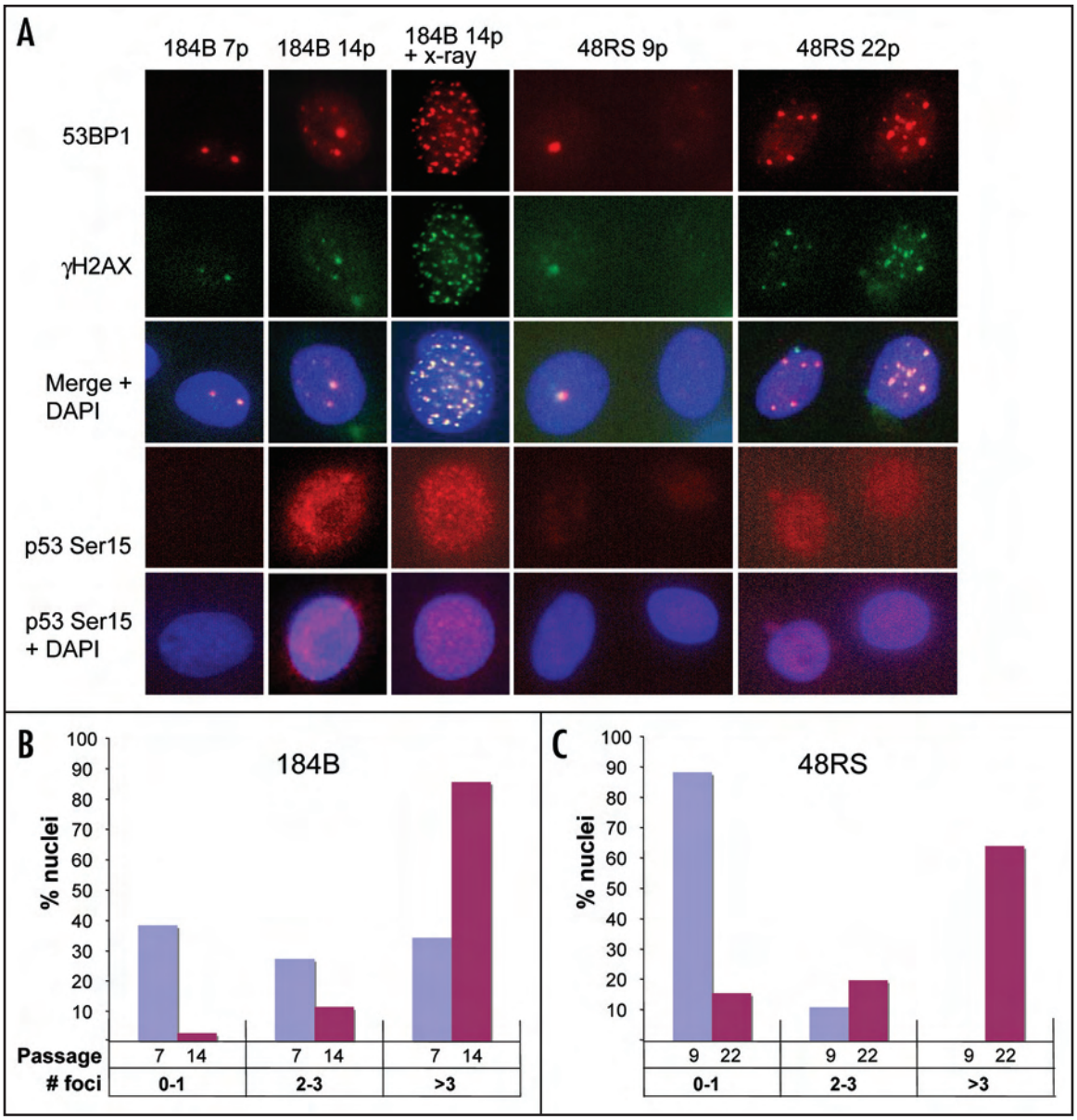

Figure 3. DNA damage responses in post-selection 184B and 48RS HMEC. (A) Representative fluorescent images of growing and agonescent post-selection HMEC, as well as x-ray irradiated HMEC, stained for p53 Ser15 (red), 53BP1 (red), phospho-histone H2AX (Ser 139) (green), and DNA (blue). Colocalization of the 53BP1 and phospho-H2AX signals is shown in yellow. (B)(C) Percentages of cells displaying 0-1, 2-3, or greater than 3 of the 53BP1 foci were calculated. For each cell population, at least five randomly selected fields were scored.

can trigger a restraining mechanism in the setting of intact p53;[45] such p53-mediated senescence mechanisms may pose a barrier to further malignant progression.[46,47] Cells which fail to arrest at agonescence die as a consequence of the genomic instability and mitotic failures produced by the critically shortened telomeres,[21] suggesting that p53 is unable to arrest all HMEC prior to acquisition of lethal or proliferation-inhibiting damage. Notably, virtually every metaphase spread examined in HMEC nearing agonescence showed gross chromosomal abnormalities, including numerous telomere associations.[21] When p53 function is abrogated in post-selection HMEC that have overcome stasis, the critically shortened telomeres produce crisis rather than agonescence; in the absence of p53-mediated checkpoint responses, virtually all the cells eventually die. Apoptosis is rare at telomere dysfunction, although it is higher during crisis than agonescence.[48] In our experiments, abrogation of p53 function by itself did not produce sustained reactivation of telo-merase activity or any immortal lines. In other reports,[49,50] rare immortalization was observed, likely due to the generation of an additional error or errors during the period of genomic instability occurring at crisis. Transduction of hTERT is sufficient to immortalize a variety of p53+ or p53- post-stasis human epithelial cell types,[28,40,51,52] further illustrating the telomere length dependence of agonescence and crisis. We have postulated that overcoming the telomere dysfunction barrier in post-selection HMEC requires generation of multiple errors that permit telomerase reactivation.[2]

In contrast with post-selection HMEC, we show here that GSE22-mediated abrogation of p53 function in early passage prestasis HMEC had no significant effect on growth of the population as a whole. Cells with and without p53 function ceased proliferation at stasis, associated with expression of p16 and SA-β-Gal, and a senescent

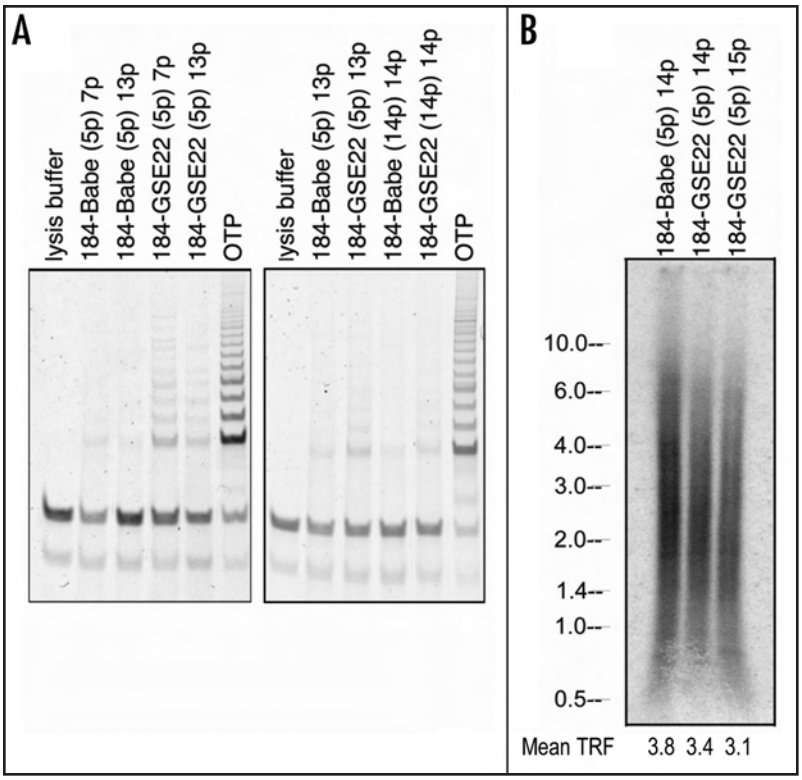

Figure 4. (A) Transduction of GSE22 in post-selection 184 HMEC does not produce significant, sustained reactivation of telomerase activity. 184B HMEC were transduced at passage 5 (5p) or 14 (14p) with GSE22 or control (Babe) vector, and assayed at the indicated passages for telomerase activity. (B). Mean TRF length of 184B-GSE22 at crisis is shorter than184B-Babe at agonescence. Genomic DNA was isolated from 184B-Babe HMEC at agonescence (14p) or from 184B-GSE22 HMEC during crisis (14p, 15p). Numbers on the left indicate the sizes of DNA molecular weight standards.

morphology. Similar results have been reported using HPVE6 inactivation of p53 function.[53] Thus p53 does not appear to enforce the initial proliferation barrier in cultured HMEC, in contrast to reports on other cell types such as human fibroblasts, keratinocytes, and astrocytes, where overcoming a first proliferation barrier has generally required loss of p53 function.[13,40,54] We propose that this difference is due to cell-type variations in stress responses.[55] Specifically, other cells may use the p53-dependent CKI p21 instead of or in addition to p16 to enforce an Rb-mediated stasis barrier. Ablation of p21 or Rb function can overcome this barrier even in the presence of functional p53.[56,57] In HMEC, p21 is not elevated at stasis,[21] and stasis can be efficiently overcome by introduction of an shRNA to p16 (Garbe J, Stampfer M, unpublished). We speculate that stresses that induce p53 may involve DNA damaging agents such as oxidative stress, and HMEC under routine culture conditions may be less susceptible to such damage than other cell types. In this regard, we have not seen any significant differences in long-term growth potential of prestasis HMEC when grown under 20% vs. 3% O_2 conditions (Garbe et al., in preparation). The absence of p53-dependent p21 induction enforcing stasis in cultured HMEC, along with the spontaneous silencing of p16 in rare HMEC grown in serum-free MCDB170 medium, presented an unusual situation that has facilitated distinguishing p53 input at the senescence barriers. It also permitted long-term growth of cultured finite lifespan HMEC (30–70 PD). These post-selection HMEC have been widely utilized, however we note that they have overcome the stasis barrier, and may possess significantly different properties and gene expression compared to prestasis HMEC derived from normal cells in vivo.[58-61]

Although p53 inactivation is not necessary to overcome stasis in HMEC, most studies with human cells have utilized agents that inactivate p53 to overcome a first proliferation barrier. Consequently, only crisis was observed at the telomere-length dependent senescence barrier in the p53(-) populations.[53,62] Since cells at agonescence are largely viable, SA-β-Gal(+), and express a senescent morphology, in the absence of additional molecular characterization, this telomere-length-dependent barrier may be equated with the viable stasis barrier. The assumption that HMEC at agonescence reflect M1/senescence led to the renaming of the earlier HMEC proliferation barrier, selection/stasis, as "M0";[41] however, our model and data indicate that no molecularly distinct "M0" exists. Rather we propose that agonescence, like M2/crisis, reflects a telomere dysfunction barrier, while stasis is similar to what has been called M1/senescence.

HMEC arrested at stasis are characterized by normal karyotypes, a low LI, viable arrest in G_1, elevated p16 levels, and a mean TRF >5 kb.[20,21,23] The cells also express SA-β-Gal, and have a senescent morphology. This molecular profile resembles what in many cultured cells has been called senescence, replicative senescence, or M1.[63] However, cellular diversity in stress responses, such as differences in sensitivity to oxidative stress-induced DNA damage, could generate variability in the phenotype seen at stasis. We suggest that what has been called stress-associated senescence due to "culture shock" also represents stasis; the greater the stress-inducing signals, the fewer PD prior to stasis. We have seen that the PD potential of cultured primary HMEC can vary from 15–60 PD, prior to a p16-associated arrest, depending upon culture conditions (Garbe et al., in preparation). An age-related increase in p16 expression is also reported for human breast, kidney, and pancreas tissues,[64-66] as well as rodent tissues,[67] suggesting that stress-induced responses may occur in vivo.

Cultured human fibroblasts commonly proliferate for more PD than epithelial cells before encountering a senescence barrier. The molecular profile of most fibroblasts called senescent contains properties more similar to those defining HMEC stasis than agonescence,[63] and overcoming this barrier by inactivation of p16/RB and p21/p53 function leads to crisis.[15,56] Some fibroblasts strains, particularly those with reduced p16 expression such as BJ, may display >80 PD in culture, and cells in such populations could encounter agonescence prior to stasis. Unlike most fibroblast strains, BJ populations at proliferative arrest exhibit karyotypic abnormalities in a minority of the cells; however most cells did not exhibit telomeric end-associations.[68] This is distinct from HMEC at agonescence, where virtually all cells showed gross chromosomal abnormalities and telomere associations,[21] indicating that at least for HMEC, telomere dysfunction does not produce a p53-mediated senescence arrest prior to the formation of gross chromosomal aberrations.

To have terminology tied to specific molecular criteria, we propose the model shown in Figure 6. The non telomere-length dependent, stress-associated senescence barrier is called stasis,[1,69] while the telomere-length dependent senescence barrier is referred to as either agonescence (when p53 is functional),[24] or crisis (when p53-dependent functions are absent). Stasis is characterized by elevated

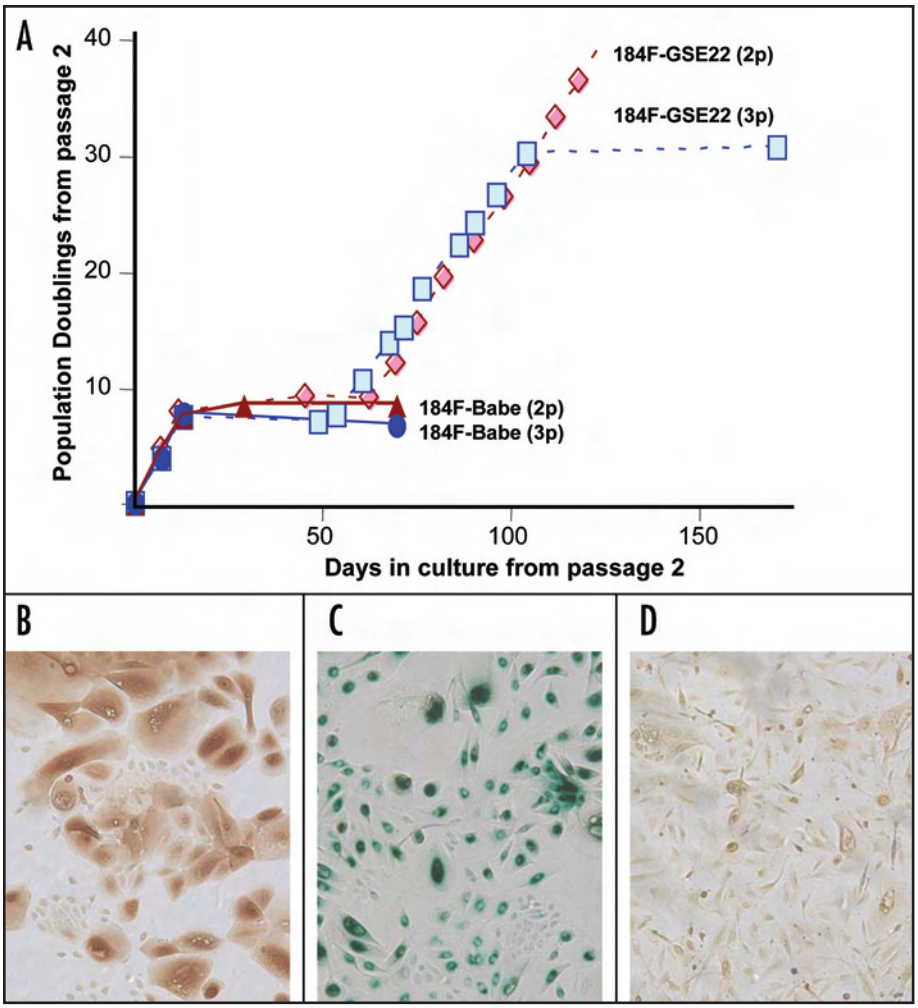

Figure 5. Transduction of GSE22 into prestasis 184F HMEC does not overcome stasis. 184F HMEC were transduced at passage 2 (2p) or 3 (3p) with GSE22 or control (Babe) vector, and proliferative potential determined. (A) All populations showed cessation of most growth by passage 5, however rare colonies appeared in the GSE22-transduced cultures that maintained growth until either a crisis-like arrest (184F-GSE22 3p) or emergence of an immortal line (184F-GSE22 2p). (B) 184F-GSE22 cells at passage 5 with a senescent morphology are p16(+) and (C) SA-β-Gal(+). (D) 184F-GSE22 (3p) shows weak staining for p16 at 9p.

levels of the CKIs p16 and/or p21, a low LI, G_1 arrest, and largely normal karyotypes; it can also be readily overcome by multiple types of errors that inactivate an Rb-mediated barrier. Agonescence is characterized by a moderate LI, mostly viable arrest at all phases of the cell cycle with some cell death, critically shortened telomeres, and widespread karyotypic abnormalities. Crisis is characterized by a high LI, widespread karyotypic abnormalities, and eventual massive cell death. The properties associated with Raf-1 induced OIS in HMEC differ from what is seen for stasis or telomere dysfunction.[7] Generic usage of the term "senescence" to refer to both telomere length-independent stasis, and barriers due to telomere dysfunction, may obscure distinctions important for understanding human cellular aging, immortalization, and carcinogenesis. For example, cultured rodent cells, which readily spontaneously immortalize, lack stringent repression of telomerase activity and may contain long telomeres.[70] What has been called senescence in rodent cells may most closely resemble Rb-mediated non telomere-length dependent stasis. Senescence in mouse embryo fibroblasts can be reversed by inactivation of RB, even in the presence of functional p53.[71]

In contrast, in long-lived organisms such as humans, stringent telomerase repression eventually leads to telomere erosion and the telomere dysfunction senescence barrier, even in cells that have overcome stasis. The genomic instability induced by telomere dysfunction is not readily reversible, and overcoming this barrier by reactivation of telomerase requires rare errors.[2] Unlike rodent cells, spontaneous transformation to immortality of human cells cultured from normal tissues is virtually nonexistent. Thus the senescence barrier responsible for enforcing stringent mortality in cultured human cells is telomere length dependent. Given the importance of senescence barriers as tumor suppressor mechanisms, as well as the potential clinical utility of markers of senescence,[14,16] use of molecularly defined nomenclature for senescence barriers may facilitate our understanding of and therapeutic approaches to human carcinogenesis.

Acknowledgements

We thank Gerri Levine for excellent technical assistance, Kathy Bjornstad and Ellie Blakely for assistance with microscopy, and Drs. Andrei Gudkov, Peter Chumakov, Christian Beausejour and Judy Campisi for reagents. This work was supported by NIH grant CA24844, Department of Defense BCRP grant W81XWH-04-1-0580 (M.R.S., J.G.), the Office of Energy Research, Office of Health and Biological Research, U.S. Department of Energy under Contract No. DE-AC03-76SF00098 (M.R.S.), NIH grant CA73952 (T.T.), Howard Hughes Medical Institute Pre-Doctoral fellowship (C.H.), and Ruth L. Kirschstein National Research Service Award Individual Fellowship CA108480-03 (EB).

References

1. Drayton S, Peters G. Immortalisation and transformation revisited. Curr Op Gen Dev 2002; 12:98-104.
2. Stampfer MR, Yaswen P. Human epithelial cell immortalization as a step in carcinogenesis. Cancer Lett 2003; 194:199-208.
3. Ben-Porath I, Weinberg RA. When cells get stressed: An integrative view of cellular senescence. J Clin Invest 2004; 113:8-13.
4. Campisi J. Senescent cells, tumor suppression, and organismal aging: Good citizens, bad neighbors. Cell 2005; 120:513-22.
5. Kim WY, Sharpless NE. The regulation of ink4/arf in cancer and aging. Cell 2006; 127:265-75.
6. Serrano M, Lin AW, McCurrach ME, Beach D, Lowe SW. Oncogenic *ras* provokes premature cell senescence associated with accumulation of *p53* and *p16^{ink4a}*. Cell 1997; 88:593-602.
7. Olsen CL, Gardie B, Yaswen P, Stampfer MR. *Raf-1*-induced growth arrest in human mammary epithelial cells is p16-independent and is overcome in immortal cells during conversion. Oncogene 2002; 21:6328-39.
8. Courtois-Cox S, Genther Williams SM, Reczek EE, Johnson BW, McGillicuddy LT, Johannessen CM, Hollstein PE, MacCollin M, Cichowski K. A negative feedback signaling network underlies oncogene-induced senescence. Cancer Cell 2006; 10:459-72.
9. Bartkova J, Rezaei N, Liontos M, Karakaidos P, Kletsas D, Issaeva N, Vassiliou LV, Kolettas E, Niforou K, Zoumpourlis VC, Takaoka M, Nakagawa H, Tort F, Fugger K, Johansson F, Sehested M, Andersen CL, Dyrskjot L, Orntoft T, Lukas J, Kittas C, Helleday T, Halazonetis TD, Bartek J, Gorgoulis VG. Oncogene-induced senescence is part of the tumorigenesis barrier imposed by DNA damage checkpoints. Nature 2006; 444:633-7.

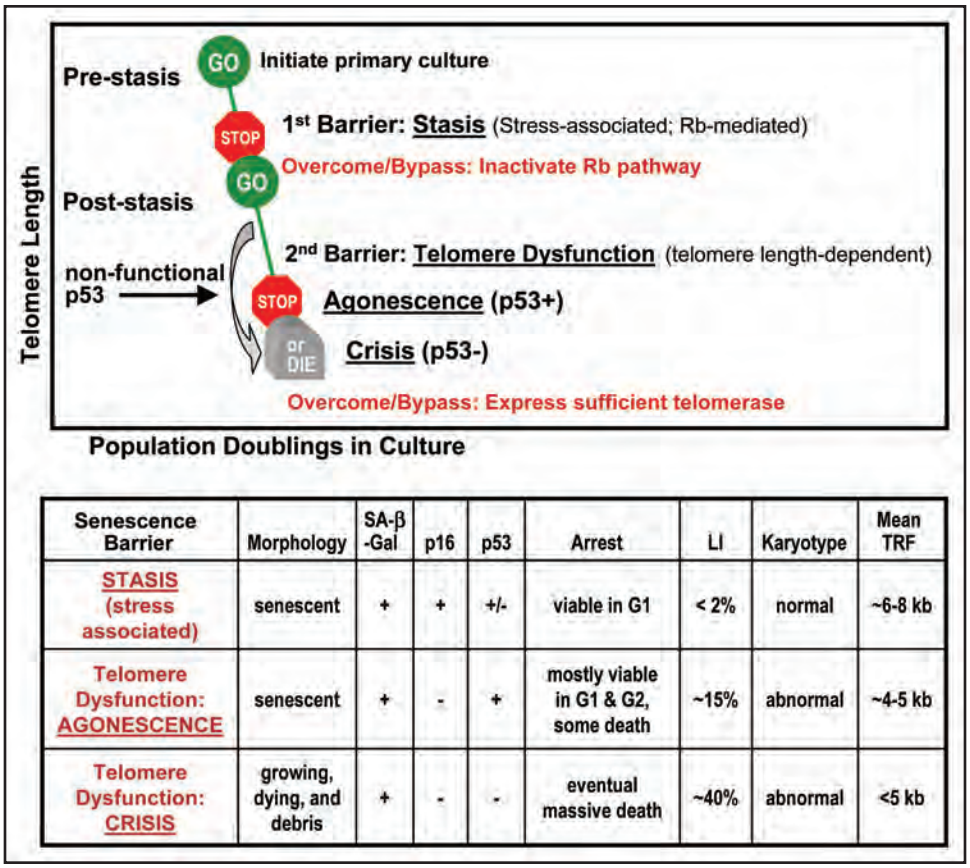

Senescence Barrier	Morphology	SA-β -Gal	p16	p53	Arrest	LI	Karyotype	Mean TRF
STASIS (stress associated)	senescent	+	+	+/-	viable in G1	< 2%	normal	~6-8 kb
Telomere Dysfunction: AGONESCENCE	senescent	+	-	+	mostly viable in G1 & G2, some death	~15%	abnormal	~4-5 kb
Telomere Dysfunction: CRISIS	growing, dying, and debris	+	-	-	eventual massive death	~40%	abnormal	<5 kb

Figure 6. Molecularly defined model for senescence barriers in cultured HMEC. This model postulates at least two mechanistically distinct barriers to indefinite proliferation in cultured HMEC. The non telomere-length dependent stasis barrier is enforced by the CKI p16. In other cell types, p53-dependent p21 expression may also enforce Rb-mediated stasis. p53-inducing stresses cells could produce distinct phenotypes from what is seen in the cultured HMEC at stasis. HMEC in vivo, or in response to DNA-damaging stresses in vitro such as radiation, might also employ p53-dependent p21 to enforce stasis. Multiple types of errors that can inactivate a stress-induced Rb-mediated barrier can overcome stasis. Many such errors (e.g., p16 silencing/mutation, RB and p53 mutations/inactivation, cyclin D1 or cdk4 overexpression) are found in early stage human carcinoma development, and could give rise to clonal hyperplastic outgrowths. The phenotype of the telomere dysfunction barrier depends upon whether or not p53 is functional. We have postulated that overcoming the telomere dysfunction barrier is an extremely rare event because it requires multiple errors to reactivate telomerase.[2] HMEC nearing arrest from telomere dysfunction have some properties similar to premalignant lesions such as DCIS, e.g., very short telomeres and genomic instability; reactivation of telomerase activity can also be detected in DCIS tissues. The phenotype of HMEC subjected to OIS is distinct from both stasis and agonescence, e.g., unlike some other cell types, there is no requirement for either p16 or p53 function for OIS in HMEC, arrest is at all phases of the cell cycle, and telomeres are not critically shortened.[7]

10. Wright WE, Pereira-Smith OM, Shay JW. Reversible cellular senescence: Implications for immortalization of normal human diploid fibroblasts. Mol Cell Biol 1989; 9:3088-92.
11. Shay JW, Wright WE, Werbin H. Toward a molecular understanding of human breast cancer: A hypothesis. Breast Can Res and Treat 1993; 25:83-94.
12. Wright WE, Shay JW. Time, telomeres and tumors: Is cellular senescence more than an anticancer mechanism. Trends Cell Biol 1995; 5:293-7.
13. Rheinwald JG, Hahn WC, Ramsey MR, Wu JY, Guo Z, Tsao H, De Luca M, Catricala C, O'Toole KM. A two-stage, p16^{ink4a}-and p53-dependent keratinocyte senescence mechanism that limits replicative potential independent of telomere status. Mol Cell Biol 2002; 22:5157-72.
14. Collado M, Serrano M. The power and the promise of oncogene-induced senescence markers. Nat Rev Cancer 2006; 6:472-6.
15. Brookes S, Rowe J, Gutierrez Del Arroyo A, Bond J, Peters G. Contribution of p16(ink4a) to replicative senescence of human fibroblasts. Exp Cell Res 2004; 298:549-59.
16. Braig M, Schmitt CA. Oncogene-induced senescence: Putting the brakes on tumor development. Cancer Res 2006; 66:2881-4.
17. Jones CJ, Kipling D, Morris M, Hepburn P, Skinner J, Bounacer A, Wyllie FS, Ivan M, Bartek J, Wynford-Thomas D, Bond JA. Evidence for a telomere-independent "clock" limiting ras oncogene-driven proliferation of human thyroid epithelial cells. Mol Cell Biol 2000; 20:5690-9.
18. Stampfer MR. Cholera toxin stimulation of human mammary epithelial cells in culture. In Vitro 1982; 18:531-7.
19. Hammond SL, Ham RG, Stampfer MR. Serum-free growth of human mammary epithelial cells: Rapid clonal growth in defined medium and extended serial passage with pituitary extract. Proc Natl Acad Sci USA 1984; 81:5435-9.
20. Garbe J, Wong M, Wigington D, Yaswen P, Stampfer MR. Viral oncogenes accelerate conversion to immortality of cultured human mammary epithelial cells. Oncogene 1999; 18:2169-80.
21. Romanov S, Kozakiewicz K, Holst C, Stampfer MR, Haupt LM, Tlsty T. Normal human mammary epithelial cells spontaneously escape senescence and acquire genomic changes. Nature 2001; 409:633-7.
22. Holst CR, Nuovo GJ, Esteller M, Chew K, Baylin SB, Herman JG, Tlsty TD. Methylation of p16(ink4a) promoters occurs in vivo in histologically normal human mammary epithelia. Cancer Res 2003; 63:1596-601.
23. Brenner AJ, Stampfer MR, Aldaz CM. Increased p16ink4a expression with onset of senescence of human mammary epithelial cells and extended growth capacity with inactivation. Oncogene 1998; 17:199-205.
24. Tlsty TD, Romanov SR, Kozakiewicz BK, Holst CR, Haupt LM, Crawford YG. Loss of chromosomal integrity in human mammary epithelial cells subsequent to escape from senescence. J Mammary Gland Biol Neoplasia 2001; 6:235-43.
25. Stampfer MR. Isolation and growth of human mammary epithelial cells. J Tissue Culture Methods 1985; 9:107-16.
26. Stampfer M, Yaswen P. Culture systems for study of human mammary epithelial cell proliferation, differentiation and transformation. Cancer Surveys 1994; 18:7-34.

27. Stampfer MR, Pan CH, Hosoda J, Bartholomew J, Mendelsohn J, Yaswen P. Blockage of EGF receptor signal transduction causes reversible arrest of normal and transformed human mammary epithelial cells with synchronous reentry into the cell cycle. Exp Cell Res 1993; 208:175-88.
28. Stampfer M, Garbe J, Levine G, Lichsteiner S, Vasserot A, Yaswen P. Expression of the telomerase catalytic subunit, hTERT, induces resistance to transforming growth factor β growth inhibition in $p16^{ink4}$ (-) human mammary epithelial cells. Proc Natl Acad Sci USA 2001; 98:4498-503.
29. Dimri GP, Lee X, Basile G, Roskelley C, Medrano EE, Rubelji I, Pereira-Smith OM, Peacocke M, Campisi J. A novel biomarker identifies senescent human cells in culture and in aging skin in vivo. Proc Natl Acad Sci USA 1995; 92:9363-7.
30. Ossovskaya VS, Mazo IA, Chernov MV, Chernova OB, Strezoska Z, Kondratov R, Stark GR, Chumakov PM, Gudkov AV. Use of genetic suppressor elements to dissect distinct biological effects of separate p53 domains. Proc Natl Acad Sci USA 1996; 93:10309-14.
31. Finer MH, Dull TJ, Qin L, Farson D, Roberts MR. *Kat*: A high-efficiency retroviral transduction system for primary human T lymphocytes. Blood 1994; 83:43-50.
32. Dull T, Zufferey R, Kelly M, Mandel RJ, Nguyen M, Trono D, Naldini L. A third-generation lentivirus vector with a conditional packaging system. J Virol 1998; 72:8463-71.
33. Naldini L, Blomer U, Gallay P, Ory D, Mulligan R, Gage FH, Verma IM, Trono D. In vivo gene delivery and stable transduction of nondividing cells by a lentiviral vector. Science 1996; 272:263-7.
34. Bodnar AG, Kim NW, Effros RB, Chiu CP. Mechanism of telomerase induction during T cell activation. Exp Cell Res 1996; 228:58-64.
35. Stampfer MR, Garbe J, Nijjar T, Wigington D, Swisshelm K, Yaswen P. Loss of p53 function accelerates acquisition of telomerase activity in indefinite lifespan human mammary epithelial cell lines. Oncogene 2003; 22:5238-51.
36. Lehman T, Modali R, Boukamp P, Stanek J, Bennett W, Welsh J, Metcalf R, Stampfer M, Fusenig N, Rogan E, Reddel R, Harris C. *P53* mutations in human immortalized epithelial cell lines. Carcinogenesis 1993; 14:833-9.
37. Wei W, Sedivy JM. Differentiation between senescence (M1) and crisis (M2) in human fibroblast cultures. Exp Cell Res 1999; 253:519-22.
38. Beausejour CM, Krtolica A, Galimi F, Narita M, Lowe SW, Yaswen P, Campisi J. Reversal of human cellular senescence: Roles of the p53 and p16 pathways. EMBO J 2003; 22:4212-22.
39. d'Adda di Fagagna F, Reaper PM, Clay-Farrace L, Fiegler H, Carr P, Von Zglinicki T, Saretzki G, Carter NP, Jackson SP. A DNA damage checkpoint response in telomere-initiated senescence. Nature 2003; 426:194-8.
40. Evans RJ, Wyllie FS, Wynford-Thomas D, Kipling D, Jones CJ. A p53-dependent, telomere-independent proliferative life span barrier in human astrocytes consistent with the molecular genetics of glioma development. Cancer Res 2003; 63:4854-61.
41. Foster SA, Galloway DA. Human papillomavirus type 16 E7 alleviates a proliferative block in early passage human mammary epithelial cells. Oncogene 1996; 12:1773-9.
42. Bond JA, Haughton MF, Rowson JM, Smith PJ, Gire V, Wynford-Thomas D, Wyllie FS. Control of replicative life span in human cells: Barriers to clonal expansion intermediate between M1 senescence and M2 crisis. Mol Cell Biol 1999; 19:3103-14.
43. Sherr CJ, DePinho RA. Cellular senescence: Mitotic clock or culture shock? Cell 2000; 102:407-10.
44. Serrano M, Blasco MA. Putting the stress on senescence. Cur Opinion Cell Bio 2001; 13:748-53.
45. Maser RS, DePinho RA. Connecting chromosomes, crisis, and cancer. Science 2002; 297:565-9.
46. Cosme-Blanco W, Shen MF, Lazar AJ, Pathak S, Lozano G, Multani AS, Chang S. Telomere dysfunction suppresses spontaneous tumorigenesis in vivo by initiating p53-dependent cellular senescence. EMBO Rep 2007; 8:497-503.
47. Feldser DM, Greider CW. Short telomeres limit tumor progression in vivo by inducing senescence. Cancer Cell 2007.
48. Goldstein JC, Rodier F, Garbe JC, Stampfer MR, Campisi J. Caspase-independent cytochrome c release is a sensitive measure of low-level apoptosis in cell culture models. Aging Cell 2005; 4:217-22.
49. Gao Q, Hauser SH, Liu XL, Wazer DE, Madoc-Jones H, Band V. Mutant *p53*-induced immortalization of primary human mammary epithelial cells. Cancer Res 1996; 56:3129-33.
50. Gollahon LS, Shay JW. Immortalization of human mammary epithelial cells transfected with mutant *p53 (273^{bis})*. Oncogene 1996; 12:715-25.
51. Kiyono T, Foster SA, Koop JJ, McDougall JK, Galloway DA, Klingelhutz AJ. Both Rb/$p16^{ink4a}$ inactivation and telomerase activity are required to immortalize human epithelial cell. Nature 1998; 396:84-8.
52. Dickson MA, Hahn WC, Ino Y, Ronfard V, Wu JY, Weinberg RA, Louis DN, Li FP, Rheinwald JG. Human keratinocytes that expess hTERT and also bypass a $p16^{ink4a}$-enforced mechanism that limits lifespan become immortal yet retain normal growth and differentiation characteristics. Mol Cell Biol 2000; 20:1436-47.
53. Wazer DE, Liu XL, Chu Q, Gao Q, Band V. Immortalization of distinct human mammary epithelial cell types by human papilloma virus 16 E6 or E7. Proc Nat Acad Sci USA 1995; 92:3687-91.
54. Shay JW, Pereira-Smith OM, Wright WE. A role for both Rb and p53 in the regulation of human cellular senescence. Exp Cell Res 1991; 196:33-9.
55. Amundson SA, Do KT, Vinikoor L, Koch-Paiz CA, Bittner ML, Trent JM, Meltzer P, Fornace Jr AJ. Stress-specific signatures: Expression profiling of p53 wild-type and -null human cells. Oncogene 2005; 24:4572-9.
56. Brown JP, Wei W, Sedivy JM. Bypass of senescence after disruption of *p21cip1/waf1* gene in normal diploid human fibroblasts. Science 1997; 277:831-4.
57. Wei W, Herbig U, Wei S, Dutriaux A, Sedivy JM. Loss of retinoblastoma but not p16 function allows bypass of replicative senescence in human fibroblasts. EMBO Rep 2003; 4:1061-6.
58. Crawford YG, Gauthier ML, Joubel A, Mantei K, Kozakiewicz K, Afshari CA, Tlsty TD. Histologically normal human mammary epithelia with silenced p16(ink4a) overexpress cox-2, promoting a premalignant program. Cancer Cell 2004; 5:263-73.
59. McDermott KM, Zhang J, Holst CR, Kozakiewicz BK, Singla V, Tlsty TD. P16(ink4a) prevents centrosome dysfunction and genomic instability in primary cells. PLoS Biol 2006; 4:e51.
60. Li Y, Pan J, Li JL, Lee JH, Tunkey C, Saraf K, Garbe JC, Whitley MZ, Jelinsky SA, Stampfer MR, Haney SA. Transcriptional changes associated with breast cancer occur as normal human mammary epithelial cells overcome senescence barriers and become immortalized. Mol Cancer 2007; 6:7.
61. Zhang J, Pickering CR, Holst CR, Gauthier ML, Tlsty TD. P16ink4a modulates p53 in primary human mammary epithelial cells. Cancer Res 2006; 66:10325-31.
62. Shay JW, Wright WE, Brasiskyte D, Van Der Haegen BA. E6 of human papillomavirus type 16 can overcome the M1 stage of immortalization in human mammary epithelial cells but not in human fibroblasts. Oncogene 1993; 8:1407-13.
63. Li GZ, Eller MS, Firoozabadi R, Gilchrest BA. Evidence that exposure of the telomere 3' overhang sequence induces senescence. Proc Natl Acad Sci USA 2003; 100:527-31.
64. Nielsen GP, Stemmer-Rachamimov AO, Shaw J, Roy JE, Koh J, Louis DN. Immunohistochemical survey of $p16^{ink4a}$ expression in normal human adult and infant tissues. Lab Invest 1999; 79:1137-43.
65. Melk A, Schmidt BM, Takeuchi O, Sawitzki B, Rayner DC, Halloran PF. Expression of p16ink4a and other cell cycle regulator and senescence associated genes in aging human kidney. Kidney Int 2004; 65:510-20.
66. Krishnamurthy J, Ramsey MR, Ligon KL, Torrice C, Koh A, Bonner-Weir S, Sharpless NE. P16ink4a induces an age-dependent decline in islet regenerative potential. Nature 2006; 443:453-7.
67. Krishnamurthy J, Torrice C, Ramsey MR, Kovalev GI, Al-Regaiey K, Su L, Sharpless NE. Ink4a/arf expression is a biomarker of aging. J Clin Invest 2004; 114:1299-307.
68. Zou Y, Sfeir A, Gryaznov SM, Shay JW, Wright WE. Does a sentinel or a subset of short telomeres determine replicative senescence? Mol Biol Cell 2004; 15:3709-18.
69. Wright WE, Shay JW. Historical claims and current interpretations of replicative aging. Nat Biotech 2002; 20:682-8.
70. Prowse KR, Greider CW. Developmental and tissue-specific regulation of mouse telomerase and telomere length. Proc Natl Acad Sci USA 1995; 92:4818-22.
71. Sage J, Miller AL, Perez-Mancera PA, Wysocki JM, Jacks T. Acute mutation of retinoblastoma gene function is sufficient for cell cycle reentry. Nature 2003; 424:223-8.

Molecular Cancer

BioMed Central

Research

Open Access

Transcriptional changes associated with breast cancer occur as normal human mammary epithelial cells overcome senescence barriers and become immortalized

Yizheng Li[1], Jing Pan[2], Jian-Liang Li[1], Jee Hyung Lee[2], Chris Tunkey[3], Katie Saraf[3], James C Garbe[4], Maryann Z Whitley[1], Scott A Jelinsky[3], Martha R Stampfer[4] and Steven A Haney*[2]

Address: [1]Section of Bioinformatics, Department of Biological Technologies, Wyeth Research, 87 Cambridge Park Drive, Cambridge, MA 02140, USA, [2]Applied Genomics, Department of Biological Technologies, Wyeth Research, 87 Cambridge Park Drive, Cambridge, MA 02140, USA, [3]Molecular Profiling and Biomarker Discovery, Department of Biological Technologies, Wyeth Research, 87 Cambridge Park Drive, Cambridge, MA 02140, USA and [4]Life Sciences Division, Lawrence Berkeley National Laboratory, Berkeley, CA 94720, USA

Email: Yizheng Li - yli@wyeth.com; Jing Pan - jpan@wyeth.com; Jian-Liang Li - jlli@wyeth.com; Jee Hyung Lee - jeehyung.lee@novartis.com; Chris Tunkey - ctunkey@crtx.com; Katie Saraf - ksaraf@wyeth.com; James C Garbe - jcgarbe@lbl.gov; Maryann Z Whitley - mwhitley@wyeth.com; Scott A Jelinsky - sjelinsky@wyeth.com; Martha R Stampfer - mrstampfer@lbl.gov; Steven A Haney* - shaney@wyeth.com

* Corresponding author

Published: 18 January 2007

Molecular Cancer 2007, **6**:7 doi:10.1186/1476-4598-6-7

Received: 11 December 2006
Accepted: 18 January 2007

This article is available from: http://www.molecular-cancer.com/content/6/1/7

Abstract

Background: Human mammary epithelial cells (HMEC) overcome two well-characterized genetic and epigenetic barriers as they progress from primary cells to fully immortalized cell lines *in vitro*. Finite lifespan HMEC overcome an Rb-mediated stress-associated senescence barrier (stasis), and a stringent, telomere-length dependent, barrier (agonescence or crisis, depending on p53 status). HMEC that have overcome the second senescence barrier are immortalized.

Methods: We have characterized pre-stasis, post-selection (post-stasis, with p16 silenced), and fully immortalized HMEC by transcription profiling and RT-PCR. Four pre-stasis and seven post-selection HMEC samples, along with 10 representatives of fully immortalized breast epithelial cell lines, were profiled using Affymetrix U133A/B chips and compared using both supervised and unsupervised clustering. Datasets were validated by RT-PCR for a select set of genes. Quantitative immunofluorescence was used to assess changes in transcriptional regulators associated with the gene expression changes.

Results: The most dramatic and uniform changes we observed were in a set of about 30 genes that are characterized as a "cancer proliferation cluster," which includes genes expressed during mitosis (*CDC2*, *CDC25*, *MCM2*, *PLK1*) and following DNA damage. The increased expression of these genes was particularly concordant in the fully immortalized lines. Additional changes were observed in IFN-regulated genes in some post-selection and fully immortalized cultures. Nuclear localization was observed for several transcriptional regulators associated with expression of these genes in post-selection and immortalized HMEC, including Rb, Myc, BRCA1, HDAC3 and SP1.

Conclusion: Gene expression profiles and cytological changes in related transcriptional regulators indicate that immortalized HMEC resemble non-invasive breast cancers, such as ductal and lobular carcinomas *in situ*, and are strikingly distinct from finite-lifespan HMEC, particularly with regard to genes involved in proliferation, cell cycle regulation, chromosome structure and the DNA damage response. The comparison of HMEC profiles with lines harboring oncogenic changes (e.g. overexpression of Her-2^{neu}, loss of p53 expression) identifies genes involved in tissue remodeling as well as proinflamatory cytokines and S100 proteins. Studies on carcinogenesis using immortalized cell lines as starting points or "normal" controls need to account for the significant pre-existing genetic and epigenetic changes inherent in such lines before results can be broadly interpreted.

Background

Genetic and epigenetic changes that occur early in the process of carcinogenesis may enable the survival and growth of cells that subsequently acquire oncogenic mutations. One early alteration in the development of human carcinomas is the acquisition of an immortal potential, associated with reactivation of endogenous *hTERT* expression and maintenance of stable telomere lengths. [1]. We have employed an *in vitro* HMEC model system to examine gene expression changes during the process of transformation of normal finite cells to immortality and malignancy [2-11]. Two mechanistically distinct barriers to unlimited proliferation have been described. The first barrier, stasis (stress-associated senescence) is associated with elevated levels of the cyclin-dependent kinase inhibitor (CKI) $p16^{INK4A}$ [6]. Stasis appears to be Rb-mediated and not directly dependent on telomere length. Cells arrested at this barrier exhibit a viable G1 arrest with a low labeling index (LI), normal karyotypes, expression of senescence -associated ß-galactosidase (SA-ß-gal) activity, and a senescent morphology [7,12]. HMEC can undergo a variable number of population doublings (PD), depending upon culture conditions, prior to encountering stasis.

Multiple types of single changes that prevent Rb-mediated growth inhibition will overcome stasis. Loss of *CDKN2A* (encoding $p16^{ink4a}$) expression, from methylation-induced *CDKN2A* promoter silencing, or mutations, is one alteration frequently observed in human breast cancers and cultured HMEC [6,13,14]. HMEC cultured in a serum-free medium can produce rare cells that spontaneously silence the p16 promoter and resume growth, a process termed selection, with the resulting post-stasis population called post-selection [3]. In the HMEC, no increase in p53, p21, or $p14^{ARF}$ levels have been seen at stasis [7] and p53 function is not required for the stasis barrier (J.G. and M.S., unpublished). Rare HMEC with silenced p16 are also observed in vivo and have been called variant HMEC (vHMEC) [15,16].

HMEC that have overcome or bypassed stasis encounter a second barrier as a consequence of telomere dysfunction. Ongoing proliferation in the absence of telomerase expression leads to critically shortened telomeres, and chromosomal aberrations [7,17]. In post-selection HMEC with functional p53, these aberrations induce a mostly viable G1 and G2 arrest (termed agonescence); if p53 is non-functional, massive cell death (crisis) ensues (J.G. and M.S., unpublished) [18]. Telomere dysfunction poses an extremely stringent barrier to human cellular immortalization; in post-selection HMEC multiple errors appear to be necessary for telomerase reactivation, and immortalization [4,8]. Since this barrier is dependent upon telomere length, ectopic overexpression of hTERT readily immortalizes post-selection HMEC [19]. HMEC can be immortalized using several different pathologically relevant agents, e.g., chemical carcinogens, over-expression of the breast cancer-associated oncogenes *c-myc* and/or *ZNF217*, and/or inactivation of p53 function [8,9,11]. Fully immortal HMEC maintain telomeres at short, stable lengths, but do not necessarily express malignancy-associated properties; overexpression of specific oncogenes can confer malignant properties [20-22].

Transcriptional profiling has proven to be a valuable technology for describing the differences between cell types and experimental treatments for many disease models, particularly cancer [23]. One of the most well-developed stratifications of human cancers has been for breast cancer [24,25]. These and other studies have shown that a common set of genes is consistently overexpressed in most cancers [26], including many cell cycle regulated genes and genes required for mitosis (e.g. *MKI67*, *PCNA*, *BIRC5*, *MYBL2*, *TOP2A*, *PLK1*, *MCM2-MCM6*, *CDC20*). The frequent identification of these genes in cancer cells suggests that they represent a common characteristic of cancers, irrespective of the cell type from which the cancers originate.

The data described here examines the changes that occur as HMEC overcome the barriers to indefinite proliferation. We show that pre-stasis and post-selection HMEC are profoundly different from fully immortalized HMEC lines, despite the fact that the immortalized lines may retain normal growth factor requirements, lack anchorage-independent growth or invasiveness, and are not tumorigenic in animal models [4]. Rather, the non-malignant immortalized lines display the cancer-associated proliferation cluster of genes frequently identified in transcriptional profiling studies of cancer cells and tissues [26].

Materials and methods

Reagents and supplies

MEBM serum-free medium was purchased from the Clonetics division of Cambrex BioScience (Walkersville, MD), and was supplemented with EGF, hydrocortisone, insulin, and BPE using Singlequot reagent packs from Clonetics, as well as 5 μg/ml transferrin (Clonetics) and 10 nM isopeterenol (Sigma). Hams F-12/DMEM (50:50) was purchased from Invitrogen or prepared by Core Technical Services (Wyeth Research), and supplemented to contain 5% FBS (Invitrogen), 2 mM pyruvate (Invitrogen), 2 mM glutamine (Invitrogen), 20 ng/ml EGF (Clonetics), 200 μg/ml cholera toxin (Sigma), 1× ITS (Clonetics), 500 ng/ml hydrocortisone (Sigma or Clonetics), and 20 mg/ml gentamycin (Invitrogen). MM medium was prepared as described [2]. Antibodies and fluorescent dyes used in High Content Screening (HCS, or quantitiative immunofluorescence) were obtained from Cell Signaling Technologies (Beverly, MA), Upstate Bio-

technologies (Lake Placid, NY), and Molecular Probes/ Invitrogen (Carlsbad, CA), as described in the supplementary material. Antibodies were screened by Western blot prior to immunofluorescence studies to verify that they recognize a single specific antigen of the expected molecular size.

Cell culture

Pre-stasis and post-selection HMEC, from specimens 48, 161, 184, 191, 195 and 239, as well as the immortally transformed lines 184A1, 184AA2, 184AA3, 184B5 were developed and characterized at LBNL, starting with reduction mammoplasty tissues; an additional post-selection HMEC strain was obtained from Clonetics. Remaining lines, as well as additional samples of 184A1 and 184B5 were obtained from ATCC (Manassas, VA). 184B5ME was derived from immortal 184B5 following stable expression of *ERBB2/Her2* and selection for anchorage independent growth (Stampfer, unpublished). Pre-stasis cells were maintained in MM media [2], and post-selection cells were maintained in MEBM prior to this study. Pre-stasis HMEC display 15–25 PD in MM, and 10–15 PD in MEBM, prior to growth arrest at stasis. For transcriptional profiling studies, all lines maintained at LBNL (listed above), as well as the post-selection HMEC purchased from Clonetics, were revived in MEBM media and cultured at 37°C with 1% CO_2. Consequently, the pre-stasis HMEC were studied as they neared stasis. Pre-stasis HMEC used in HCS were cultured in MM medium. Fully immortalized cell lines obtained from ATCC (184A1, 184B5, MCF10A, MCF10A-2 and MCF12A) were cultured in DMEM/Ham's F-12 medium, at 37°C with 10% CO_2, as they were maintained prior to crypreservation.

RNA labeling, GeneChip hybridizations and expression analysis

Cells to be prepared for RNA extraction were revived from cryopreservation and cultured to 80% confluence in a single T-75 flask, trypsinized under conditions appropriate for each line, and split 1:4 into four new T-75 flasks. When cells reached 80% confluence three of the flasks were trypsinized, lysed and total RNA isolated using the Midiprep RNA isolation kit from Qiagen, according to manufacturers instructions.

An 11-point standard curve of bacterial cRNA control samples was added prior to hybridization as described [27,28]. Three independent replicates were generated per cell type at the indicated stage. Affymetrix's MAS5 algorithm was used to generate expression measures including Signal values and Absent/Present calls (Affymetrix (2001) *Microarray Suite User Guide*, Version 5. [29]. A global scaling normalization was applied to the raw signal intensity. Briefly, a 2% trimmed-mean was calculated per chip, and was scaled to an arbitrary value of 100. A scaled Signal value was then computed for each gene by multiplying its original Signal intensity with the scale factor (100/ trimmed-mean). Subsequently, genes were filtered to remove those with uninformative or noisy expression changes across the entire samples. A gene is selected for downstream analysis if its expression exceeds 50 (scaled) Signal unit in at least one sample. Analysis of variance (ANOVA) was performed with log2 transformation on the scaled Signals of several cell lineage groups (see details below). Data was analyzed using several analytical approaches, including unsupervised clustering [30], supervised clustering [31,32], and principal components analysis. For the unsupervised clustering, genes that are filtered based on the Pvalues from one-way analysis of variance (ANOVA) on four cell lineage groups as well as greater than 2 fold difference among the four groups. These groups consist of 1) all finite lifespan cells, 2) $p53^{+/+}$ immortalized 184A1 and 184B5, 3) $p53^{-/-}$ immortalized 184AA2 and 184AA3, and 4) immortalized non-184 derived cells (including MCF10A, MCF10A-2, and MCF12A).

Promoter analysis

Genes identified as unique classes in a subset of post-selection HMEC were examined in detail (see Results for a complete list of genes). Initially, the 500 bp upstream of the transcription start site for each gene was examined for well-characterized transcription binding sites using two algorithms, Match and Clover [33,34]. For most of the groups, strong assignments of specific promoter binding sites could be identified using both algorithms. One class (Class B in the Results) was less definitive, so the region was extended to 2 kb prior to the transcription start site for those genes.

Taqman™ quantitative PCR

Primer sets for 15 genes analyzed by Taqman™ analysis were obtained from Applied Biosystems (Foster City, CA) and used according to standard protocols. Genes tested are listed in the Results section.

High content screening

Cells were seeded at 5000 cells/well in a 96-well black wall, clear bottom Packard ViewPlate, and incubated in MM, MEBM or DMEM/F-12 medium for pre-stasis, post-selection and immortalized HMEC, respectively, for 48 hours. Cells were washed with PBS, and fixed with pre-warmed 4% paraformaldehyde for 10 minutes. Cells were washed 2× with PBS, permeabilized with 0.2% Triton X-100 for 3–5 minutes, and washed 2× with PBS again. Cells were stained with primary antibodies in 1% BSA/PBS. Primary antibodies were used as follows: E2F1 (BD/Pharmagin, 1:200 dilution), E2F4 (Abcam, 1:400), Rb (Cell Signaling Technologies, 1:400), p107 (Santa Cruz, 1:200), BRCA1 (Abcam, 1:200), p53 (Cell Signaling Tech-

nologies, 1:200), SP1 (Upstate Biotechnologies, 1:400), NF-κB (Cellomics, 1:200). Cells were washed 3× with PBST (0.05% Tween-20), and stained with DAPI and secondary antibodies of appropriate species/isotype specificity and conjugated to either Alexa-488 or Alexa-594. Cells were washed again 3× with PBST; 100 μl of PBS was added and plates were sealed with an adhesive cover.

Quantitative immunofluorescence was performed using a Cellomics ArrayScan V^{ti}. Images were taken using a 20× objective and data was collected for a minimum of 1000 valid cells per well. Valid cells are defined as having nuclei with expected DNA content (defined by DAPI fluorescence intensity), nuclei size and shape typical for the cell line/type, and well-separated from neighboring cells, such that cytoplasmic regions could be clearly resolved. DNA content and antigen intensity were quantitated for each cell, and the nuclear-cytoplasmic ratio for each antigen was determined by a mask derived from the DAPI staining, which was used to define the nucleus, and a region surrounding the nucleus (which was specific for each cell line/type) was used to define the cytoplasm. Quantitation was performed using either the Compartmental Analysis or Nuclear Translocation BioApplications, from Cellomics.

Results

Transcriptional profiling of pre-stasis, post-selection and immortalized HMEC

To better understand the extent to which pre-stasis, post-selection and immortalized HMEC represent distinct cell types, we compared several samples of these cultures by transcriptional profiling; the HMEC samples characterized are described in Table 1. The finite lifespan pre-stasis and post-selection HMEC are referred to as strains or cell types from a specific source, and culture conditions (including stage) are noted for each particular sample. The relationships between samples in this study, their origins, are indicated graphically in Figure 1. Triplicate cultures for each sample were grown under the conditions indicated in the Methods, and in Table 1, following which the total RNA was isolated, labeled and hybridized to the Affymetrix U133A/B GeneChips.

Principal Component Analysis (PCA) was used to visualize the gross relationships among the cell types, as shown in Figure 2A. The first three components, which explains about 60% of the total variation, are displayed in a three dimensional graph. The pre-stasis HMEC (in red) and post-selection HMEC (in pink) are clearly separated from the immortalized lines (in blue, black and green) along the first principal component axis. Thus, transcriptional profiling defines the transition from finite lifespan to fully immortalized HMEC as the most significant change in HMEC progression. The pre-stasis and post-selection HMEC are also well segregated within their unique space. In addition, the fully immortalized lines that either do not express *p53* or are transduced with *ERBB2/Her2* (green and blue, respectively) are distinguished from the rest of the immortalized lines (black). According to the PCA, there are no significant differences between the fully immortalized lines derived from various methods of

Table 1: Cell Types and Lines Used in This Study

Cell Name	Source	Stage	Growth Media
48L	LBNL	Pre-stasis, finite lifespan strain	MM (MEBM)***
161	LBNL	Pre-stasis, finite lifespan strain	MM (MEBM)
184	LBNL	Pre-stasis, finite lifespan strain	MM (MEBM)
195L	LBNL	Pre-stasis, finite lifespan strain	MM (MEBM)
48R	LBNL	Post-selection, finite lifespan strain	MEBM
161	LBNL	Post-selection, finite lifespan strain	MEBM
184	LBNL	Post-selection, finite lifespan strain	MEBM
195L	LBNL	Post-selection, finite lifespan strain	MEBM
191	LBNL	Post-selection, finite lifespan strain	MEBM
239	LBNL	Post-selection, finite lifespan strain	MEBM
HMEC-1001-13	Clonetics	Post-selection, finite lifespan strain**	MEBM
184A1	LBNL	Fully immortal cell line	MEBM
184B5	LBNL	Fully immortal cell line	MEBM
184AA2	LBNL	Fully immortal cell line	MEBM
184AA3	LBNL	Fully immortal cell line	MEBM
184B5ME	LBNL	Fully immortal cell line	MEBM
184A1*	ATCC	Fully immortal cell line	DMEM/F-12
184B5*	ATCC	Fully immortal cell line	DMEM/F-12
MCF-10A	ATCC	Fully immortal cell line	DMEM/F-12
MCF-10A-2	ATCC	Fully immortal cell line	DMEM/F-12
MCF-12A	ATCC	Fully immortal cell line	DMEM/F-12

*designated as 184A1(a) and 184B5(a) in other tables and figures

**stage defined by transcriptional profile

***cells isolated from reduction mammoplasty tissues and expanded in MM media to passages 2–3, then cultured in serum-free MEBM media for transcriptional profiling

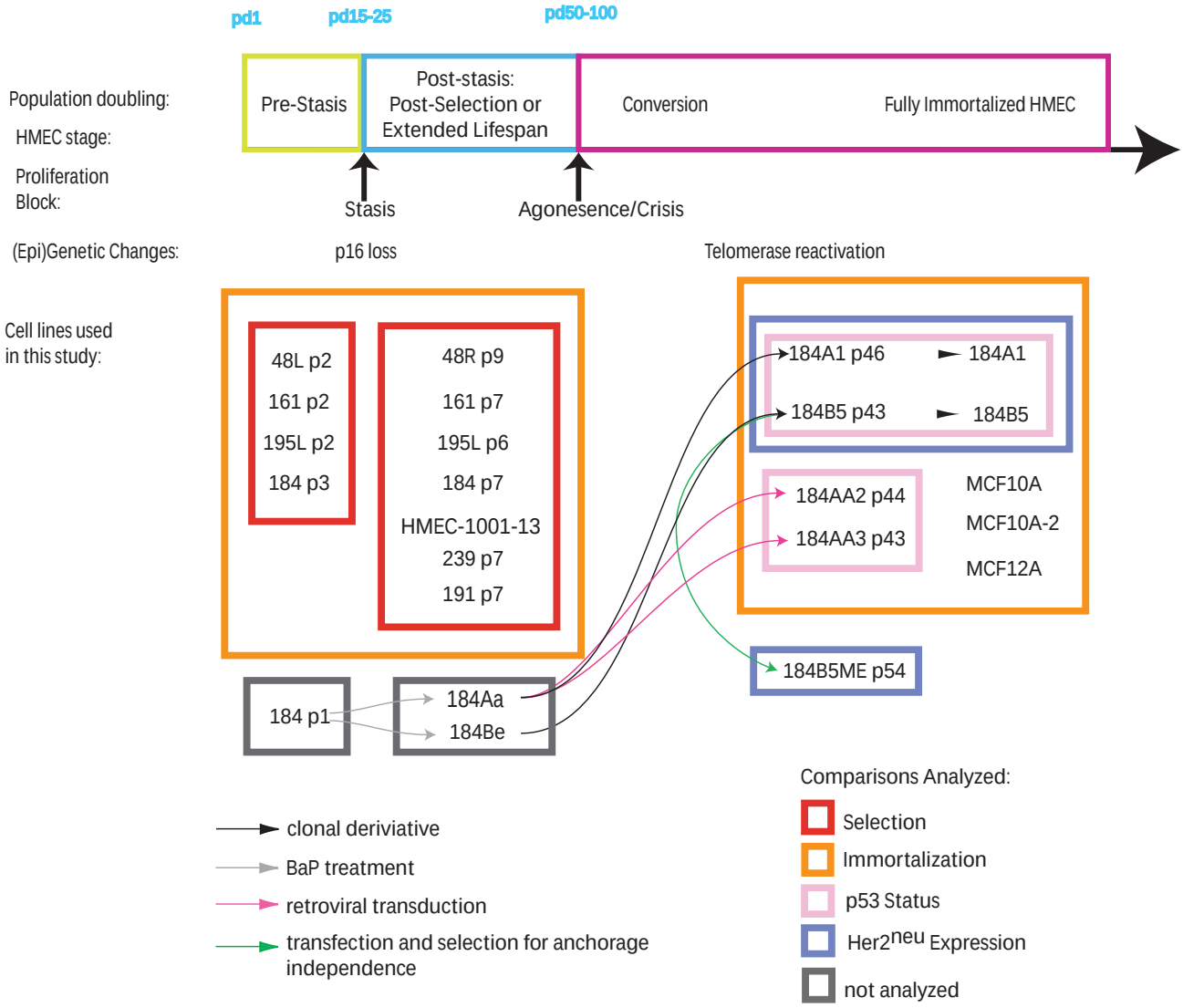

Figure 1

Graphic relationship of cell lines profiled in this study. Cell lines characterized in this study are shown with reference to their stage in transformation. The pre-stasis HMEC used were cultured for 2–3 passages before analysis, and reach stasis by passages 3–5. Rare isolates of cells grown in serum-free media (MEBM) emerge spontaneously from stasis, associated with the absence of p16 expression due to promoter silencing, and continue growing as post-selection HMEC until reaching a second, proliferation barrier (telomere dysfunction). This barrier is highly stringent, and spontaneous immortalization has never been observed in cells that were not mutagenized or virally transduced during pre-stasis or post-selection growth. HMEC grown in MM do not spontaneously give rise to post-selection cells, however primary populations exposed to the chemical carcinogen benzo(a)pyrene (BaP) have produced rare clonal isolates with post-stasis growth, associated with absence of p16 expression due to mutation or promoter silencing. These non-spontaneously arising post-stasis cells are referred to as *extended lifespan*, and may harbor additional errors due to the carcinogen exposure. Overcoming the telomere dysfunction barrier is associated with reactivation of telomerase activity. The fully immortalized lines 184A1 and 184B5 were derived from extended lifespan post-stasis cells grown in MM and exposed to BaP in primary culture. Exposure of extended lifespan 184Aa cells to retroviral infection resulted in two cell lines that had lost both copies of the *TP53* gene. The cell lines profiled in this study are shown relative to the profiling analyses performed. Comparisons used to analyze selection and immortalization, as well as the influence of p53 and ERBB2/Her2 status are shown by colored boxes and identified in the key at the lower left of the figure.

immortalization, or from lines maintained at LBNL versus those obtained from ATCC. Unsupervised (or Eisen) clustering of the genes that change following selection and immortalization for most of the samples is shown in Figure 2B. These data reflect the 1 342 genes that are filtered based on the Pvalues from one-way analysis of variance (ANOVA), as described in the supplementary material.

Gene expression changes following selection

Gene expression changes that distinguish pre-stasis from post-selection cells were identified using GeneCluster [31], and the results are shown in Figure 3A. The figure characterizes a large set of concordantly-regulated genes in the pre-stasis strains, and a high level of concordance in four of the six post-selection HMEC (200 genes for each class). Among these top-200 genes in the pre-stasis cell types, the largest number of genes we identified are involved in the extra-cellular matrix (ECM), including structural proteins and matrix remodeling enzymes (listed in supplementary Additional file 1). Examples include many collagen and kallikrein genes. Genes that increase expression level in post-selection HMEC include a large number of genes associated with proliferation and the cell cycle. These genes are strongly associated with cancer cell growth, and increase in expression directly with tumor grade. Specific examples include *BIRC5*, A and B type cyclin genes, *CDC2*, and the *MCM* chromosomal proteins. The increased expression of these genes is dependent on E2F transcription factors and reflects the proliferative state a cell. Since the pre-stasis cells were nearing stasis, the increased expression of the genes in the post-selection HMEC may reflect either a loss of Rb repression (consistent with a loss of p16), or could reflect the relative proliferative state of these pre-stasis and post-selection cells.

The two discordant post-selection HMEC we observed in Figure 3A (195L and 1001-13), suggest that additional molecular events can occur during selection; these samples also show a loss of p16 expression (results not shown), a definitive event for post-selection HMEC. In order to probe further into the changes that occur during selection, we compared the four sets of HMEC studied as pre-stasis and post-selection samples. For this analysis, we identified genes that increase expression in post-selection HMEC, as compared to the corresponding pre-selection sample. Four patterns were observed. The genes we identified in each group are listed in Table 2, and the expression changes we observe for three of the groups are shown in Figure 3B. The group not explicitly shown in Figure 3B is uniformly down-regulated in all four pairs. Genes expressed exclusively in post-selection 195L HMEC (Group A) fall into two categories: genes previously identified as cancer-associated (including several antigens proposed as cancer biomarkers), and genes induced by interferons [35]. Among the cancer-associated genes, the *Cancer-Testis Antigen 2* (*CTAG-2*) is very strongly expressed (30-fold according to the GeneChip data), as are *ARH-GDIB*/*Ly-GDI*, and *IGFBP6*. The cytokine induced genes [35] include a set previously reported as increasing in post-selection HMEC, such as *IFIT1*, *IFITM1*, *G1P2* and *OAS1* [36]. The genes that are unique to 48 HMEC (Group B) include several transcription factors and cell cycle proteins whose roles in cancer or breast tissue development have not been well characterized to date, including *NUCKS*, *SON* and *HOXB2*. Group C includes many genes previously associated with cancer cell proliferation.

Since these geneset classes were comprised of a relatively small number of genes, we performed promoter analyses, to see if these sets are linked in specific pathways. Promoter binding sites we were able to identify are listed in Table 2. For Group A, interferon-responsive elements were found for most of the genes, but not the cancer/metastasis-associated genes (*BST2* is an exception), consistent with previous studies that did not identify these genes as IFN-regulated [35]. Instead, several genes in this group have been shown to be direct or indirect targets of p53 and Myc. A common element in the regulation of both p53/Myc and IFN-regulated genes is *BRCA1*, and in particular, BRCA1 is essential for the activation of stress and inflammatory response genes following treatment with interferons [37]. Group B was less well-defined by specific binding sites near the promoter, but an extended analysis (2 kb) identified SP1, E2F, MAZ and NF-Y binding sites for many genes. These binding sites were also identified in the genes of Group C, especially the E2F, NF-Y and SP1 sites, which is consistent previous work [38,39]. Group D, genes significantly repressed in post-selection HMEC, may be under the control of MAZ (Myc-associated zinc finger protein), as binding sites were found in 19 of 22 genes examined, which is consistent with previous observations that increased Myc can repress ECM genes [40-42]. In conclusion, although distinct gene expression patterns could be observed for each of the pre-stasis/post-selection HMEC pairs we have characterized, in each case strong associations could be made between the promoters of each class and the proliferation and cell cycle transcription factors, particularly E2F, SP-1, NF-Y and the Myc-related MAZ. The distinguishing features for each of these expression classes is likely to be found in additional, unique pathways such as BRCA1-mediated regulation.

Gene expression changes that distinguish finite life span HMEC from immortally transformed HMEC

The most significant transition observed in this study is that of immortalization. Genes whose expression are reduced in the immortalized lines include a significant number that suppress angiogenesis, contribute to the ECM, or regulate the actin cytoskeleton. Many of these genes were identified as down-regulated in HMEC follow-

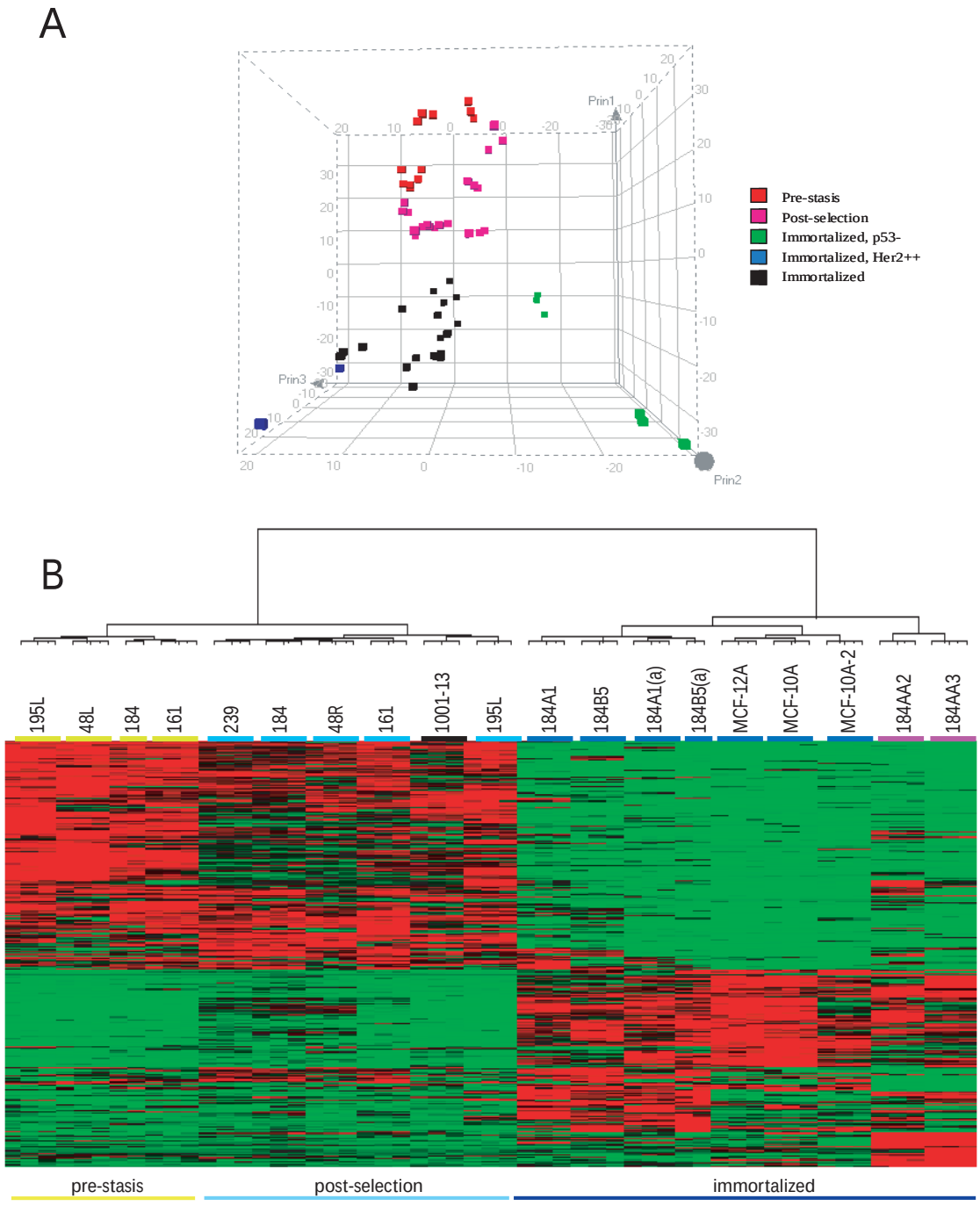

Figure 2

Relationship of HMEC as determined by transcriptional profiles. **A**. Data from 2319 genes were used to determine the number of principal components of the data. Three components were identified, and the contribution of the components to the transcription profile of each cell line samples are shown in the figure. Individual replicates for each cell line are shown. Cell lines grouped in **Figure 1** are shown in **Figure 2A** as shown in the legend. Vertical axis is PC1, the first, and therefore the strongest. principal component. **B**. Unsupervised clustering of HMEC. All genes that change expression in one or more samples were used to cluster the cell types and lines by overall similarity. Cell types and lines are identified by color under the designations: pre-stasis HMEC: light green; post-selection HMEC: light blue; fully immortalized HMEC: dark blue; $p53^{-/-}$ fully immortal HMEC: burgundy, and lines not formally characterized: black. Samples of 184A1 and 184B5 designated by (a) were obtained from ATCC.

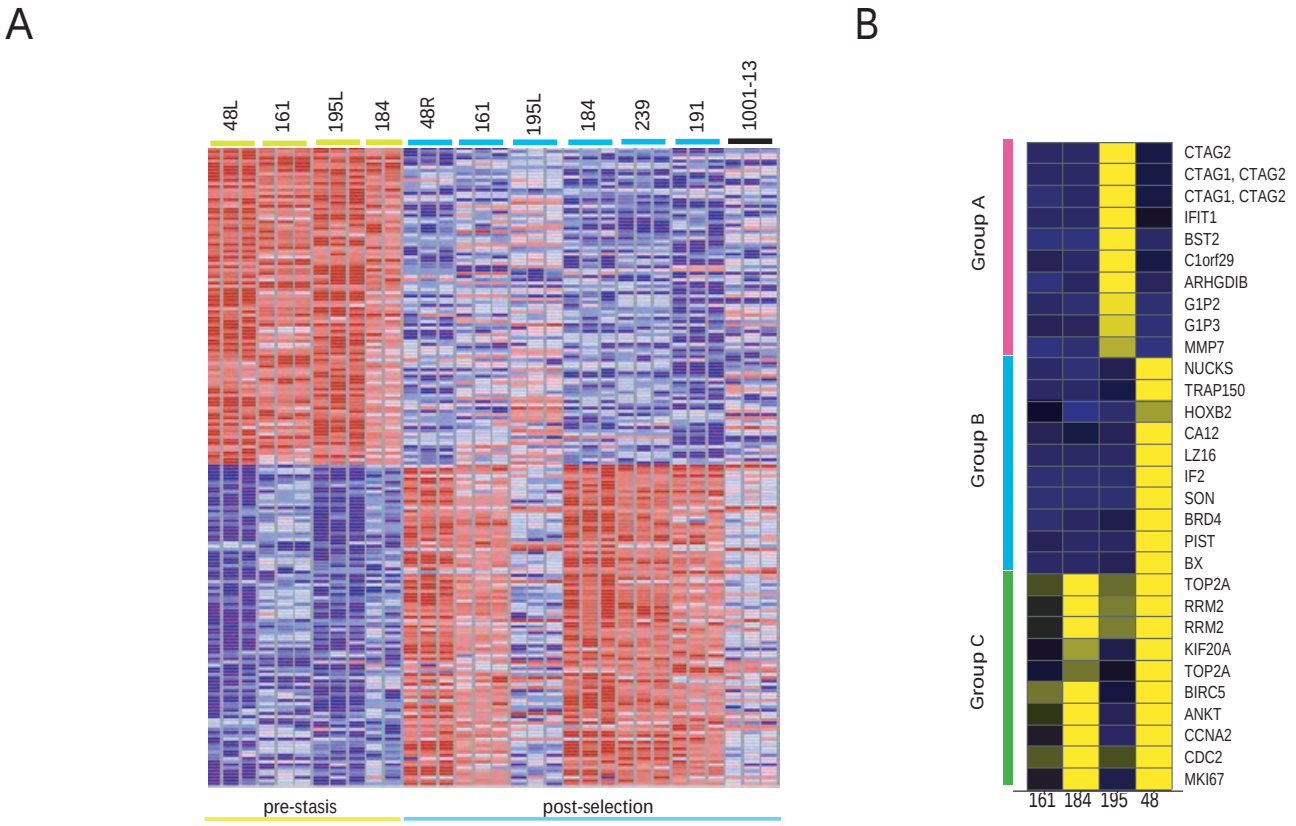

Figure 3

***Supervised Clustering of Pre-stasis, and Post-selection HMEC*. A**. Gene expression values were normalized and characterized for the significance of overexpression in one group relative to other groups in the comparison. The top 50 genes that are significantly overexpressed in one group are shown. All pre-stasis and post-selection cell types have been used. Analysis was performed in GeneCluster, and the color bar describing how normalized values are depicted is shown at the bottom of the figure. **B**. Distinct classes of genes over-expressed in post-selection HMEC. Genes showing one of three specific patterns of expression in the four pairs of pre-stasis and post-selection samples are diagramed. The top 10 qualifiers (based on fold change) are shown (some genes are represented by more than one qualifier).

ing selection as well; some are further down-regulated in the immortalized lines, as shown in Figure 4A. These comparisons include multiple independent samples from each stage, including four distinct fully immortalized cell lines, and three additional samples from either different sources (184A1 and 184B5 from ATCC) or two separate isolates from the same experiment (MCF-10A and MCF-10A-2) [43]. The genes identified in each group are described in Additional file 2. Collectively, the pre-stasis and post-selection samples are distinguished most strongly by changes to the ECM and cell-cell communication genes, particularly collagens, kallikrein, matrix metalloproteinase and serpin proteinases; genes that affect the actin cytoskeleton are also noted (both actin and actin-interactors, such as actinin, nidogen, transgelin, and palladin, genes). Several well-recognized classes of genes are up-regulated in fully immortalized lines, including the commonly observed "proliferation cluster" described above. These genes were also observed to be up-regulated in the post-selection, compared to pre-stasis HMEC. Fewer of these "proliferation genes" are identified in the fully immortalized samples following a three-way comparison, but this is because GeneCluster identifies the most definitive group of genes for each class, and since some of the post-selection samples express increased levels of genes such as *MCM2* and *STK12*, they are not unique to either the post-selection or the fully immortalized HMEC.

We have examined the expression of the cancer cell proliferation class of genes directly in Figure 4B. In this example, the absolute expression levels of each gene listed in the figure are displayed directly (rather than the ratio of post-selection over pre-stasis expression levels in Figure 3B). These genes are compared to equal subsets of genes

Table 2: Genes and Promoter Elements That Define Post-Selection HMEC Gene Expression Classes

Geneset Classes	Genes	Promoter Elements
Group A		
IFN genes	IFIT1, BST2, G1P2, G1P3, IFIT2, OAS1, IFI44, IFIT4	IRF, ILR, IRL
Non-IFN genes	CTAG2, ARHGDI-B/Ly-GDI, MMP7, PLAU, CALB1, SLC1A6, MDA5, FXYD5, HMOX1	
Group B	NUCKS, HDAC3, TRAP150, HOXB2, SON, IF2, LZ16, ANLN, BBX, TOP1, H4FG, SFRP1, KTN1, GTAR, BAZ1A, PK428, FALZ, TTC3, DNCL12, RBM9	SP1
Group C	TOP2A, RRM2, KIF20A, BIRC5, ANKT, CCNA2, CDC2, MKI67, CDC20, MCM5, HMMR, IL-1B, PRC1, PMSCL1, MADL1, DLG7	E2F, NF-Y, B-Myb
Group D	H11, COL11A1, IGFBP5, CNN1, COMP, LGALS7, CLDN7, KLK6, KLK7, KLK10, KLK11 KRT23, LOXL4, THY1, FLJ21841	MAZ, MAZR, MEF-3

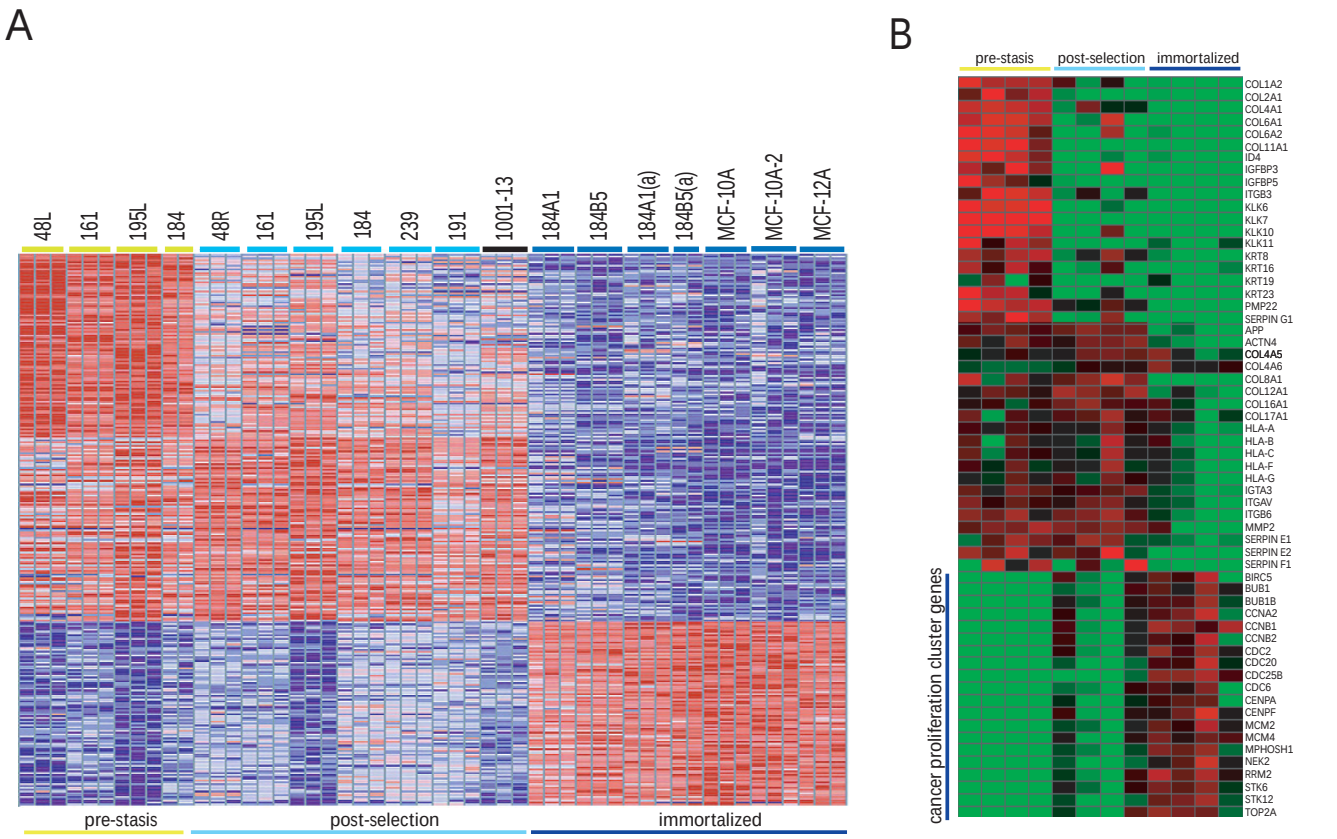

Figure 4

Supervised Clustering of Pre-stasis, Post-selection and Immortalized HMEC. **A**. Gene expression values were normalized and characterized for the significance of over-expression in one group relative to other groups in the comparison. The top 200 genes (of 1342) that are significantly over-expressed in one group are shown. All pre-stasis, post-selection and immortalized HMEC (except the *p53*$^{-/-}$ and *ERBB2/Her2* transfected variants) have been grouped. The top 100 genes (of 1440) that are over-expressed in one group relative to the other two are presented. Analysis was performed in GeneCluster. **B**. *Expression of a subset of highly concordant genes in pre-stasis, post-selection and fully immortalized HMEC*. Gene-normalized expression of 60 genes identified in the figure are shown for four representatives each for the three groups of HMEC. Samples are (left to right): 48L, 161, 195L and 184; 48R, 161, 195L, and 184; 184A1, 184B5, MCF-10A and MCF12A.

that show maximal levels of expression in the pre-stasis and post-selection HMEC samples. As can be observed in the figure, genes showing maximal expression in the pre-stasis samples are robust, whereas those showing maximal expression in the post-selection are less strongly definitive of post-selection cells. The "proliferation cluster" genes show strongest expression in the fully immortalized HMEC lines, however expression of these genes is heterogeneous for both the post-selection and fully immortalized sets. Increased expression can be observed for the post-selection 48R and 184 samples (as was seen for some of these genes in Figure 3B), and lesser expression is seen for MCF-12A. However, the rise in expression of this group of genes as HMEC progress from pre-stasis through fully immortalized stages is clear.

Gene expression changes observed in p53$^{-/-}$ cell lines

HMEC lines that have lost p53 during immortalization show distinctive changes in transcriptional profiles when compared to closely related lines that have retained p53 function. The complete list of genes is presented in the supplementary Additional file 3. When we explicitly look for genes whose expression changes are common to the p53 status of the lines derived from specimen 184 cells, several genes showing concordant changes between *p53*$^{+/+}$ 184A1 and 184B5 versus *p53*$^{-/-}$ 184AA2 and 184AA3 are observed. *SIAH2*, *Lipocalin 2*, *Asparagine synthase* and *Keratin 15* are all upregulated in both 184AA2 and 184AA3, relative to both 184A1 and184B5. Genes down-regulated in the p53$^{-/-}$ lines include several that are explicitly regulated by p53 (including *RRM2* and *TP53INP1*). A comparison of the two *p53*$^{+/+}$ and the two *p53*$^{-/-}$ lines shows that additional gene expression changes unique to each line have occurred. Examples include *DUSP1* and *BIRC3*, expressed at significantly higher levels 184AA3 than in 184AA2, and *FABP4*, *IFI27*, *HRASLS3*, and *Fibulin 1*, expressed much more robustly in 184A1 than in 184B5. The complete list of genes is presented in the supplementary Additional file 4 and Additional file 5.

Gene expression changes resulting from ectopic expression of Her2

The events characterized thus far in this study concern HMEC immortalization; however, additional events are critical to malignancy. To connect these studies directly to changes that occur following an oncogenic event, we have compared one immortalized HMEC line, 184B5, with a derivative that ectopically expresses the *ERBB2*/*Her2* oncogene, 184B5ME. *ERBB2*/*Her2* is frequently over-expressed in breast cancer, and is transforming simply by being over-expressed, so this line models clinically relevant features of breast cancer. Over-expression of *ERBB2*/*Her2* in 184B5 results in anchorage independent growth, a malignancy-associated property, while over-expression of oncogenic *ERBB2*/*Her2* in 184B5 can confer tumorigenicity [21]. Gene expression changes seen for 184B5ME that are distinct from its parent are listed in the supplementary Additional file 6. Genes showing increased expression include many that were down-regulated in post-selection HMEC, including kallikreins *KLK6* and *KLK7*, and *cystatin E*/*M*. These phenotypic reversions may play a role in the transition to invasive cancer [44]. Additional gene expression changes include a dramatic increase in the expression of *IL24* and significant changes in *BIRC3*, *HRASLS3*, and *PTGES*. Genes showing down-regulation as a consequence of *ERBB2*/*Her2* overexpression include many of the IFN genes that showed increased expression following selection (in 195L) or immortalization (in 184A1, 184B5 and others).

Real-time PCR measurement for selected genes identified in this study

The results presented comprise a large study of human mammary cell samples that have not been characterized by transcriptional profiling previously, and the gene expression patterns are either new or not previously associated with non-cancerous cell lines. As such we wished to validate the findings by corroborating the gene expression changes observed by genechips with an independent method. 15 genes were chosen from the data to be validated by Taqman™ quantitative PCR. Genes that change following selection (*PMP22*/*GAS3* and several insulin-like growth factor binding protein (IGFBP) genes: *IGFBP2*, *IGFBP3*, *IGFBP4*, *IGFBP5*, *IGFBP6*, and *IGFBP7*), as well as genes that change in immortalized lines (*CCNB1*, *CDC2*, *CDC25B*, *HDAC3*, *MYC*, and *STK6*) were evaluated by RT-PCR in 17 cell types, comprising pre-stasis, post-selection and fully immortalized samples, and the results compared to expression data from the oligonucleotide arrays. The concordance between expression of a gene as measured by oligonucleotide array and Taqman™ assays were generally quite good; in 14 cases, only minor discordances can be observed (see Figure 5). *HDAC3* was an exception. The expression level changes of three probes sets for *HDAC3* on the Affymetrix U133 GeneArrays, and the Taqman™ primer set, were highly discordant, so we were not able to validate the expression changes of this gene by RT-PCR, however were able to show significant changes in HDAC3 protein expression and localization by immunofluorescence microscopy (described below).

Transcriptional regulatory factors are localized to the nucleus following selection and immortalization

We explored the changes that occur in several critical regulators of cell cycle progression and chromosomal stability by quantitative fluorescence microscopy, or High Content Screening (HCS). These factors were chosen based on patterns observed in the transcription profiling data as ones that would be expected to change as HMEC progress past senescence barriers, based on the gene

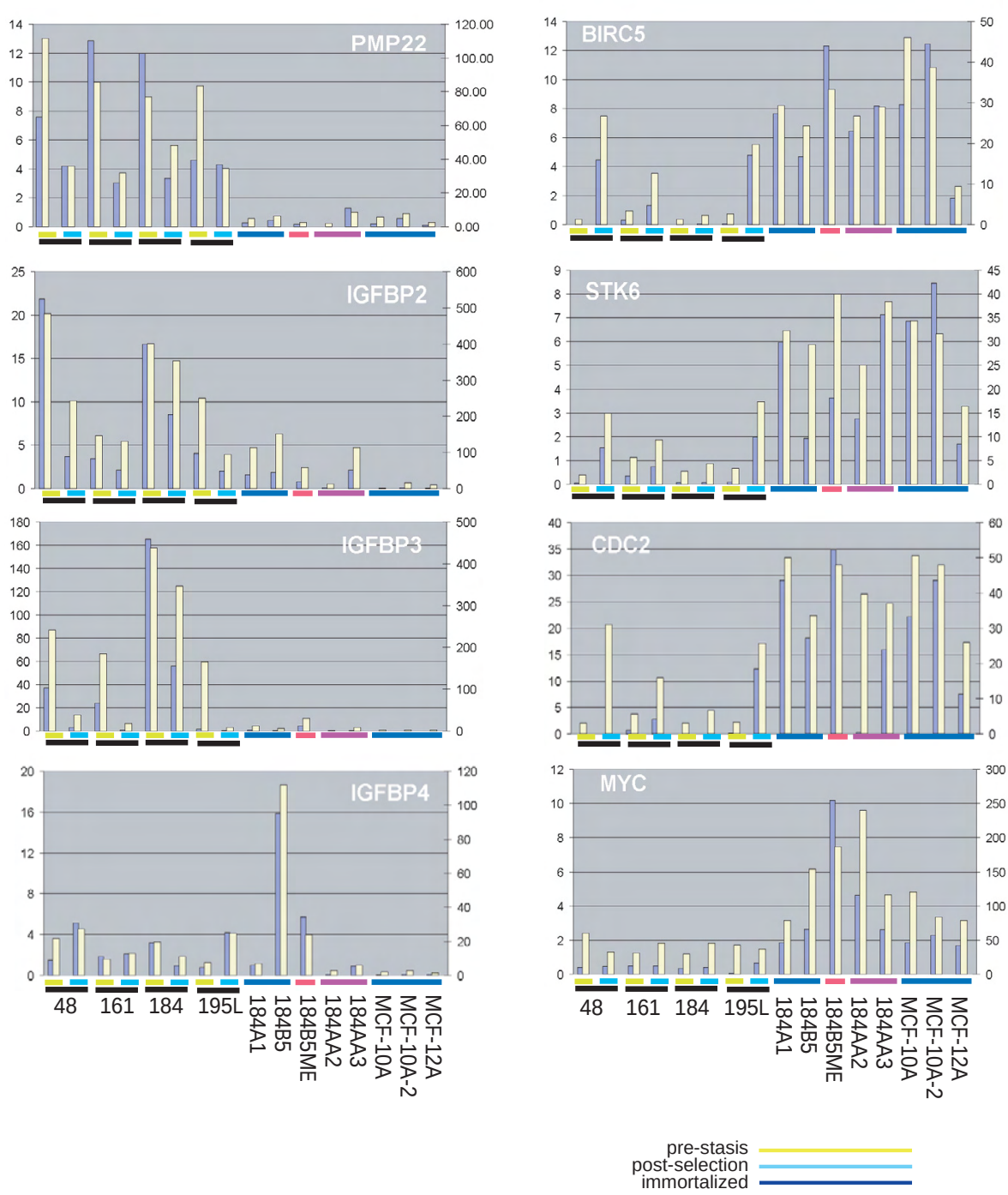

Figure 5

Real-time PCR measurements of gene identified in transcriptional profiling analyses. Representative genes from groups identified as changing expression during selection or immortalization were characterized by real-time PCR analysis (Taq-Man™). Genes were selected as representative of classes were described in this study. Each gene is presented as a separate graph, as identified in the figure. Cell lines are presented in the same order in each graph, as listed in the bottom left panel. The finite lifespan samples are shown as pairs, with the pre-stasis sample on the left and the post-selection sample on the right. For each cell line, expression data from Affymetrix GeneChips are shown as blue bars, according to the scale at the left of the graphs. Expression data from real-time PCR of the same samples are shown as yellow bars, according to the scale at the right of the graphs.

expression patterns we observe. Example images are shown in Figure 6A. For these images, Rb is shown in red and DNA is shown in blue. In the pre-stasis 184 HMEC, Rb is punctate and is evenly distributed between the nucleus and cytoplasm. In post-selection 184 HMEC and in immortalized lines such as 184A1 (shown in the figure) and 184B5 (not shown), Rb is very strongly localized to the nucleus, and the staining is no longer punctate. The nuclear/cytoplasmic ratio (determined using least 1000 cells per sample for three samples each) are shown in Figure 6B for Rb and 8 other proteins. The ratio for Rb in pre-stasis cells is 0.5–2, whereas for post-selection and immortalized HMEC it is greater than 100. Similar dramatic changes are observed for HDAC3, BRCA1, p53 and the general transcription factor SP1. BRCA1 and c-Myc are localized in the cytoplasm in pre-stasis HMEC, but to the nucleus in post-selection and immortalized HMEC. For other proteins associated with G1 progression (E2F1, E2F4 and p107), the differential is in the range of two to four-fold.

Discussion

Transcriptional profiles and quantitative immunofluoresence of HMEC reveal significant cancer-associated changes following both selection and immortalization

The effect of malignant transformation (oncogenesis) on gene expression has been studied extensively in both cell lines and tissues in an effort to characterize the causes of cancer at the molecular level [45]. Gene signatures commonly found in breast and other human cancers include those critical for the cell cycle, chromosomal stability and proliferation; the extent of the increase in the expression of this signature correlates with tumor grade and poorer prognosis [26,46]. A separate signature of IFN-regulated genes has also been observed in ductal carcinoma *in situ* (DCIS) [47] and has been associated with metastasis to the lymph nodes in aggressive breast cancers [48]. We have observed both of these signatures in non-malignant, immortally transformed, HMEC lines that had overcome the two senescence barriers to immortalization, despite these lines retaining many characteristics of finite lifespan epithelial cells.

Transcriptional changes in gene families associated with mammary epithelial biology or breast cancer in post-selection and fully immortalized HMEC

There are several gene families that we identified in this study which have direct connections to breast epithelial biology and breast cancer, which we can summarize:

(A) Several IGFBPs show reduced expression in post-selection HMEC and immortalized lines, including IGFBP2 (minor decreases overall, but larger in the $p53^{-/-}$ lines), *IGFBP3* and *IGFBP5* (very large decreases in immortal HMEC). Levels of *IGFBP4* were significantly reduced in 184B5ME relative to 184B5. IGFBPs are frequently observed to be reduced in breast cancers, and these reductions are associated with increased sensitivity to IGF-I and IGF-II [49,50].

(B) *BRCA1*, a gene deleted in about 5% of women with breast cancer, encodes a protein that interacts with many other proteins [51]. These complexes recognize and orchestrate the repair of DNA damage. Many genes that encode proteins that interact with BRCA1 were identified in this study as genes that increase expression following either selection or immortalization. *BAP*, *RAD51*, *CSE1L* and *RFC4* all increased expression following selection in a pattern similar to the E2F-regulated genes identified as Group C in Figure 3B. *MYC*, *RAD50* and *RFC3* increased expression in fully immortalized lines, including the $p53^{-/-}$ lines. These changes suggest the possibility that BRCA1-mediated functions are affected by overcoming stasis and/or immortalization, which is supported by the significant change in localization of BRCA1 to the nucleus in post-selection HMEC.

(C) The increased expression of a well-characterized cluster of IFN-regulated genes was observed in some lines in this study, as well as in other studies of HMEC [36], and in a taxol-resistant MCF-7 line [52]. The IFN-dependent stress response is mediated by BRCA1 [37,53]. Therefore, since we have noted expression changes in many genes associated with BRCA1 function, as well as in BRCA1 abundance and localization in post-selection HMEC, IFN gene signature may reflect changes in BRCA1-mediated functions.

(D) Inhibitors of Differentiation (ID) genes are important regulators of differentiation by dominantly interfering with the function of bHLH proteins during embryogenesis, neurodevelopment and cancer. Part of their function is through the repression of CKIs, including p16. Some functions have been attributed to specific members, including the interaction of ID2 with Rb [54], and the expression of *BRCA1* by ID4 [55], which is in turn repressed by BRCA1 [56]. In this study, *ID1* is expressed at higher levels in the immortalized lines (184AA2 is an exception), while *ID4* is repressed in post-selection HMEC and all of the immortalized lines.

(E) S100 proteins comprise a large family of calcium-activated proteins that function in homo- and hetero-dimers to regulate many intra- and extra-cellular targets [57]. Their increased expression in cancer and inflammatory diseases has provoked interest in this family as potential drug targets and clinical biomarkers. We observe increases in the expression of *S100A8* and *S100A9*, which comprise the heterodimer Calprotectin, following selection and fur-

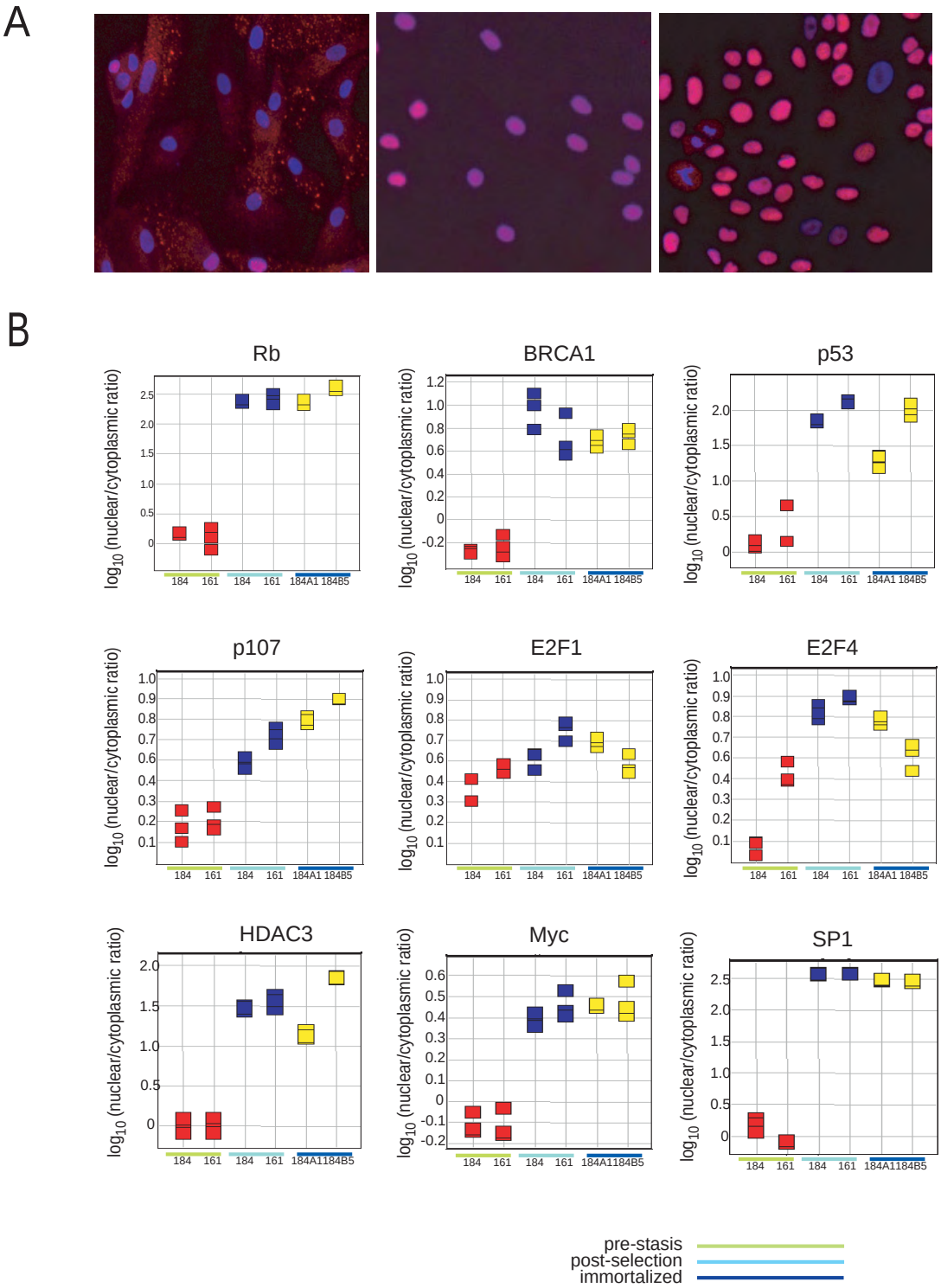

Figure 6

High Content Screening of proteins associated with cell cycle progression and chromosomal stability. (A) Immunofluorescent images of Rb (red) and DNA (blue) obtained using a Cellomics ArrayScan Vti are shown for pre-stasis 184 HMEC (left), post-selection 184 HMEC (center) and the 184A1 cell line (right). (B) Quantitation of the nuclear/cytoplasmic ratio is shown for pre-stasis 184 and 161 HMEC, post-stasis 184 and 161 HMEC and the cell lines 184A1 and 184B5, as indicated in the figure panels. Antigens quantitated in each panel are identified above the panel.

ther dramatic increases following immortalization. Increased expression of *S100P* is seen in DCIS [58], and was also observed in several of the immortalized lines, particularly 184B5ME, the *ERBB2/Her2* transduced line. Increased expression of S100A7, also known as psoriasin, is seen in both DCIS and IDC, particularly ER negative breast cancers [59]; increased expression was observed in several immortalized lines, most strongly in 184AA3.

Transcriptional changes that occur following genetic changes associated with invasive cancer

p53 imposes a cell cycle arrest when chromosomal breakage or damage is detected, and its loss in breast cancer is associated with increased chromosomal instability and a more aggressive subtype [60]. The two $p53^{-/-}$ lines we have characterized show a number of transcriptional changes that are expected of $p53^{-/-}$ cell lines, as well as changes unique to the two lines. Of note is expression of the IFN-induced genes observed in post-selection 195L cells and in the 184AA3 line. This may indicate a common molecular event occurred following selection of the 195L cells and the immortalization of the 184AA3 cells. Further studies on the changes common and unique to $p53^{-/-}$ HMEC lines may be important in understanding differences between $p53^{+/+}$ and $p53^{-/-}$ cell lines and breast cancers in overcoming senescence barriers and immortalizing.

In data presented here, transfection of an immortalized line with a clinically-relevant oncogene, *ERBB2/Her2*, showed fewer transcriptional changes than were observed following selection or immortalization, and these changes were generally limited to genes involved in invasive growth and motility. Specifically, expression of the proliferation geneset was not dramatically altered, but there was increased expression of genes encoding the secreted proteases Cystatin E/M, and Kallikrein 6, as well as tissue plasminogen activator. Such changes could enable these cells to grow invasively in breast tissue.

Activation of transcriptional regulators associated with gene expression changes in post-selection and immortalized HMEC, telomerase reactivation and cancer

In quiescent or unstimulated cells, many transcription factors are excluded from the nucleus and localize to the nucleus upon activation [61]. In the case of BRCA1, nuclear retention has been shown to suppress its pro-apoptotic functions [62]. The proliferation, cell cycle and DNA damage response genes identified in the gene expression signatures we observe are supported by the changes in the localization of several associated regulatory proteins and transcription factors, as determined by quantitative immunofluorescence. Based on previous studies linking regulatory pathways to gene expression, the relationship between the gene expression signatures and the regulatory factor localizations we observe are concordant. Proteins directly responsive to p16/CDK4 activation, particularly Rb, show striking changes in cytoplasmic/nuclear distribution in both post-selection and fully immortalized HMEC, compared to pre-stasis HMEC. Additional proteins also showing strong changes in localization are BRCA1, p53, HDAC3, Myc and SP1. Each of these proteins have well characterized roles in oncogenesis and in the regulation of hTERT [63-66], a critical event in immortalization [1,5]. These changes are consistent with both the transcriptional profiles we have generated of post-selection and fully immortal HMEC, as well as with what is known about the role of these factors on telomerase regulation.

The relationship between immortalized HMEC and DCIS

Taken together, these data support a classification of immortalized breast epithelial cell lines as *in vitro* models of highly dysregulated epithelial cells, rather than as perpetually growing models of normal breast epithelia. Gene expression patterns we have identified in the comparison of finite-lifespan and immortalized HMEC lines are highly similar to changes observed in DCIS and invasive human breast cancers [47,67,68], and are consistent with other similarities between immortal HMEC lines and DCIS. Specifically, short telomeres and moderate chromosomal instability, as well as telomerase re-activation, are common to many early-stage tumors [69], including the breast [17]. In addition, p16 expression is lost in post-selection, as it is in vHMEC [15,16], which are proposed to be premalignant breast cancer precursors *in vivo*. In contrast, we observe that a cell line, 184B5ME, which grows invasively in tissue culture and in *in vivo* models, shows fewer changes.

DCIS is a complex disease [70], often requiring no immediate treatment in the strict sense, however it is not currently possible to forecast when, or if, progression to IDC will occur. This necessitates an aggressive strategy, even in cases where it may be effectively managed by substantially simpler, cheaper, and less emotionally challenging modes [71]. The ability to characterize DCIS, and to target it explicitly when it manifests invasive potential, is a critical need with regard to effective breast cancer treatment strategies. In particular, established markers for breast cancer, including Ki-67, p53, Her-2^{neu} and ER expression are very effective for identifying aggressive, invasive cancers, and for determining the most effect treatment strategy in these cases, but are less informative about the likelihood that a well-contained DCIS will progress to invasive cancer. Currently, some of the best indicators of DCIS progression risk are cytological, including grade, necrosis and architectural patterns [72]. Additional molecular markers, particularly those that correlate strongly (or better, explain) the histological patterns used to stage DCIS would be very val-

uable. Some additional molecular markers are emerging. COX-2 has been identified as a marker of vHMEC [15,16], and expression levels have been correlated with DCIS grade, as well [73]. For these reasons, recognizing immortalized HMEC as resembling early-stage cancers would facilitate a formal interrogation of their genetics and physiology for clues to how DCIS occurs, and to the factors that can enable DCIS to progress.

Use of post-selection and immortalized HMEC to study normal mammary cell biology and breast cancer

Immortalized cell lines have been used to address complex problems in cancer [74] and epithelial cell biology [75] precisely because they allow for controlled experiments to be performed and theories of breast cancer to be tested. In studies of oncogenesis, the non-malignant status of immortalized lines allows for the specific steps in full malignant transformation to be examined, such as by the introduction of activated oncogenes [76,77]. However, in many cases immortalized cell lines are referred to and used as "normal" cells. This inaccurate characterization may obscure understanding of the multiple errors that permit immortal transformation, and thus aspects of early stage carcinogenesis. While established breast cancer cell lines are usually derived from advanced, metastatic tumors (particularly pleural effusions), and therefore are quite different from immortalized cell lines, immortalized lines themselves have undergone extensive genetic and epigenetic changes, especially in frequently studied aspects of oncogenesis, such as G1 checkpoint function and the DNA damage response. The use of immortalized HMEC as "normal" controls for tumor-derived lines can impede our ability to understand early stages of carcinogenesis, and obscure the potential of treating DCIS-stage changes as additional targets for clinical benefit.

Conclusion

Gene expression profiles and cytological changes in related transcriptional regulators indicate that immortalized HMEC resemble non-invasive breast cancers, such as ductal and lobular carcinomas *in situ*, and are strikingly distinct from finite-lifespan HMEC, particularly with regard to genes involved in proliferation, cell cycle regulation, chromosome structure and the DNA damage response. The comparison of HMEC profiles with lines harboring oncogenic changes (e.g. overexpression of Her-2^{neu}, loss of p53 expression) identifies genes involved in tissue remodeling as well as proinflamatory cytokines and S100 proteins. Studies on carcinogenesis using immortalized cell lines as starting points or "normal" controls need to account for the significant pre-existing genetic and epigenetic changes inherent in such lines before results can be broadly interpreted.

Abbreviations

LI, labeling index; HMEC, human mammary epithelial cells; CKI, cyclin-dependent kinase inhibitor, DCIS, ductal carcinoma in situ; IDC, invasive ductal carcinoma; PD, population doubling; ANOVA, analysis of variance; CIN, chromosomal instability; IGFBP; insulin-like growth factor binding protein; SA-b-gal, senescence associated beta-galactosidase; ECM, extracellular matrix; HCS, high content screening.

Competing interests

The author(s) declare that they have no competing interests.

Authors' contributions

JP, JHL, CT, and KS performed experiments and analyzed primary data. YL, J-JL, MW, SJ and SH analyzed normalized data and interpreted results. JG and MS developed cell lines and analyzed normalized data. JP performed cell-based assays on the transcription factors and regulatory proteins. JP and SH analyzed data from the cell-based assays. YL, MS and SH wrote the manuscript. All authors read and approved the final version of the manuscript.

Additional material

Additional file 1

Table s1: Genes Expressed Concordantly in Pre-Stasis and Post-Selection Cell Types. Compilation of genelists that distinguish the two classes of finite-lifespan HMEC strains.
Click here for file
[http://www.biomedcentral.com/content/supplementary/1476-4598-6-7-S1.doc]

Additional file 2

Table s2. Genes Concordantly Expressed in Pre-stasis, Post-selection or Fully Immortalized HMEC. Compilations of genelists that define the three classes of non-malignant HMEC cell strains and lines.
Click here for file
[http://www.biomedcentral.com/content/supplementary/1476-4598-6-7-S2.doc]

Additional file 3

Table s3: Genes Expressed Concordantly in $p53^{+/+}$ (184A1 and 184B5) or $p53^{-/-}$ (184AA2 and 184AA3) HMEC. Compilations of commonly expressed genes in multiple wild type and $p53^{-}$ immortalized HMEC cell lines.
Click here for file
[http://www.biomedcentral.com/content/supplementary/1476-4598-6-7-S3.doc]

Additional file 4

Table s4. Gene Expression changes of $p53^{+}$ cell lines 184A1 versus 184B5. Compilations of genelists and expression statistics of genes expressed uniquely in two p53 wild type HMEC cell lines.
Click here for file
[http://www.biomedcentral.com/content/supplementary/1476-4598-6-7-S4.doc]

Additional file 5

Table s5. Gene Expression changes of p53+ cell lines 184A1 versus 184B5. Compilations of genelists and expression statistics of genes expressed uniquely in two p53- HMEC cell lines.
Click here for file
[http://www.biomedcentral.com/content/supplementary/1476-4598-6-7-S5.doc]

Additional file 6

Table s6. Gene Expression Changes Resulting from Expression of ERB-B2/Her2neu in 184B5. Compilations of genelists and expression statistics of genes that change expression following overexpression of the Her-2neu oncogene.
Click here for file
[http://www.biomedcentral.com/content/supplementary/1476-4598-6-7-S6.doc]

Acknowledgements

Work performed at LBNL was supported by the Department of Defense BCRP grant W81XWH-04-1-0580 to M.R.S and contract AC03-76SF00098 to the University of California from the US Department of Energy.

References

1. Meyerson M, Counter CM, Eaton EN, Ellisen LW, Steiner P, Caddle SD, Ziaugra L, Beijersbergen RL, Davidoff MJ, Liu Q, Bacchetti S, Haber DA, Weinberg RA: **hEST2, the putative human telomerase catalytic subunit gene, is up-regulated in tumor cells and during immortalization.** *Cell* 1997, **90:**785-795.
2. Stampfer M: **Cholera toxin stimulation of human mammary epithelial cell in culture.** In *vitro* 1982, **18:**531-537.
3. Hammond SL, Ham RG, Stampfer MR: **Serum-free growth of human mammary epithelial cells: Rapid clonal growth in defined medium and extended serial passage with pituitary extract.** *Proceedings of the National Academy of Sciences, USA* 1984, **81:**5435-5439.
4. Stampfer MR, Yaswen P: **Human epithelial cell immortalization as a step in carcinogenesis.** *Cancer Letters* 2003, **194:**199-208.
5. Stampfer MR, Bodnar A, Garbe J, Wong M, Pan A, Villeponteau B, Yaswen P: **Gradual phenotypic conversion associated with immortalization of cultured human mammary epithelial cells.** *Molecular and Cellular Biology* 1997, **8:**2391-2405.
6. Brenner AJ, Stampfer MR, Aldaz CM: **Increased p16 expression with first senescence arrest in human mammary epithelial cells and extended growth capacity with p16 inactivation.** *Oncogene* 1998, **17:**199-205.
7. Romanov S, Kozakiewicz K, Holst C, Stampfer MR, Haupt LM, Tlsty TD: **Normal human mammary epithelial cells spontaneously escape senescence and aquire genomic changes.** *Nature* 2001, **409:**633-637.
8. Nonet G, Stampfer MR, Chin K, Gray JW, Collins CC, Yaswen P: **The ZNF217 gene amplified in breast cancers promotes immortalization of human mammary epithelia cells.** *Cancer Research* 2001, **61:**1250-1254.
9. Stampfer MR, Garbe J, Nijjar T, Wiginton D, Swisshelm K, Yaswen P: **Loss of p53 function accelerates acquisition of telomerase activity in indefinite lifespan human mammary epithelial cell lines.** *Oncogene* 2003, **22:**5238-5251.
10. Strunnikova M, Schagdarsurengin U, Kehlen A, Garbe JC, Stampfer MR, Dammann R: **Chromatin inactivation precedes de novo DNA methylation during the progressive epigenetic silencing of the RASSF1A promoter.** *Molecular and Cellular Biology* 2005, **25:**3923-3933.
11. Stampfer MR, Bartley JC: **Induction of transformation and continuous cell lines from normal human mammary epithelial cells after exposure to benzo(a)pyrene.** *Proceedings of the National Academy of Sciences, USA* 1985, **82:**2394-2398.
12. Garbe J, Wong M, Wigington D, Yaswen P, Stampfer MR: **Viral oncogenes accelerate conversion to immortality of cultured human mammary epithelial cells.** *Oncogene* 1999, **18:**2169-2180.
13. Geradts J, Wilson PA: **High frequency of aberrant p16INK4A expression in human breast cancer.** *American Journal of Pathology* 1996, **149:**15-20.
14. Baylin SB, Herman JG, Graff JR, Vertino PM, Issa JP: **Alterations in DNA methylation: a fundemental aspect of neoplasia.** *Advances in Cancer Research* 1998, **72:**141-196.
15. Crawford YG, Gauthier ML, Joubel A, Mantei K, Kozakiewicz K, Afshar CA, Tlsty TD: **Histologically normal human mammary epithelia with silenced p16(INK4a) overexpress COX-2, promoting a premalignant program.** *Cancer Cell* 2004, **5:**263-273.
16. Holst CR, Nuovo GJ, Esteller M, Chew K, Baylin SB, Herman JG, Tlsty TD: **Methylation of p16(INK4a) promoters occurs in vivo in histologically normal human mammary epithelia.** *Cancer Research* 2003, **63:**1596-1601.
17. Chin K, de Solorzano CO, Knowles D, Jones A, Chou W, Rodriguez EG, Kuo WL, Ljung BM, Chew K, Myambo K, Miranda M, Krig S, Garbe J, Stampfer M, Yaswen P, Gray JW, Lockett SJ: **In situ analyses of genome instability in breast cancer.** *Nature Genetics* 2004, **36:**984-988.
18. Goldstein JC, Rodier F, Garbe JC, Stampfer MR, Campisi J: **Caspase-independent cytochrome c release is a sensitive measure of low-level apoptosis in cell culture models.** *Aging Cell* 2005, **4:**217-222.
19. Stampfer MR, Garbe J, Levine G, Lichtsteiner S, Vasserot AP, Yaswen P: **Expression of the telomerase catalytic subunit, hTERT, induces resistance to transforming growth factor beta growth inhibition in p16INK4A(-) human mammary epithelial cells.** *Proceedings of the National Academy of Sciences, USA* 2001, **98:**4498-4503.
20. Clark R, Stampfer MR, Milley R, O'Rourke , Walen KH, Kriegler M, Kopplin JMC F.: **Transformation of human mammary epithelial cells by oncogenic retroviruses.** *Cancer Research* 1988, **48:**4689-4694.
21. Pierce JH, Arnstein P, DiMarco E, Artrip J, Kraus MH, Lonardo F, Di Fiore PP, Aaronson SA: **Oncogenic potential of erbB-2 in human mammary epithelial cells.** *Oncogene* 1991, **6:**1189-1194.
22. Frittitta L, Vigneri R, Stampfer MR, Goldfine ID: **Insulin receptor overexpression in 184B5 human mammary epithelial cells induces a ligand-dependent transformed phenotype.** *Journal of Cellular Biochemistry* 1995, **57:**666-669.
23. Slonim DK: **From patterns to pathways: gene expression data analysis comes of age.** *Nature Genetics* 2002, **32(s502-s508.):**.
24. Perou CM, Sorlie T, Eisen MB, van de Rijn M, Jeffrey SS, Rees CA, Pollack JR, Ross DT, Johnsen H, Akslen LA, Fluge O, Pergamenschikov A, Williams C, Zhu SX, Lonning PE, Borresen-Dale AL, Brown PO, Botstein D: **Molecular portraits of human breast tumours.** *Nature* 2000, **406:**747-752.
25. Sorlie T, Perou CM, Tibshirani R, Aas T, Geisler S, Johnsen H, Hastie T, Eisen MB, van de Rijn M, Jeffrey SS, Thorsen T, Quist H, Matese JC, Brown PO, Botstein D, Eystein Lonning P, Borresen-Dale AL: **Gene expression patterns of breast carcinomas distinguish tumor subclasses with clinical implications.** *Proceedings of the National Academy of Sciences, USA* 2001, **98:**10869-10874.
26. Whitfield ML, George LK, Grant GD, Perou CM: **Common markers of proliferation.** *Nature Reviews Cancer* 2006, **6:**99-106.
27. Byrne MC, Whitley MZ, Follettie MT: **Preparation of mRNA for expression monitoring.** In *Current Protocols in Molecular Biology* John Wiley and Sons; 2000:22.2.1-22.2.13.
28. Hill AA, Brown EL, Whitley MZ, Tucker-Kellogg G, Hunter CP, Slonim DK: **Evaluation of normalization procedures for oligonucleotide array data based on spiked cRNA controls.** *Genome Biology* 2001, **2:**0055.1-55.13.
29. Affymetrix I: **http://www.affymetrix.com/support/technical/manuals.affx.** .
30. Eisen MB, Spellman PT, Brown POB D.: **Cluster analysis and display of genome-wide expression patterns.** *Proceedings of the National Academy of Sciences, USA* 1998, **95:**14863-14868.
31. Golub TR, Slonim DK, Tamayo P, Huard C, Gaasenbeek M, Mesirov JP, Coller H, Loh ML, Downing JR, Caligiuri MA, Bloomfield CD, Lander ES: **Molecular classification of cancer: class discovery and class prediction by gene expression monitoring.** *Science* 1999, **286:**531-537.
32. Reich M, Ohm K, Angelo M, Tamayo P, Mesirov JP: **GeneCluster 2.0: an advanced toolset for bioarray analysis.** *Bioinformatics* 2004, **20:**1797-1798.
33. Frith M, Fu Y, Yu L, Chen JF, Hansen U, Weng Z: **Detection of functional DNA motifs via statistical over-representation.** *Nucleic Acids Research* 2004, **32:**1372-1381.
34. Kel AE, Gossling E, Reuter I, Cheremushkin E, Kel-Margoulis OV, Wingender E: **MATCH: A tool for searching transcription factor binding sites in DNA sequences.** *Nucleic Acids Research* 2003, **31:**3576-3579.
35. Der SD, Zhou A, Williams BR, Silverman RH: **Identification of genes differentially regulated by interferon alpha, beta, or gamma**

using oligonucleotide arrays. *Proceedings of the National Academy of Sciences, USA* 1998, **95:**15623-15628.
36. Zhang H, Herbert BS, Pan KH, Shay JW, Cohen SN: **Disparate effects of telomere attrition on gene expression during replicative senescence of human mammary epithelial cells cultured under different conditions.** *Oncogene* 2004, **23:**6193-6198.
37. Andrews HN, Mullan PB, McWilliams S, Sebelova S, Quinn JE, Gilmore PM, McCabe N, Pace A, Koller B, Johnston PG, Haber DA, Harkin DP: **BRCA1 regulates the interferon gamma-mediated apoptotic response.** *Journal of Biological Chemistry* 2002, **277:**26225-26232.
38. Muller H, Bracken AP, Vernell R, Moroni MC, Christians F, Grassilli E, Prosperini E, Vigo E, Oliner JD, Helin K: **E2Fs regulate the expression of genes involved in differentiation, development, proliferation, and apoptosis.** *Genes and Developement* 2001, **15:**267-285.
39. Ren B, Cam H, Takahashi Y, Volkert T, Terragni J, Young RA, Dynlacht BD: **E2F integrates cell cycle progression with DNA repair, replication, and G(2)/M checkpoints.** *Genes and Developement* 2002, **16:**245-256.
40. Coller HA, Grandori C, Tamayo P, Colbert T, Lander ES, Eisenman RN, Golub TR: **Expression analysis with oligonucleotide microarrays reveals that MYC regulates genes involved in growth, cell cycle, signaling, and adhesion.** *Proceedings of the National Academy of Sciences, USA* 2000, **97:**3260-3265.
41. Lawlor ER, Soucek L, Brown-Swigart L, Shchors K, Bialucha CU, Evan GI: **Reversible kinetic analysis of Myc targets in vivo provides novel insights into Myc-mediated tumorigenesis.** *Cancer Research* 2006, **66:**4591-4601.
42. Watson JD, Oster SK, Shago M, Khosravi F, Penn LZ: **Identifying genes regulated in a Myc-dependent manner.** *Journal of Biological Chemistry* 2002, **277:**36921-36930.
43. Paine TM, Soule HD, Pauley RJ, Dawson PJ: **Characterization of epithelial phenotypes in mortal and immortal human breast cells.** *International Journal of Cancer* 1992, **50:**463-473.
44. Zhang J, R. S, Dai Q, Song J, Barlow SC, Yin L, Sloane BF, Miller FR, Meschonat C, Li BD, Abreo F, Keppler D: **Cystatin m: a novel candidate tumor suppressor gene for breast cancer.** *Cancer Research* 2004, **64:**6957-6964.
45. Rhodes DR, Kalyana-Sundaram S, Mahavisno V, Barrette TR, Ghosh D, Chinnaiyan AM: **Mining for regulatory programs in the cancer transcriptome.** *Nature Genetics* 2005, **37:**579-583.
46. Dai H, van't Veer L, Lamb J, He YD, Mao M, Fine BM, Bernards R, van de Vijver M, Deutsch P, Sachs A, Stoughton R, Friend S: **A cell proliferation signature is a marker of extremely poor outcome in a subpopulation of breast cancer patients.** *Cancer Research* 2005, **65:**4059-4066.
47. Seth A, Kitching R, Landberg G, Xu J, Zubovits J, Burger AM: **Gene expression profiling of ductal carcinomas in situ and invasive breast tumors.** *Anticancer Research* 2003, **23:**2043-2051.
48. Huang E, Cheng SH, Dressman H, Pittman J, Tsou MH, Horng CF, Bild A, Iversen ES, Liao M, Chen CM, West M, Nevins JR, Huang AT: **Gene expression predictors of breast cancer outcomes.** *Lancet* 2003, **361:**1590-1596.
49. Pollak MN, Schernhammer ES, Hankinson SE: **Insulin-like growth factors and neoplasia.** *Nature Reviews Cancer* 2004, **4:**505-518.
50. Yu H, Rohan T: **Role of the insulin-like growth factor family in cancer development and progression.** *Journal of the National Cancer Institute* 2000, **92:**1472-1489.
51. Deng CX, Brodie SG: **Roles of BRCA1 and its interacting proteins.** *Bioessays* 2000, **22:**728-737.
52. Luker KE, Pica CM, Schreiber RD, Piwnica-Worms D: **Overexpression of IRF9 confers resistance to antimicrotubule agents in breast cancer cells.** *Cancer Research* 2001, **61:**6540-6547.
53. Gilmore PM, McCabe N, Quinn JE, Kennedy RD, Gorski JJ, Andrews HN, McWilliams S, Carty M, Mullan PB, Duprex WP, Liu ET, Johnston PG, Harkin DP: **BRCA1 interacts with and is required for paclitaxel-induced activation of mitogen-activated protein kinase kinase kinase 3.** *Cancer Research* 2004, **64:**4184-4154.
54. Lasorella A, Noseda M, Beyna M, Yokota Y, Iavarone A: **Id2 is a retinoblastoma protein target and mediates signalling by Myc oncoproteins.** *Nature* 2000, **407:**592-598.
55. Beger C, Pierce LN, Kruger M, Marcusson EG, Robbins JM, Welcsh P, Welch PJ, Welte K, King MC, Barber JR, Wong-Staal F: **Identification of Id4 as a regulator of BRCA1 expression by using a ribozyme-library-based inverse genomics approach.** *Proceedings of the National Academy of Sciences, USA* 2001, **98:**130-135.
56. Welcsh PL, Lee MK, Gonzalez-Hernandez RM, Black DJ, Mahadevappa M, Swisher EM, Warrington JA, King MC: **BRCA1 transcriptionally regulates genes involved in breast tumorigenesis.** *Proceedings of the National Academy of Sciences, USA* 2002, **28:**7560-7565.
57. Donato R: **S100: a multigenic family of calcium-modulated proteins of the EF-hand type with intracellular and extracellular functional roles.** *International Journal of Biochemistry and Cell Biology* 2001, **33:**637-668.
58. Poola I, DeWitty RL, Marshalleck JJ, Bhatnagar R, Abraham J, Leffall LD: **Identification of MMP-1 as a putative breast cancer predictive marker by global gene expression analysis.** *Nature Medicine* 2005, **11:**481-483.
59. Emberley ED, Niu Y, Njue C, Kliewer EV, Murphy LC, Watson PH: **Psoriasin (S100A7) expression is associated with poor outcome in estrogen receptor-negative invasive breast cancer.** *Clinical Cancer Research* 2003, **2627-2631:**.
60. Miller LD, Smeds J, George J, Vega VB, Vergara L, Ploner A, Pawitan Y, Hall P, Klaar S, Liu ET, Bergh J: **An expression signature for p53 status in human breast cancer predicts mutation status, transcriptional effects, and patient survival.** *Proceedings of the National Academy of Sciences, USA* 2005, **102:**13550-13555.
61. Ziegler EC, Ghosh S: **Regulating inducible transcription through controlled localization.** *SciSTKE* 2005, **284:**re6.
62. Fabbro M, Schuechner S, Au WW, Henderson BR: **BARD1 regulates BRCA1 apoptotic function by a mechanism involving nuclear retention.** *Experimental Cell Research* 2004, **298:**661-673.
63. Won J, Yim J, Kim TK: **Sp1 and Sp3 recruit histone deacetylase to repress transcription of human telomerase reverse transcriptase (hTERT) promoter in normal human somatic cells.** *Journal of Biological Chemistry* 2002, **277(38230-383238.):**.
64. Cong YS, Bacchetti S: **Histone deacetylation is involved in the transcriptional repression of hTERT in normal human cells.** *Journal of Biological Chemistry* 2000, **275:**35665-35668.
65. Kyo S, Takakura M, Taira T, Kanaya T, Itoh H, Yutsudo M, Ariga H, Inoue M: **Sp1 cooperates with c-Myc to activate transcription of the human telomerase reverse transcriptase gene (hTERT).** *Nucleic Acids Research* 2000, **28:**669-677.
66. Li H, Lee TH, Avraham H: **A novel tricomplex of BRCA1, Nmi, and c-Myc inhibits c-Myc-induced human telomerase reverse transcriptase gene (hTERT) promoter activity in breast cancer.** *Journal of Biological Chemistry* 2002, **277:**20965-20973.
67. Porter D, Lahti-Domenici J, Keshaviah A, Bae YK, Argani P, Marks J, Richardson A, Cooper A, Strausberg R, Riggins GJ, Schnitt S, Gabrielson E, Gelman R, Polyak K: **Molecular markers in ductal carcinoma in situ of the breast.** *Molecular Cancer Research* 2003, **1:**362-375.
68. Zhao H, Langerod A, Ji Y, Nowels KW, Nesland JM, Tibshirani R, Bukholm IK, Karesen R, Botstein D, Borresen-Dale AL, Jeffrey SS: **Different gene expression patterns in invasive lobular and ductal carcinomas of the breast.** *Molecular Biology of the Cell* 2004, **15:**2523-2536.
69. Meeker AK, Hicks JL, Iacobuzio-Donahue CA, Montgomery EA, Westra WH, Chan TY, Ronnett BM, De Marzo AM: **Telomere length abnormalities occur early in the initiation of epithelial carcinogenesis.** *Clinical Cancer Research* 2004, **10:**3317-3326.
70. Burstein HJ, Polyak K, Wong JS, Lester SC, Kaelin CM: **Ductal Carcinoma in Situ of the Breast.** *New England Journal of Medicine* 2004, **350:**1430-1441.
71. Baxter NN, Virnig BA, Durham SB, Tuttle TM: **Trends in the Treatment of Ductal Carcinoma In Situ of the Breast.** *Journal of the National Cancer Institute* 2004, **96:**443-448.
72. Tsikitis VL, Chung MA: **Biology of ductal carcinoma in situ classification based on biologic potential.** *American Journal of Clinical Oncology* 2006, **29:**305-310.
73. Boland GP, Butt IS, Prasad R, Knox WF, Bundred NJ: **COX-2 expression is associated with an aggressive phenotype in ductal carcinoma in situ.** *British Journal of Cancer* 2004, **90:**423-429.
74. Adler AS, Lin M, Horlings H, Nuyten DS, van de Vijver MJ, Chang HY: **Genetic regulators of large-scale transcriptional signatures in cancer.** *Nature Genetics* 2006, **38:**421-430.
75. Debnath J, Mills KR, Collins NL, Reginato MJ, Muthuswamy SK, Brugge JS: **The role of apoptosis in creating and maintaining luminal space within normal and oncogene-expressing mammary acini.** *Cell* 2002, **111:**29-40.
76. Thompson EW, Torri J, Sabol M, Sommers CL, Byers S, Valverius EM, Martin GR, Lippman ME, Stampfer MR, Dickson RB: **Oncogene-induced basement membrane invasiveness in human mammary epithelial cells.** *Clinical and Experimental Metastasis* 1994, **12:**181-194.
77. Wang B, Soule HD, FR. M: **Transforming and oncogenic potential of activated c-Ha-ras in three immortalized human breast epithelial cell lines.** *Anticancer Research* 1997, **17:**4387-4394.

Table s1: Genes Expressed Concordantly in Pre-Stasis and Post-Selection Cell Types

Genes expressed in pre-stasis HMEC	
Cytoskeleton	
ACTA2	actin, alpha 2, smooth muscle, aorta
ACTG2	actin, gamma 2, smooth muscle, enteric
CDH2	cadherin 2, type 1, N-cadherin (neuronal)
CNN3	calponin 3, acidic
MACF1	microtubule-actin crosslinking factor 1
MAP2	microtubule-associated protein 2
TPM2	tropomyosin 2 (beta)
TUBB	tubulin, beta polypeptide
Extracellular Matrix and Cell-Cell Communication	
ADAMTS1	a disintegrin-like and metalloprotease (reprolysin type) with thrombospondin type 1 motif, 1
ADAMTS5	a disintegrin-like and metalloprotease (reprolysin type) with thrombospondin type 1 motif, 5 (aggrecanase-2)
CAST	calpastatin, calpain inhibitor
COL1A2	collagen, type I, alpha 2
COL2A1	collagen, type II, alpha 1 (primary osteoarthritis, spondyloepiphyseal dysplasia, congenital)
COL4A1	collagen, type IV, alpha 1
COL6A1	collagen, type VI, alpha 1
COL6A2	collagen, type VI, alpha 2
CPA4	carboxypeptidase A4
CST6	cystatin E/M
CTGF	connective tissue growth factor
DSC2	desmocollin 2
EDIL3	EGF-like repeats and discoidin I-like domains 3
EGFL5	EGF-like-domain, multiple 5
ENC1	ectodermal-neural cortex (with BTB-like domain)
ITGB3	integrin, beta 3 (platelet glycoprotein IIIa, antigen CD61)
KLK10	kallikrein 10
KLK5	kallikrein 5
KLK6	kallikrein 6 (neurosin, zyme)
KLK7	kallikrein 7 (chymotryptic, stratum corneum)
KRT23	keratin 23 (histone deacetylase inducible)
MCAM	melanoma cell adhesion molecule
MGP	matrix Gla protein
NET-6	transmembrane 4 superfamily member tetraspan NET-6
PLOD	procollagen-lysine, 2-oxoglutarate 5-dioxygenase (lysine hydroxylase, Ehlers-Danlos syndrome type VI)
PMP22	peripheral myelin protein 22
RSN	restin (Reed-Steinberg cell-expressed intermediate

	filament-associated protein)
TIMP3	tissue inhibitor of metalloproteinase 3 (Sorsby fundus dystrophy, pseudoinflammatory)
TMEPAI	transmembrane, prostate androgen induced RNA
Protein Metabolism and Turnover	
CTSB	cathepsin B
UCHL1	ubiquitin carboxyl-terminal esterase L1 (ubiquitin thiolesterase)
Protein Secretion	
GCNT1	glucosaminyl (N-acetyl) transferase 1, core 2 (beta-1,6-N-acetylglucosaminyltransferase)
TRAM	translocating chain-associating membrane protein
Metabolism and Homeostasis	
BPGM	2,3-bisphosphoglycerate mutase
CLIC3	chloride intracellular channel 3
LIPG	lipase, endothelial
LOXL2	lysyl oxidase-like 2
SLC16A4	solute carrier family 16 (monocarboxylic acid transporters) , member 4
SLC17A5	solute carrier family 17 (anion/sugar transporter), member 5
Transcription and Translation	
GLIS2	Kruppel-like zinc finger protein GLIS2
IRX1	iroquois homeobox protein 1
Signal Transduction	
OXTR	oxytocin receptor
RSU1	Ras suppressor protein 1
STAC	src homology three (SH3) and cysteine rich domain
SORT1	sortilin 1; NTr co-receptor for nerve growth factor
Cell Cycle	
CDKN2B	cyclin-dependent kinase inhibitor 2B (p15, inhibits CDK4)
Other	
DESC1	DESC1 protein
DKFZP564G202	DKFZP564G202 protein
FLJ11036	hypothetical protein FLJ11036
FLJ40021	hypothetical protein FLJ40021
KIAA0275	KIAA0275 gene product
KIAA1497	KIAA1497 protein
LBH	likely ortholog of mouse limb-bud and heart gene

LOC115207	hypothetical protein BC013764
LOC91663	hypothetical protein BC013995
LOC92689	hypothetical protein BC001096
MIG2	mitogen inducible 2
PPAP2A	phosphatidic acid phosphatase type 2A
SPG3A	spastic paraplegia 3A (autosomal dominant)
TRIM2	tripartite motif-containing 2
WSB2	likely ortholog of mouse WD-40-repeat-containing protein with a SOCS box 2

Genes expressed in post-selection HMEC

Extracellular Matrix and Cell-Cell Communication

CSPG2	chondroitin sulfate proteoglycan 2 (versican)
DLG7	discs, large homolog 7 (Drosophila)
IFI16	interferon, gamma-inducible protein 16
IL18	interleukin 18 (interferon-gamma-inducing factor)
IL1A	interleukin 1, alpha
ITGB3BP	integrin beta 3 binding protein (beta3-endonexin)
HBP17	heparin-binding growth factor binding protein
PLAB	prostate differentiation factor; GDF15
PMSCL1	polymyositis/scleroderma autoantigen 1, 75kDa
PLAU	plasminogen activator, urokinase
S100A8	S100 calcium binding protein A8 (calgranulin A)
SERPINA1	serine (or cysteine) proteinase inhibitor, clade A (alpha-1 antiproteinase, antitrypsin), member 1
SERPINB3	serine (or cysteine) proteinase inhibitor, clade B (ovalbumin), member 3

Protein Metabolism and Turnover

HSPC150	HSPC150 protein similar to ubiquitin-conjugating enzyme
PSMB8	proteasome (prosome, macropain) subunit, beta type, 8 (large multifunctional protease 7)
UBE2C	ubiquitin-conjugating enzyme E2C
UHRF1	ubiquitin-like, containing PHD and RING finger domains, 1

Metabolism and Homeostasis

DHFR	dihydrofolate reductase
PAICS	phosphoribosylaminoimidazole carboxylase, phosphoribosylaminoimidazole succinocarboxamide synthetase

Transcription and Translation

ANKT	nucleolar protein ANKT
LYAR	hypothetical protein FLJ20425
MKI67	antigen identified by monoclonal antibody Ki-67
RAMP	RA-regulated nuclear matrix-associated protein

Signal Transduction	
GG2-1	TNF-induced protein; TNFAIP8, oncogenic negative regulator of extrinsic apoptosis
LGN	LGN protein; GPSM2, regulator of heterotrimeric G-protein signaling
MELK	maternal embryonic leucine zipper kinase
SHCBP1	likely ortholog of mouse Shc SH2-domain binding protein 1
TOPK	T-LAK cell-originated protein kinase
VRP	vascular Rab-GAP/TBC-containing
Cell Cycle	
BIRC5	baculoviral IAP repeat-containing 5 (survivin)
BUB1	BUB1 budding uninhibited by benzimidazoles 1 homolog (yeast)
BUB3	BUB3 budding uninhibited by benzimidazoles 3 homolog (yeast)
CCNA2	cyclin A2
CCNB1	cyclin B1
CCNB2	cyclin B2
CDC2	cell division cycle 2, G1 to S and G2 to M
CDC25B	cell division cycle 25B
CDKN3	cyclin-dependent kinase inhibitor 3 (CDK2-associated dual specificity phosphatase)
CKS1B	CDC28 protein kinase regulatory subunit 1B
CSE1L	CSE1 chromosome segregation 1-like (yeast)
GMNN	geminin, DNA replication inhibitor
MAD2L1	MAD2 mitotic arrest deficient-like 1 (yeast)
MCM2	MCM2 minichromosome maintenance deficient 2, mitotin (S. cerevisiae)
MCM6	MCM6 minichromosome maintenance deficient 6 (MIS5 homolog, S. pombe) (S. cerevisiae)
MCM7	MCM7 minichromosome maintenance deficient 7 (S. cerevisiae)
NASP	nuclear autoantigenic sperm protein (histone-binding)
PCNA	proliferating cell nuclear antigen
PRC1	protein regulator of cytokinesis 1
RFC4	replication factor C (activator 1) 4, 37kDa
RRM2	ribonucleotide reductase M2 polypeptide
SMC4L1	SMC4 structural maintenance of chromosomes 4-like 1 (yeast)
STK12	serine/threonine kinase 12
TOP2A	topoisomerase (DNA) II alpha 170kDa
ZWINT	ZW10 interactor
Other	
C10orf3	chromosome 10 open reading frame 3

C20orf1	chromosome 20 open reading frame 1
CMG2	capillary morphogenesis protein 2
DKFZp762E1312	hypothetical protein DKFZp762E1312
FLJ20354	hypothetical protein FLJ20354
HMGB2	high-mobility group box 2
HMGN2	high-mobility group nucleosomal binding domain 2
IER5	immediate early response 5
KIAA0101	KIAA0101 gene product
KIAA0186	KIAA0186 gene product
KIAA1393	KIAA1393 protein
LOC113115	hypothetical protein BC011716
LOC134147	hypothetical protein BC001573
LOC51659	HSPC037 protein
MGC34923	hypothetical protein MGC34923
PRO2000	PRO2000 protein
PSIP2	PC4 and SFRS1 interacting protein 2
SRPX	sushi-repeat-containing protein, X chromosome

Table s2. Genes Concordantly Expressed in Pre-stasis, Post-selection or Fully Immortalized HMEC

Genes over-expressed in pre-stasis HMEC		
Cytoskeleton		
	ACTA2	actin, alpha 2, smooth muscle, aorta
	ACTG2	actin, gamma 2, smooth muscle, enteric
	CDH2	cadherin 2, type 1, N-cadherin (neuronal)
	MAP2	microtubule-associated protein 2
	RSN	restin (Reed-Steinberg cell-expressed intermediate filament-associated protein)
	TPM2	tropomyosin 2 (beta)
Extracellular Matrix and Cell-Cell Interactions		
	ADAMTS5	a disintegrin-like and metalloprotease (reprolysin type) with thrombospondin type 1 motif, 5 (aggrecanase-2)
	COL1A2	collagen, type I, alpha 2
	COL2A1	collagen, type II, alpha 1 (primary osteoarthritis, spondyloepiphyseal dysplasia, congenital)
	COL4A1	collagen, type IV, alpha 1
	COL4A2	collagen, type IV, alpha 2
	COL6A1	collagen, type VI, alpha 1
	COL6A2	collagen, type VI, alpha 2
	CST6	cystatin E/M
	CTSB	cathepsin B
	DSC2	desmocollin 2
	EGFL5	EGF-like-domain, multiple 5
	GJA5	gap junction protein, alpha 5, 40kDa (connexin 40)
	IGFBP3	insulin-like growth factor binding protein 3
	ITGB3	integrin, beta 3 (platelet glycoprotein IIIa, antigen CD61)
	KLK6	kallikrein 6 (neurosin, zyme)
	KLK7	kallikrein 7 (chymotryptic, stratum corneum)
	KLK10	kallikrein 10
	KRT23	keratin 23 (histone deacetylase inducible)
	LIPG	lipase, endothelial
	LOC143903	layilin
	LTBP2	latent transforming growth factor beta binding protein 2
	MGP	matrix Gla protein
	MIG2	mitogen inducible 2
	MOX2	antigen identified by monoclonal antibody MRC OX-2
	NET-6	transmembrane 4 superfamily member tetraspan NET-6
	NY-REN-25	NY-REN-25 antigen
	PMP22	peripheral myelin protein 22
	SERPING1	serine (or cysteine) proteinase inhibitor, clade G (C1 inhibitor), member 1, (angioedema, hereditary)

	SPP1	secreted phosphoprotein 1 (osteopontin, bone sialoprotein I, early T-lymphocyte activation 1)
	TIMP3	tissue inhibitor of metalloproteinase 3 (Sorsby fundus dystrophy, pseudoinflammatory)
	WNT5B	wingless-type MMTV integration site family, member 5B
Metabolism		
	BPGM	2,3-bisphosphoglycerate mutase
	CLIC3	chloride intracellular channel 3
	FADS3	fatty acid desaturase 3
	SLC16A4	solute carrier family 16 (monocarboxylic acid transporters), member 4
Protein Biogenesis and Turnover		
	SELM	selenoprotein SelM
	UCHL1	ubiquitin carboxyl-terminal esterase L1 (ubiquitin thiolesterase)
Protein Secretion		
	COPZ2	coatomer protein complex, subunit zeta 2
	DESC1	DESC1 protein
	EHD3	EH-domain containing 3
	GCNT1	glucosaminyl (N-acetyl) transferase 1, core 2 (beta-1,6-N-acetylglucosaminyltransferase)
	SEC14L2	SEC14-like 2 (S. cerevisiae)
	SORT1	sortilin 1
	TRAM	translocating chain-associating membrane protein
Signal Transduction		
	CHRNB1	cholinergic receptor, nicotinic, beta polypeptide 1 (muscle)
	OXTR	oxytocin receptor
Transcription and Translation		
	GLIS2	Kruppel-like zinc finger protein GLIS2
	LMCD1	LIM and cysteine-rich domains 1
	RBP1	retinol binding protein 1, cellular
	RUNX1	runt-related transcription factor 1 (acute myeloid leukemia 1; aml1 oncogene)
Other		
	AF1Q	ALL1-fused gene from chromosome 1q
	ALEX2	armadillo repeat protein ALEX2
	DESC1	DESC1 protein
	DKFZP564G202	DKFZP564G202 protein
	DKFZP586H2123	DKFZP586H2123 protein
	FLJ14054	hypothetical protein FLJ14054
	FLJ40021	hypothetical protein FLJ40021

	KIAA0275	KIAA0275 gene product
	KIAA0599	KIAA0599 protein
	KIAA1161	KIAA1161 protein
	KIAA1497	KIAA1497 protein

Genes over-expressed in post-selection HMEC

Cytoskeleton		
	ACTN1	actinin, alpha 1
	ACTN4	actinin, alpha 4
	KIAA0992	palladin, interacts with a-actinin
	NID	nidogen (enactin)
	TAGLN	transgelin
	SRPX	sushi-repeat-containing protein, X chromosome
	TPM4	tropomyosin 4
	BEX1	brain expressed, X-linked 1
	C20orf80, CRIP2	chromosome 20 open reading frame 80, cysteine-rich protein 2
	P311	P311 protein
Extracellular Matrix and Cell-Cell Interactions		
	ADAM23	a disintegrin and metalloproteinase domain 23
	ADAMTS1	a disintegrin-like and metalloprotease (reprolysin type) with thrombospondin type 1 motif, 1
	CMG2	capillary morphogenesis protein 2, anthrax co-receptor with TEM-8
	CNTN1	contactin 1
	CNTN3	contactin 3 (plasmacytoma associated)
	COL5A2	collagen, type V, alpha 2
	CSPG2	chondroitin sulfate proteoglycan 2 (versican)
	CTGF	connective tissue growth factor
	DRAPC1	hypothetical protein DRAPC1, regulated be b-catenin
	EDIL3	EGF-like repeats and discoidin I-like domains 3
	FN1	fibronectin 1
	FZD7	frizzled homolog 7 (Drosophila)
	GJB2	gap junction protein, beta 2, 26kDa (connexin 26)
	HNT	neurotrimin
	ITGB6	integrin, beta 6
	KRT6B	keratin 6B
	L1CAM	L1 cell adhesion molecule (hydrocephalus, stenosis of aqueduct of Sylvius 1, MASA (mental retardation, aphasia, shuffling gait and adducted thumbs) syndrome, spastic paraplegia 1)
	MIA	melanoma inhibitory activity
	MMP10	matrix metalloproteinase 10 (stromelysin 2)
	MMP14	matrix metalloproteinase 14 (membrane-inserted)
	MMP2	matrix metalloproteinase 2 (gelatinase A, 72kDa gelatinase, 72kDa type IV collagenase)
	MPPE1	metallo phosphoesterase

	PCDH19	protocadherin 19
	PLAU	plasminogen activator, urokinase
	PTHLH	parathyroid hormone-like hormone
	SERPINA1	serine (or cysteine) proteinase inhibitor, clade A (alpha-1 antiproteinase, antitrypsin), member 1
	SERPINE2	serine (or cysteine) proteinase inhibitor, clade E (nexin, plasminogen activator inhibitor type 1), member 2
	TMEM2	transmembrane protein 2
	TRA1	tumor rejection antigen (gp96) 1
	TRAP150	thyroid hormone receptor-associated protein, 150 kDa subunit
	TTC3	tetratricopeptide repeat domain 3
	VLDLR	very low density lipoprotein receptor
Metabolism		
	ATP1B1	ATPase, Na+/K+ transporting, beta 1 polypeptide
	CAT	catalase
	CLN2	ceroid-lipofuscinosis, neuronal 2, late infantile (Jansky-Bielschowsky disease)
	GCLM	glutamate-cysteine ligase, modifier subunit
	HEPH	hephaestin; iron homeostasis, macular degenration linked
	KMO	kynurenine 3-monooxygenase (kynurenine 3-hydroxylase)
	SLC7A8	solute carrier family 7 (cationic amino acid transporter, y+ system), member 8
Protein Biogenesis and Turnover		
	BHLHB3	basic helix-loop-helix domain containing, class B, 3; lysosomal protease
	CTSB	cathepsin B
	CTSL2	cathepsin L2
	PA200	proteasome activator 200 kDa
	TPST1	tyrosylprotein sulfotransferase 1
Protein Secretion		
	CALU	calumenin
	LPHH1	latrophilin 1
Signal Transduction		
	ARK5	KIAA0537 gene product, IGF-1 signaling, metastasis and invasion of myeloma cells
	INHBA	inhibin, beta A (activin A, activin AB alpha polypeptide)
	IQGAP1	IQ motif containing GTPase activating protein 1
	MYLK	myosin, light polypeptide kinase
	PTK7	PTK7 protein tyrosine kinase 7
	SPRY2	sprouty homolog 2 (Drosophila), neg regul EGFR signaling, dn-reg in PrCa
Transcription and Translation		
	HDAC3	histone deacetylase 3

Other	
C20orf80, CRIP2	chromosome 20 open reading frame 80, cysteine-rich protein 2
DKFZP564K0322	hypothetical protein DKFZp564K0322
DKFZp564O1278, FLJ22774	hypothetical protein DKFZp564O1278, hypothetical protein FLJ22774
DKFZP761F241	hypothetical protein DKFZp761F241
FLJ10856	hypothetical protein FLJ10856
FLJ20481	hypothetical protein FLJ20481
FLJ31810	hypothetical protein FLJ31810
FLJ90440	hypothetical protein FLJ90440
MGC12335	hypothetical protein MGC12335
Genes over-expressed in fully immortalized HMEC	
Cytoskeleton	
STOML2	stomatin (EPB72)-like 2; raft assocation
ECM and Cell-Cell Communication	
8D6A	8D6 antigen
C1QBP, MGC4189	complement component 1, q subcomponent binding protein, hypothetical protein MGC4189
IL18	interleukin 18 (interferon-gamma-inducing factor)
LRPPRC	leucine-rich PPR-motif containing
NMU	neuromedin U
PDZK3	PDZ domain containing 3
PTGES	prostaglandin E synthase; PIG12, p53-induced
SECTM1	secreted and transmembrane 1
HDGF	hepatoma-derived growth factor (high-mobility group protein 1-like)
Metabolism and Homeostasis	
ADA	adenosine deaminase
ADPRT	ADP-ribosyltransferase (NAD+; poly (ADP-ribose) polymerase); PARP
ATP5O	ATP synthase, H+ transporting, mitochondrial F1 complex, O subunit (oligomycin sensitivity conferring protein)
CLNS1A	chloride channel, nucleotide-sensitive, 1A
CYC1	cytochrome c-1
DC12, SCNN1A	DC12 protein, sodium channel, nonvoltage-gated 1 alpha
EEG1	likely ortholog of mouse embryonic epithelial gene 1, transporter
IMPDH2	IMP (inosine monophosphate) dehydrogenase 2
KYNU	kynureninase (L-kynurenine hydrolase)
MAOA	monoamine oxidase A
MCCC2	methylcrotonoyl-Coenzyme A carboxylase 2 (beta)
MFTC	mitochondrial folate transporter/carrier
OXA1L	oxidase (cytochrome c) assembly 1-like
SDHB	succinate dehydrogenase complex, subunit B, iron sulfur (Ip)

SLC21A12	solute carrier family 21 (organic anion transporter), member 12
SORD	sorbitol dehydrogenase
SUCLG1	succinate-CoA ligase, GDP-forming, alpha subunit
Protein Biogenesis and Turnover	
CABC1	chaperone, ABC1 activity of bc1 complex like (S. pombe)
HS6ST2	heparan sulfate 6-O-sulfotransferase 2
HSPA9B	heat shock 70kDa protein 9B (mortalin-2)
HSPD1	heat shock 60kDa protein 1 (chaperonin)
PPT1	palmitoyl-protein thioesterase 1 (ceroid-lipofuscinosis, neuronal 1, infantile)
TRAP1	heat shock protein 75
USP3	ubiquitin specific protease 3
Protein Secretion	
MAL2	mal, T-cell differentiation protein 2
Signal Transduction	
ADRB2	adrenergic, beta-2-, receptor, surface
DDEF1	development and differentiation enhancing factor 1, ARF GAP
DDX18	DEAD/H (Asp-Glu-Ala-Asp/His) box polypeptide 18 (Myc-regulated)
FKBP5	FK506 binding protein 5
VIP32	hypothetical protein PP5395, activator of MAPK signaling
Cell Cycle	
CDC25B	cell division cycle 25B
CDCA7	cell division cycle associated 7
CKS1B	CDC28 protein kinase regulatory subunit 1B
NEK2	NIMA (never in mitosis gene a)-related kinase 2
STK6	serine/threonine kinase 6
Transcription and Translation	
DKC1	dyskeratosis congenita 1, dyskerin; ribosomal function, binds TERC
DSIPI	delta sleep inducing peptide, immunoreactor; GILZ, IL-10 induced, antiinflamatory and antiapoptotic role
EEF1D	eukaryotic translation elongation factor 1 delta (guanine nucleotide exchange protein)
EIF3S6	eukaryotic translation initiation factor 3, subunit 6 48kDa
FBL	fibrillarin; nucleolar protein required for rRNA processing
FTSJ2	FtsJ homolog 2 (E. coli), nucleolar rRNA methyl-transferase
GEMIN5	gem (nuclear organelle) associated protein 5
ID3	inhibitor of DNA binding 3, dominant negative helix-loop-helix protein
KARS	lysyl-tRNA synthetase
MAGOH	mago-nashi homolog, proliferation-associated (Drosophila); nucleolar exon-junction complex protein
MRPL22	mitochondrial ribosomal protein L22

	MRPL3	mitochondrial ribosomal protein L3
	MRPL30	mitochondrial ribosomal protein L30
	MRPS27	mitochondrial ribosomal protein S27
	MYC	v-myc myelocytomatosis viral oncogene homolog (avian)
	NOL5A	nucleolar protein 5A (56kDa with KKE/D repeat)
	NOLA2	nucleolar protein family A, member 2 (H/ACA small nucleolar RNPs)
	NOLC1	nucleolar and coiled-body phosphoprotein 1
	NUP133	nucleoporin 133kDa
	PRPF4	PRP4 pre-mRNA processing factor 4 homolog (yeast)
	RFC4	replication factor C (activator 1) 4, 37kDa
	RIP60	replication initiation region protein (60kD)
	RPC5	RNA polymerase III 80 kDa subunit RPC5
	Rpo1-2	similar to DNA-directed RNA polymerase I (135 kDa)
	RPS21	ribosomal protein S21
	SNX5	sorting nexin 5
	TCERG1	transcription elongation regulator 1 (CA150)
	TCOF1	Treacher Collins-Franceschetti syndrome 1; pre-rRNA methylation, neural crest and macular degeneration linked
	WDR3	WD repeat domain 3
	ZRF1	zuotin related factor 1; MPHOSH11, ribosomal co-chaparone
Other		
	C20orf44	chromosome 20 open reading frame 44
	CECR5	cat eye syndrome chromosome region, candidate 5, CHR22
	CGI-09	CGI-09 protein
	DKFZP564M182	DKFZP564M182 protein
	DKFZp762L0311	hypothetical protein DKFZp762L0311
	FLJ10407	hypothetical protein FLJ10407
	FLJ10439	hypothetical protein FLJ10439
	FLJ12436	hypothetical protein FLJ12436
	JTB	jumping translocation breakpoint
	MTX1	metaxin 1
	TH1L	TH1-like (Drosophila)

Table s3: Genes Expressed Concordantly in $p53^{+/+}$ (184A1 and 184B5) or $p53^{-/-}$ (184AA2 and 184AA3) HMEC.

Genes overexpressed in $p53^{+/+}$ HMEC lines over $p53^{-/-}$ HMEC lines		
	Cytoskeleton	
	CYFIP2	cytoplasmic FMR1 interacting protein 2
	EMS1	ems1 sequence (mammary tumor and squamous cell carcinoma-associated (p80/85 src substrate); cortactin, part of 11q13 amplicon
	FAT	FAT tumor suppressor homolog 1 (Drosophila)
	FLNB	filamin B, beta (actin binding protein 278)
	RAI14	retinoic acid induced 14
	TRIM22	tripartite motif-containing 22
	TRIM5	tripartite motif-containing 5
	TUBA3	tubulin, alpha 3
	TUBB-5	tubulin beta-5
	WDR1	WD repeat domain 1
	ECM and Cell-Cell Communication	
	ADM	adrenomedullin
	BST2	bone marrow stromal cell antigen 2
	CD59	CD59 antigen p18-20 (antigen identified by monoclonal antibodies 16.3A5, EJ16, EJ30, EL32 and G344)
	COL12A1	collagen, type XII, alpha 1
	FAP	fibroblast activation protein, alpha
	FBN1	fibrillin 1 (Marfan syndrome)
	FBN2	fibrillin 2 (congenital contractural arachnodactyly)
	FLRT3	fibronectin leucine rich transmembrane protein 3
	FN1	fibronectin 1
	FSTL1	follistatin-like 1
	HAS3	hyaluronan synthase 3
	HBP17	heparin-binding growth factor binding protein
	HSPG2	heparan sulfate proteoglycan 2 (perlecan)
	IFITM1, PTS	6-pyruvoyltetrahydropterin synthase, interferon induced transmembrane protein 1 (9-27)
	IGFBP6	insulin-like growth factor binding protein 6
	IGSF4	immunoglobulin superfamily, member 4
	ITGB5	integrin, beta 5
	KIAA1260	neuroligin
	KRT15	keratin 15
	LIF	leukemia inhibitory factor (cholinergic differentiation factor)
	LTBP2	latent transforming growth factor beta binding protein 2
	LTBP3	latent transforming growth factor beta binding protein 3

	NRCAM	neuronal cell adhesion molecule
	PLAC8	placenta-specific 8
	PMP22	peripheral myelin protein 22
	SDCCAG8	serologically defined colon cancer antigen 8
	SRI	sorcin
	SYT8	synaptotagmin VIII
	TEM6	tumor endothelial marker 6
	TIMP3	tissue inhibitor of metalloproteinase 3 (Sorsby fundus dystrophy, pseudoinflammatory)
	TMEM2	transmembrane protein 2
	TMEPAI	transmembrane, prostate androgen induced RNA
	TSPAN-1	tetraspan 1
Metabolism and Homeostasis		
	ADH5	alcohol dehydrogenase 5 (class III), chi polypeptide
	ALDH1A3	aldehyde dehydrogenase 1 family, member A3
	ALDH3A1	aldehyde dehydrogenase 3 family, memberA1
	ARL7	ADP-ribosylation factor-like 7
	DPYSL4	dihydropyrimidinase-like 4
	FLJ23462	duodenal cytochrome b
	FXYD3	FXYD domain containing ion transport regulator 3
	FXYD5	FXYD domain containing ion transport regulator 5
	GABRE	gamma-aminobutyric acid (GABA) A receptor, epsilon
	GAMT	guanidinoacetate N-methyltransferase
	GYS1	glycogen synthase 1 (muscle)
	INPP5D	inositol polyphosphate-5-phosphatase, 145kDa
	KCNJ15	potassium inwardly-rectifying channel, subfamily J, member 15
	KCNN4	potassium intermediate/small conductance calcium-activated channel, subfamily N, member 4
	PKD2	polycystic kidney disease 2 (autosomal dominant)
Protein Biogenesis and Turnover		
	CASP6	caspase 6, apoptosis-related cysteine protease
	CAST	calpastatin
	CTSD	cathepsin D (lysosomal aspartyl protease)
	CXX1	CAAX box 1
	FBXL2	F-box and leucine-rich repeat protein 2
	LAMP2	lysosomal-associated membrane protein 2
	MIPEP	mitochondrial intermediate peptidase
	MSRA	methionine sulfoxide reductase A
	NEDD4L	neural precursor cell expressed, developmentally down-regulated 4-like
	PSMC2	proteasome (prosome, macropain) 26S subunit, ATPase, 2
	SPG3A	spastic paraplegia 3A (autosomal dominant)

Protein Secretion		
	CPA4	carboxypeptidase A4
	GALNT1	UDP-N-acetyl-alpha-D-galactosamine:polypeptide N-acetylgalactosaminyltransferase 1 (GalNAc-T1)
	N33	Putative prostate cancer tumor suppressor
	SEC14L2	SEC14-like 2 (S. cerevisiae)
	SULF2.	similar to glucosamine-6-sulfatases
	VAMP8	vesicle-associated membrane protein 8 (endobrevin)
Signal Transduction		
	ADORA2B	adenosine A2b receptor
	ARHGDIB	Rho GDP dissociation inhibitor (GDI) beta
	ANKRD3	ankyrin repeat domain 3; PKCd-interacting protein kinase
	COPS3	COP9 constitutive photomorphogenic homolog subunit 3 (Arabidopsis)
	DXS1283E	GS2 gene; phospholipase A2
	FYN	FYN oncogene related to SRC, FGR, YES
	EPS8R2	EPS8-related protein 2; EGFR substrate
	G1P3	interferon, alpha-inducible protein (clone IFI-6-16)
	GPR48	G protein-coupled receptor 48
	GRP58	glucose regulated protein, 58kDa
	HRASLS3	HRAS-like suppressor 3
	NOTCH1	Notch homolog 1, translocation-associated (Drosophila)
	PIK3C3	phosphoinositide-3-kinase, class 3
	PSTPIP2	proline-serine-threonine phosphatase interacting protein 2
	SH3BGRL	SH3 domain binding glutamic acid-rich protein like
Transcription and Translation		
	CSTF1	cleavage stimulation factor, 3' pre-RNA, subunit 1, 50kDa
	HNRPDL	heterogeneous nuclear ribonucleoprotein D-like
	HOXC10	homeo box C10
	PCNA	proliferating cell nuclear antigen
	PCNP, POLR2L	PEST-containing nuclear protein, polymerase (RNA) II (DNA directed) polypeptide L, 7.6kDa
	RBM3	RNA binding motif protein 3
	RBM8A	RNA binding motif protein 8A
	RBPMS	RNA-binding protein gene with multiple splicing
	RPL28	ribosomal protein L28
	RPS27L	ribosomal protein S27-like
	SFRS11	splicing factor, arginine/serine-rich 11
	TP53	tumor protein p53 (Li-Fraumeni syndrome)
	ZDHHC2	zinc finger, DHHC domain containing 2
	ZIC2	Zic family member 2 (odd-paired homolog, Drosophila); TF involved in brain development
	ZNF195	zinc finger protein 195

Cell Cycle and DNA Replication		
	CDT1	DNA replication factor
	RRM2	ribonucleotide reductase M2 polypeptide
Other		
	APXL	apical protein-like (Xenopus laevis)
	BNIP3L	BCL2/adenovirus E1B 19kDa interacting protein 3-like; proapoptotic mitochondial BH3 protein
	BTBD3	BTB (POZ) domain containing 3
	C11orf13	chromosome 11 open reading frame 13
	C7orf10	chromosome 7 open reading frame 10
	CGI-125	CGI-125 protein
	CGI-145	CGI-145 protein
	D4S234E	DNA segment on chromosome 4 (unique) 234 expressed sequence
	DKFZp434L142	hypothetical protein DKFZp434L142
	DKFZP564K1964	DKFZP564K1964 protein
	DKFZp564O1278, FLJ22774	hypothetical protein DKFZp564O1278, hypothetical protein FLJ22774
	DKFZp762E1312	hypothetical protein DKFZp762E1312
	FLJ12436	hypothetical protein FLJ12436
	FLJ21313	hypothetical protein FLJ21313
	FLJ32104	hypothetical protein FLJ32104
	FLJ90586	hypothetical protein FLJ90586
	HRB2	HIV-1 rev binding protein 2
	HSPC022	HSPC022 protein
	KIAA0186	KIAA0186 gene product
	KIAA0864	KIAA0864 protein
	KIAA0937	KIAA0937 protein
	KIAA1039	KIAA1039 protein
	KIAA1102	KIAA1102 protein
	KIAA1337	KIAA1337 protein
	KIAA1474	KIAA1474 protein
	KIAA1500	KIAA1500 protein
	KIAA1695	hypothetical protein FLJ22297
	KIAA1946	KIAA1946 protein
	LCN7	Lipocalin 7
	LOC132671	LOC132671
	LOC51219	clone FLB5214
	LOC51659	HSPC037 protein
	LOC92689	hypothetical protein BC001096
	MGC10796	hypothetical protein MGC10796
	MSTP031	MSTP031 protein
	NDRG3	NDRG family member 3
	NPD009	NPD009 protein

	PRO1331	hypothetical protein PRO1331
	REN	likely ortholog of mouse induced by retinoic acid, EGF and NGF
	TP53INP1	tumor protein p53 inducible nuclear protein 1

Genes overexpressed in $p53^{-/-}$ HMEC lines over $p53^{+/+}$ HMEC

Cytoskeleton		
	MAP2	microtubule-associated protein 2
	MAP7	microtubule-associated protein 7
	Spir-1	Spir-1 protein; Actin nucleation protein
	TUBE	epsilon-tubulin
ECM and Cell-Cell Communication		
	ANPEP	alanyl (membrane) aminopeptidase (aminopeptidase N, aminopeptidase M, microsomal aminopeptidase, CD13, p150)
	APBB2	amyloid beta (A4) precursor protein-binding, family B, member 2 (Fe65-like)
	APOE	apolipoprotein E
	BACE2	beta-site APP-cleaving enzyme 2
	COL1A1	collagen, type I, alpha 1
	COL5A2	collagen, type V, alpha 2
	CRELD1	cysteine-rich with EGF-like domains 1
	DSC2	desmocollin 2
	E48	lymphocyte antigen 6 complex, locus D
	F2R	coagulation factor II (thrombin) receptor
	HLA-B	major histocompatibility complex, class I, B
	HLA-C	major histocompatibility complex, class I, C
	HLA-F	major histocompatibility complex, class I, F
	HLA-G	HLA-G histocompatibility antigen, class I, G
	K6HF	cytokeratin type II
	KRT16	keratin 16 (focal non-epidermolytic palmoplantar keratoderma)
	MFAP2	microfibrillar-associated protein 2
	MGC4809	serologically defined breast cancer antigen NY-BR-20
	NAV2	neuron navigator 2
	P4HA2	procollagen-proline, 2-oxoglutarate 4-dioxygenase (proline 4-hydroxylase), alpha polypeptide II
	PLOD	procollagen-lysine, 2-oxoglutarate 5-dioxygenase (lysine hydroxylase, Ehlers-Danlos syndrome type VI)
	PROCR	protein C receptor, endothelial (EPCR)
	PSK-1	type I transmembrane receptor (seizure-related protein)
	RSN	restin (Reed-Steinberg cell-expressed intermediate filament-associated protein)
	SERPINA3	serine (or cysteine) proteinase inhibitor, clade A (alpha-1 antiproteinase, antitrypsin), member 3

	STC2	stanniocalcin 2
	SORT1	sortilin 1; g-secretase substrate
	THBD	thrombomodulin
	TSLP	thymic stromal lymphopoietin
	VLDLR	very low density lipoprotein receptor
Metabolism and Homeostasis		
	ALDOC	aldolase C, fructose-bisphosphate
	ARG2	arginase, type II
	ASNS	asparagine synthetase
	BCAT1	branched chain aminotransferase 1, cytosolic
	CBS	cystathionine-beta-synthase
	CTH	cystathionase (cystathionine gamma-lyase)
	CYC1	cytochrome c-1
	ENO2	enolase 2, (gamma, neuronal)
	FACL1, FACL2	fatty-acid-Coenzyme A ligase, long-chain 1, fatty-acid-Coenzyme A ligase, long-chain 2
	FACL2	fatty-acid-Coenzyme A ligase, long-chain 2
	GFPT1	glutamine-fructose-6-phosphate transaminase 1
	GLDC	glycine dehydrogenase (decarboxylating; glycine decarboxylase, glycine cleavage system protein P)
	GPX3	glutathione peroxidase 3 (plasma)
	HMCS	molybdenum cofactor sulfurase
	MTHFD2	methylene tetrahydrofolate dehydrogenase (NAD+ dependent), methenyltetrahydrofolate cyclohydrolase
	OSBPL1A	oxysterol binding protein-like 1A
	PRH1	proline-rich protein HaeIII subfamily 1
	PYCR1	pyrroline-5-carboxylate reductase 1
	SLC1A4	solute carrier family 1 (glutamate/neutral amino acid transporter), member 4
	SLC7A8	solute carrier family 7 (cationic amino acid transporter, y+ system), member 8
	SPP2	sphingosine 1-phosphate phosphohydrolase 2
	TXNIP	thioredoxin interacting protein
	UGCG	UDP-glucose ceramide glucosyltransferase
Protein Biogenesis and Turnover		
	BTG1	B-cell translocation gene 1, anti-proliferative
	CTSC	cathepsin C
	DNAJB6	DnaJ (Hsp40) homolog, subfamily B, member 6
	ENSA	endosulfine alpha
	FBXO5	F-box only protein 5
	HSPA9B	heat shock 70kDa protein 9B (mortalin-2)
	LAMP3	lysosomal-associated membrane protein 3
	PSA	phosphoserine aminotransferase

	SIAH2	seven in absentia homolog 2 (Drosophila)
	STCH	stress 70 protein chaperone, microsome-associated, 60kDa
Protein Secretion		
	ARL4	ADP-ribosylation factor-like 4
Signal Transduction		
	cig5	vipirin; IFNg-induced GTP binding protein
	EPHB3	EphB3
	FZD7	frizzled homolog 7 (Drosophila)
	IL15RA	interleukin 15 receptor, alpha
	IL1RN	interleukin 1 receptor antagonist
	LRP16	LRP16 protein
	MYLK	myosin, light polypeptide kinase
	NET1	neuroepithelial cell transforming gene 1; RHO GTP exchange factor
	NOTCH3	Notch homolog 3 (Drosophila)
	PAWR	PRKC, apoptosis, WT1, regulator
	STK3	serine/threonine kinase 3 (STE20 homolog, yeast)
Transcription and Translation		
	AARS	alanyl-tRNA synthetase
	CBX4	chromobox homolog 4 (Pc class homolog, Drosophila)
	CEBPG	CCAAT/enhancer binding protein (C/EBP), gamma
	DDX18	DEAD/H (Asp-Glu-Ala-Asp/His) box polypeptide 18 (Myc-regulated)
	DKC1	dyskeratosis congenita 1, dyskerin; binds TERC
	GAS6, SC65	growth arrest-specific 6, nucleolar autoantigen (55kD) similar to rat synaptonemal complex protein
	H4F2	H4 histone, family 2
	HDAC3	histone deacetylase 3
	HEY1	hairy/enhancer-of-split related with YRPW motif 1
	HSF1	heat shock transcription factor 1
	IFRD1	interferon-related developmental regulator 1; binds SIN3 complex
	JDP2	jun dimerization protein 2
	KLF4	Kruppel-like factor 4 (gut)
	LARS	leucyl-tRNA synthetase
	LGN	LGN protein, binds GPCRs
	LPHH1	latrophilin 1; GPCR
	MARS	methionine-tRNA synthetase
	NEUGRIN	mesenchymal stem cell protein DSC92; neuronal differentiation nuclear factor
	NFIL3	nuclear factor, interleukin 3 regulated
	NOLC1	nucleolar and coiled-body phosphoprotein 1

	NUP155	nucleoporin 155kDa
	RPL17	ribosomal protein L17
	SSRP1	structure specific recognition protein 1
	SUPV3L1	suppressor of var1, 3-like 1 (S. cerevisiae)
	TCOF1	Treacher Collins-Franceschetti syndrome 1
	TRAP25	TRAP/Mediator complex component
	XPOT	exportin, tRNA (nuclear export receptor for tRNAs)
Cell Cycle and DNA Replication		
	BOP1	block of proliferation 1
	CDCA1	cell division cycle associated 1
	CDKN2A	cyclin-dependent kinase inhibitor 2A (melanoma, p16, inhibits CDK4)
	CDKN2B	cyclin-dependent kinase inhibitor 2B (p15, inhibits CDK4)
	CDKN3	cyclin-dependent kinase inhibitor 3 (CDK2-associated dual specificity phosphatase)
	CENPA	centromere protein A, 17kDa
	TACC2	transforming, acidic coiled-coil containing protein 2
Other		
	AUTS2	autism susceptibility candidate 2
	C1orf24	chromosome 1 open reading frame 24
	C20orf97	chromosome 20 open reading frame 97
	DKFZP566B183	DKFZP566B183 protein
	EBAG9	estrogen receptor binding site associated, antigen, 9
	FEM1B	fem-1 homolog b (C. elegans)
	FLJ10134	hypothetical protein FLJ10134
	FLJ11196	acheron
	FLJ12895	hypothetical protein FLJ12895
	FLJ14007	hypothetical protein FLJ14007
	FLJ20035	hypothetical protein FLJ20035
	FLJ20150	hypothetical protein FLJ20150
	FLJ20360	hypothetical protein FLJ20360
	FLJ20591	exosome component Rrp41
	FLJ20748	hypothetical protein FLJ20748
	FLJ20989	hypothetical protein FLJ20989
	IFIT2	interferon-induced protein with tetratricopeptide repeats 2
	KIAA0703	KIAA0703 gene product
	KIAA0830	KIAA0830 protein
	KIAA1357	KIAA1357 protein
	KIAA1373	KIAA1373 protein
	LOC55862	uncharacterized hypothalamus protein HCDASE
	LOC56965	hypothetical protein from EUROIMAGE 1977056
	MGC10946	hypothetical protein MGC10946
	MGC12335	hypothetical protein MGC12335

	MGC14801	hypothetical protein MGC14801
	MGC34923	hypothetical protein MGC34923
	MGC4504	hypothetical protein MGC4504
	PTD015	PTD015 protein

Table s4. Gene Expression changes of p53+ cell lines 184A1 versus 184B5

Gene Family and Name		Description	Ratio*
(1) Signal transduction			
Ligands and secreted factors			
	IGFBP7	insulin-like growth factor binding protein 7	52
	EREG	Epiregulin, EGF-like	
	DNER	delta-notch-like EGF repeat-containing transmembrane	8
	NMU	GPR66 ligand, obesity	6
	IGFBP4	Insulin-like binding protein 4	0.06
	CXCL14	chemokine (C-X-C motif) ligand 14	0.07
	EDIL3	EGF-like repeats and discoidin I-like domains 3	0.12
	SFRP1	secreted frizzled-related protein 1	0.12
	CXCL1, CXCL2	chemokine (C-X-C motif) ligand 1 (melanoma growth stimulating activity, alpha), chemokine (C-X-C motif) ligand 2	0.15
	IL8	interleukin 8	0.18
	CXCL1	chemokine (C-X-C motif) ligand 1 (melanoma growth stimulating activity, alpha)	0.21
	DTR	diphtheria toxin receptor (heparin-binding epidermal growth factor-like growth factor)	0.25
Receptors and signaling proteins			
	HRASLS3	HRAS-like suppressor 3	29
	IRS1	insulin receptor substrate 1	25
	PKIB	protein kinase (cAMP-dependent, catalytic) inhibitor beta	9
	TNFAIP2	tumor necrosis factor, alpha-induced protein 2	8
	DUSP1	dual specificity phosphatase 1	0.08
	GPR	putative G protein coupled receptor	0.22
	IFNGR1	interferon gamma receptor 1	0.24
(2) Transcription and translation			
	FABP4	fatty acid binding protein 4, adipocyte	47
	KOC1	IGF-II mRNA-binding protein 3	9
	H2BFS,H2BFT	H2B histone family, member S, H2B histone family, member T	6

	H1F2	H1 histone family, member 2	6
	FKSG14	leucine zipper protein FKSG14	6
	H2AFO	H2A histone family, member O, H2A histone family, member Q	5
	H1F0	H1 histone family, member 0	4
	H2BFT	H2B histone family, member T	4
	ATF3	activating transcription factor 3	0.21
(2) ECM			
Proteases			
	MMP2	matrix metalloproteinase 2 (gelatinase A, 72kDa gelatinase, 72kDa type IV collagenase)	10
	KLK5	Kallikrein 5	0.04
	SERPINB2	Serine (or cysteine) proteinase inhibitor, clade B (ovalbumin), member2	0.06
	CTSB	cathepsin B	0.09
	KLK8	kallikrein 8 (neuropsin/ovasin)	0.1
	SERPINB13	serine (or cysteine) proteinase inhibitor, clade B (ovalbumin), member 13	0.14
	SERPINB3	serine (or cysteine) proteinase inhibitor, clade B (ovalbumin), member 3	0.17
	CTSC	cathepsin C	0.21
	SERPINB4	serine (or cysteine) proteinase inhibitor, clade B (ovalbumin), member 4	0.25
	SERPINB7	serine (or cysteine) proteinase inhibitor, clade B (ovalbumin), member 7	0.25
Structural and secreted proteins			
	AGR2	anterior gradient 2 homolog (Xenepus laevis)	20
	FBLN1	fibulin 1, Integrin and nidogen binding protein	17
	LCP1	lymphocyte cytosolic protein 1 (L-plastin)	10
	FBN1	fibrillin 1 (Marfan syndrome)	8
	EPS8	Epidermal growth factor receptor pathway substrate 8	8
	SPARC	secreted protein, acidic, cysteine-rich (osteonectin)	7
	TNC	tenascin C (hexabrachion)	6
	PCSK1N	Proprotein convertase subtilisin/kexin type 1 inhibitor	5
	MGP`	Matrix Gla protein	4
	KRTHB1	Keratin, hair, basic, 1	0.02
	SPP1	Serected phosphoprotein1 (osteopontin, bone sialoprotein, I, early T-lymphocyte activation 1	0.04
	PI3	Protease inhibitor 3, (SKALP)	0.06
	CSPG2	chondroitin sulfate proteoglycan 2 (versican)	0.07
	FN1	Fibronectin 1	0.07
	MAGP2	Microfibril-associated glycoprotein-2	0.12

	KRT14	keratin 14 (epidermolysis bullosa simplex, Dowling-Meara, Koebner)	0.16
	THBD	thrombomodulin	0.21
(4) Cytoskeleton			
	FN1	fibronectin 1	0.07
	CALML3	calmodulin-like 3	0.07
	TAGLN	transgelin	0.15
	MAIL	molecule possessing ankyrin repeats induced by lipopolysaccharide (MAIL), homolog of mouse	0.15
(5) Interferon responsive			
	IFI27	interferon, alpha-inducible protein 27	52
	G1P3	interferon, alpha-inducible protein (clone IFI-6-16)	5
(6) Apoptosis			
	ASC/PYCARD	apoptosis-associated speck-like protein containing a CARD	10

*Ratio is the fold change of gene expression changes of 184A1 over 184B5.

Table s5. Gene Expression changes of p53^{-} cell lines 184AA2 versus 184AA3

Gene Family		Description	Ratio*
(1) Transcription and Translation			
	MLAT4	myxoid liposarcoma associated protein 4	4.63
	SSA2	Sjogren syndrome antigen A2 (60kDa, ribonucleoprotein autoantigen SS-A/Ro)	0.22
	ANGPTL4	angiopoietin-like 4	0.22
	LRRFIP1	leucine rich repeat (in FLII) interacting protein 1	0.24
	SDC3	syndecan 3 (N-syndecan)	0.24
	DREV1	CGI-81 protein	0.24
	ALEX2	armadillo repeat protein ALEX2	0.25
(2) Signal Transduction			
Ligands and secreted factors			
	DKK1	dickkopf homolog 1 (Xenopus laevis)	25.75
	IGFBP3	insulin-like growth factor binding protein 3	20
	CX3CL1	chemokine (C-X3-C motif) ligand 1	11.67
	IL1F9	interleukin 1 family, member 9	9.71
	S100A7	S100 calcium binding protein A7 (psoriasin 1)	9.25
	CXCL16	chemokine (C-X-C motif) ligand 16	8.71
	LTB	lymphotoxin beta (TNF superfamily, member 3)	8.14
	IGFBP4	insulin-like growth factor binding protein 4	7.89
	IL1B	interleukin 1, beta	7.86
	NRG1	neuregulin 1, ERB-B2/HER2neu ligand	7.33
	PDGFA	platelet-derived growth factor alpha polypeptide	6.33
	CYR61	cysteine-rich, angiogenic inducer, 61	6.1
	HBP17	heparin-binding growth factor binding protein	5.64
	GAS6, SC65	growth arrest-specific 6, nucleolar autoantigen (55kD) similar to rat synaptonemal complex protein	5.5
	JAG1	jagged 1 (Alagille syndrome)	5.18
	FGF11	fibroblast growth factor 11	4.88
	VEGFC	vascular endothelial growth factor C	4.52
	IGFBP2	insulin-like growth factor binding protein 2, 36kDa	4.46
	CKLFSF7	chemokine-like factor super family 7	4.1
	BMP1	bone morphogenetic protein 1	4
	CCL20	chemokine (C-C motif) ligand 20	0.04
	TFPI2	tissue factor pathway inhibitor 2	0.06
	SFRP1	secreted frizzled-related protein 1	0.08
	IL18	interleukin 18 (interferon-gamma-inducing factor)	0.11
	S100P	S100 calcium binding protein P	0.17

	S100A9	S100 calcium binding protein A9 (calgranulin B)	0.19
	WNT5A	wingless-type MMTV integration site family, member 5A	0.19
	LTBP1	latent transforming growth factor beta binding protein 1	0.21
Receptors and Signaling Components			
	TNFRSF21	tumor necrosis factor receptor superfamily, member 21	18.25
	FEZ1	fasciculation and elongation protein zeta 1 (zygin I)	13.33
	PARG1	PTPL1-associated RhoGAP 1	11.5
	FGFR2	fibroblast growth factor receptor 2 (bacteria-expressed kinase, keratinocyte growth factor receptor, craniofacial dysostosis 1, Crouzon syndrome, Pfeiffer syndrome, Jackson-Weiss syndrome)	9
	TNFRSF21	tumor necrosis factor receptor superfamily, member 21	8.4
	ARTN	artemin	7.75
	TNFSF10	tumor necrosis factor (ligand) superfamily, member 10	7.69
	PTPRZ1	protein tyrosine phosphatase, receptor-type, Z polypeptide 1	7.67
	AXL	AXL receptor tyrosine kinase	7.52
	PPP1R3C	protein phosphatase 1, regulatory (inhibitor) subunit 3C	7.38
	CCND2	cyclin D2	6.33
	G0S2	putative lymphocyte G0/G1 switch gene	6.17
	NOTCH1	Notch homolog 1, translocation-associated (Drosophila)	5.67
	DDR1	discoidin domain receptor family, member 1	5.28
	RDC1	G protein-coupled receptor	5.14
	PTPRF	protein tyrosine phosphatase, receptor type, F	5.13
	PPP1R14C	protein phosphatase 1, regulatory (inhibitor) subunit 14C	4.85
	TIP-1	Tax interaction protein 1	4.29
	CDC42EP3	CDC42 effector protein (Rho GTPase binding) 3	4.16
	CHRNB1	cholinergic receptor, nicotinic, beta polypeptide 1 (muscle)	4
	SNK	serum-inducible kinase	4
	SAMSN1	SAM domain, SH3 domain and nuclear localisation signals, 1	0.03
	FKBP5	FK506 binding protein 5	0.04
	DUSP1	dual specificity phosphatase 1	0.05
	BIRC3	baculoviral IAP repeat-containing 3	0.05
	TOP1	topoisomerase (DNA) I	0.06
	NUCKS	similar to rat nuclear ubiquitous casein kinase 2	0.09
	NFKBIA	nuclear factor of kappa light polypeptide gene enhancer in B-cells inhibitor, alpha	0.09
	PK428	Ser-Thr protein kinase related to the myotonic dystrophy protein kinase	0.1
	TRAP150	thyroid hormone receptor-associated protein, 150 kDa subunit	0.11
	TREM1	triggering receptor expressed on myeloid cells 1	0.11

*Ratio is the fold change of gene expression changes of 184AA2 over 184AA3.

Table s6. Gene Expression Changes Resulting from Expression of ERB-B2/Her2^{neu} in 184B5

Gene Family	Description	Ratio*
(1) Signal Transduction		
Ligands and secreted factors		
IL24	interleukin 24	22.11
TFPI2	tissue factor pathway inhibitor 2	4.27
IGFBP4	insulin-like growth factor binding protein 4	0.05
CXCL14	chemokine (C-X-C motif) ligand 14	0.05
CXCL1, CXCL2	chemokine (C-X-C motif) ligand 1 (melanoma growth stimulating activity, alpha), chemokine (C-X-C motif) ligand 2	0.08
TNFSF10	tumor necrosis factor (ligand) superfamily, member 10	0.11
DLL1	delta-like 1 (Drosophila)	0.13
TGFB2	transforming growth factor, beta 2	0.16
DKK3, RIG	dickkopf homolog 3 (Xenopus laevis), regulated in glioma	0.2
CCL20	chemokine (C-C motif) ligand 20	0.22
CXCL14	chemokine (C-X-C motif) ligand 14	0.22
S100A8	S100 calcium binding protein A8 (calgranulin A)	0.24
Receptors and other membrane proteins		
SPRR1A	small proline-rich protein 1A	0.23
SH3BGRL	SH3 domain binding glutamic acid-rich protein like	0.24
RDC1	G protein-coupled receptor	0.24
MLP	MARCKS-like protein	0.24
DRAPC1	hypothetical protein DRAPC1	0.25
AKAP12	A kinase (PRKA) anchor protein (gravin) 12	10.88
DNAJB6	DnaJ (Hsp40) homolog, subfamily B, member 6	4.13
PPFIA1	protein tyrosine phosphatase, receptor type, f polypeptide (PTPRF), interacting protein (liprin), alpha 1	4
HRASLS3		4
MYL9	myosin, light polypeptide 9, regulatory	0.08
TREM2	triggering receptor expressed on myeloid cells 2	0.13
FEZ1	fasciculation and elongation protein zeta 1 (zygin I)	0.16
EFNA1	ephrin-A1	0.16

DUSP1	dual specificity phosphatase 1	0.16
(2) Transcription and gene expression		
FOS	v-fos FBJ murine osteosarcoma viral oncogene homolog	0.21
ZFP36	zinc finger protein 36, C3H type, homolog (mouse)	0.24
(3) ECM and Cell-Cell Communication		
Proteases		
CST6	cystatin E/M	12.5
PLAT	plasminogen activator, tissue	6.29
KLK6	kallikrein 6 (neurosin, zyme)	5.27
SERPINB3	serine (or cysteine) proteinase inhibitor, clade B (ovalbumin), member 3	0.2
SERPINB4	serine (or cysteine) proteinase inhibitor, clade B (ovalbumin), member 4	0.21
SPUVE	protease, serine, 23	0.23
Structural and Secreted Proteins		
ESDN	endothelial and smooth muscle cell-derived neuropilin-like protein	8.5
COL13A1	collagen, type XIII, alpha 1	6.22
SCEL	sciellin	4.67
PLAC8	placenta-specific 8	4.63
KRT8	keratin 8	4.56
SPRR1B	small proline-rich protein 1B (cornifin)	0.12
GJB2	gap junction protein, beta 2, 26kDa (connexin 26)	0.12
KRT6B	keratin 6B	0.12
SEMA3C	sema domain, immunoglobulin domain (Ig), short basic domain, secreted, (semaphorin) 3C	0.15
C1R	complement component 1, r subcomponent	0.16
FLRT3	fibronectin leucine rich transmembrane protein 3	0.16
KRT16	keratin 16 (focal non-epidermolytic palmoplantar keratoderma)	0.17
FLRT3	fibronectin leucine rich transmembrane protein 3	0.21
ITGB6	integrin, beta 6	0.21
PI3	protease inhibitor 3, skin-derived (SKALP)	0.22
T1A-2	lung type-I cell membrane-associated glycoprotein	0.22
DSC3	desmocollin 3	0.23
CSPG2	chondroitin sulfate proteoglycan 2 (versican)	0.23
PCDH19	protocadherin 19	0.25

(5) Cytoskeleton		
HPCAL1	hippocalcin-like 1	4.65
TAGLN	transgelin	0.07
BPAG1	bullous pemphigoid antigen 1, 230/240kDa	0.18
DD96	epithelial protein up-regulated in carcinoma, membrane associated protein 17	0.2
NS1-BP	NS1-binding protein	0.25
(6) Metabolism		
ASNS	asparagine synthetase	7.89
ALDH3A1	aldehyde dehydrogenase 3 family, memberA1	0.19
CA12	carbonic anhydrase XII	0.22
AKR1C3	aldo-keto reductase family 1, member C3 (3-alpha hydroxysteroid dehydrogenase, type II)	0.22
(7) IFN-Regulated Genes		
IFIT1	interferon-induced protein with tetratricopeptide repeats 1	0.06

*Ratio is the fold change of gene expression changes of 184B5ME over 184B5.